


12-4-2009

Analyzing Spatial Patterns in Reefscape Ecology Via Remote Sensing, Benthic Habitat Mapping, and Morphometrics

Shanna K. Dunn

Nova Southeastern University, sdunn31@hotmail.com

Follow this and additional works at: https://nsuworks.nova.edu/occ_stuetd

 Part of the [Marine Biology Commons](#), and the [Oceanography and Atmospheric Sciences and Meteorology Commons](#)

Share Feedback About This Item

NSUWorks Citation

Shanna K. Dunn. 2009. *Analyzing Spatial Patterns in Reefscape Ecology Via Remote Sensing, Benthic Habitat Mapping, and Morphometrics*. Master's thesis. Nova Southeastern University. Retrieved from NSUWorks, Oceanographic Center. (234) https://nsuworks.nova.edu/occ_stuetd/234.

This Thesis is brought to you by the HCNSO Student Work at NSUWorks. It has been accepted for inclusion in HCNSO Student Theses and Dissertations by an authorized administrator of NSUWorks. For more information, please contact nsuworks@nova.edu.

NOVA SOUTHEASTERN UNIVERSITY OCEANOGRAPHIC CENTER

ANALYZING SPATIAL PATTERNS IN REEFSCAPE
ECOLOGY VIA REMOTE SENSING, BENTHIC HABITAT
MAPPING, AND MORPHOMETRICS

By

Shanna K. Dunn

Submitted to the Faculty of
Nova Southeastern University Oceanographic Center
in partial fulfillment of the requirements for
the degree of Master of Science with a specialty in:

Marine Environmental Science

Nova Southeastern University

December 4, 2009

Submitted in Partial Fulfillment of the Requirements for the Degree of

**Masters of Science:
Marine Environmental Science**

**Thesis of
SHANNA K. DUNN**

Nova Southeastern University
Oceanographic Center

December 2009

Approved:

Thesis Committee

Major Professor : _____
Samuel Purkis, Ph.D.

Committee Member : _____
Bernhard Riegl, Ph.D.

Committee Member : _____
Eric Hochberg, Ph.D.

TABLE OF CONTENTS

Table of Contents	3
List of Tables	4
List of Figures	4
Acknowledgements	5
Abstract	6
1. Introduction	7
1.1 <i>Statement of purpose</i>	9
1.2 <i>Spatial patterns in coral reefs</i>	9
1.3 <i>Landscape ecology concepts and spatial metrics</i>	11
1.4 <i>Development of high spatial resolution coral reef mapping</i>	13
1.5 <i>Coupling thematic habitat maps with digital elevation models</i>	16
1.6 <i>Utility of habitat maps: marine protected area design and modeling</i>	17
2. Methods	18
2.1 <i>Study sites</i>	18
2.1.1 <i>Vieques, Puerto Rico</i>	21
2.1.2 <i>Andavadoaka, Madagascar</i>	25
2.1.3 <i>Saipan, Commonwealth of the Northern Mariana Islands</i>	31
2.2 <i>Data processing</i>	36
2.3 <i>Morphometric calculations</i>	40
3. Results	43
4. Discussion	59
4.1 <i>Habitat class percentages</i>	59
4.2 <i>Mean habitat depth and rugosity</i>	59
4.3 <i>Neighborhood transitions</i>	61
4.4 <i>Exceedance probability</i>	62
4.5 <i>Compactness and principle axes ratio</i>	65
4.6 <i>Fractal dimension and fractal span</i>	67
4.7 <i>Error analysis</i>	69
4.8 <i>Summary: quantified spatial patterns and future research</i>	70
5. Conclusion	73
References	74
Appendices	84
<i>Appendix I: Benthic habitat maps and keys</i>	
A. <i>Vieques</i>	
B. <i>Andavadoaka</i>	
C. <i>Saipan</i>	
<i>Appendix II: Digital elevation models</i>	
A. <i>Vieques</i>	
B. <i>Andavadoaka</i>	
C. <i>Saipan</i>	

LIST OF TABLES

Table 1: Data summary for three study sites	20
Table 2: Regression errors for Figure 16 plots of depth vs. rugosity	47
Table 3: R^2 values derived from embedded relative transition matrices	50
Table 4: Exceedance probability outputs for habitats and sites	54

LIST OF FIGURES

Figure 1: World map indicating study site locations	19
Figure 2: Vieques Landsat MSS image featuring the Vieques National Wildlife Refuge polygonal boundary	22
Figure 3: Vieques IKONOS mosaic with groundtruth points plotted	22
Figure 4: Vieques surficial geology map	24
Figure 5: Andavadoaka QuickBird and SPOT images featuring the Velondriake marine protected area boundary	26
Figure 6: Andavadoaka QuickBird image with groundtruth points plotted	27
Figure 7: Madagascar surficial geology map	30
Figure 8: Saipan IKONOS mosaic featuring terrestrial and marine conservation boundaries	32
Figure 9: Saipan IKONOS mosaic with groundtruth points plotted	33
Figure 10: Saipan surficial geology map	35
Figure 11: Andavadoaka spectral bathymetry model	37
Figure 12: Data processing flow chart	39
Figure 13: Habitat percentages of total mapped areas	44
Figure 14: Percentages of consolidated and unconsolidated benthic classes	45
Figure 15: Mean habitat depths	46
Figure 16: Mean habitat depth vs. mean habitat rugosity	47
Figure 17: Embedded relative transition matrices	49
Figure 18: Exceedance probabilities by site	52
Figure 19: Exceedance probabilities by habitat	53
Figure 20: Semi-log plots of compactness vs. patch area	55
Figure 21: Semi-log plots of principle axes ratio vs. patch area	56
Figure 22: Fractal dimension vs. compactness	57
Figure 23: Cumulative percentage vs. fractal span	58
Figure 24: Geographic distribution of tropical cyclone paths	68

ACKNOWLEDGEMENTS

I would like to sincerely thank my principle advisor Dr. Sam Purkis for his guidance and support during this thesis project. The knowledge I have gained by working as an employee in Dr. Purkis' lab has helped me build a foundation for a future career path and I will always be grateful. Sam, thank you for all the encouragement during countless meetings and for sharing your time and wisdom. Gwilym Rowlands, thank you for being a comrade and for teaching me about the world of remote sensing and GIS, as well as the science behind creating marine habitat maps. I will certainly miss working with you and sharing life with you; I wish you all the best.

Many thanks to my committee members Dr. Bernhard Riegl and Dr. Eric Hochberg for their expert advice and for always challenging me to think autonomously. Kevin Kohler, I would like to show appreciation for your inspiring outlook on life, thanks for the many lively conversations.

To my parents, Jim and Kathy Dunn, your respect for education has always been a guiding factor in my life. Thank you so much for the love and support throughout my academic journey. Ryan Dunn, my dynamic brother, your liberated spirit has been a continual source of motivation, words just cannot express how much you mean to me.

Abe Gleason, the love of my life, thank you for being my best friend and partner. I owe my deepest gratitude to you for your patience and devotion during the course of my graduate studies.

Fellow OC grad students, Katy, Paola, Nesti, Alex, Greg, Kristi, Kristian, Dani, thank you for your friendship and intellectual insights during our time in this graduate program. You will all be missed dearly.

Much appreciation goes to the following people and agencies for contributing data to my thesis work: Raj Roy and Blue Ventures, the National Coral Reef Institute, Sam Purkis, Bernhard Riegl, and the National Oceanic and Atmospheric Administration.

KEY WORDS: coral reef ecosystems, habitat mapping, remote sensing, metrics, spatial patterns, geographic information system (GIS), IKONOS, QuickBird, LiDAR, digital elevation model (DEM), landscape ecology, marine protected area (MPA)

ABSTRACT

A growing number of scientists are investigating applications of landscape ecology principles to marine studies, yet few coral reef scientists have examined spatial patterns across entire reefscape with a holistic ecosystem-based view. This study was an effort to better understand reefscape ecology by quantitatively assessing spatial structures and habitat arrangements using remote sensing and geographic information systems (GIS).

Quantifying recurring patterns in reef systems has implications for improving the efficiency of mapping efforts and lowering costs associated with collecting field data and acquiring satellite imagery. If a representative example of a reef is mapped with high accuracy, the data derived from habitat configurations could be extrapolated over a larger region to aid management decisions and focus conservation efforts.

The aim of this project was to measure repeating spatial patterns at multiple scales (10s m² to 10s km²) and to explain the environmental mechanisms which have formed the observed patterns. Because power laws have been recognized in size-frequency distributions of reef habitat patches, this study further investigated whether the property exists for expansive reefs with diverse geologic histories.

Intra- and inter-reef patch relationships were studied at three sites: Andavadoaka (Madagascar), Vieques (Puerto Rico), and Saipan (Commonwealth of the Northern Mariana Islands). *In situ* ecological information, including benthic species composition and abundance, as well as substrate type, was collected with georeferenced video transects. LiDAR (Light Detection and Ranging) surveys were assembled into digital elevation models (DEMs), while vessel-based acoustic surveys were utilized to empirically tune bathymetry models where LiDAR data were unavailable. A GIS for each site was compiled by overlying groundtruth data, classifications, DEMs, and satellite images. Benthic cover classes were then digitized and analyzed based on a suite of metrics (*e.g.* patch complexity, principle axes ratio, and neighborhood transitions).

Results from metric analyses were extremely comparable between sites suggesting that spatial prediction of habitat arrangements is very plausible. Further implications discussed include developing an automated habitat mapping technique and improving conservation planning and delimitation of marine protected areas.

1. INTRODUCTION

This study merges concepts in geomorphology and landscape ecology. From a geomorphology perspective, studying reef formations and the processes that shape them enables us to understand the geologic history and dynamics of the physical system. The landscape (*i.e.* reefscape) ecology viewpoint conveys the need to improve our understanding of the relationship between spatial patterns and ecological processes on multiple scales.

Modern reef ecosystem morphology strongly depends on the nature of sea-level fluctuations, antecedent seafloor surfaces, disturbances, ambient oceanographic conditions, and the flora and fauna that contribute to reef accretion and sediment accumulation (Kennedy and Woodroffe 2002). Thus, geomorphic and ecologic processes are intimately linked in coral reef ecosystems. In one direction, geomorphic processes and bathymetry shape the distribution of biota. Conversely, in the other direction, biota modify geomorphic processes and bathymetry by accreting calcium carbonate (Stallins 2006). These interactions, firmly rooted in biogeomorphologic theory, describe ecological succession as a variable approaching a variable, an ever-changing process with an open end. The purpose of mapping and analyzing the structures and biota of reef ecosystems is to better understand the foremost factors that have influenced their construction, their current phases, and possible future trajectories.

Applying landscape ecology concepts to marine ecology is a relatively recent endeavor undertaken by the oceanographic community. Landscape ecologists have been successful in describing the patterns and processes of terrestrial environments using landscape-level metrics (Grober-Dunsmore *et al.* 2008a). As advances in GIS, remote sensing, and computer technologies continue to emerge, marine scientists are better equipped to quantify spatial patterns in marine ecology and geomorphology (Hinchey *et al.* 2008). Remote sensing, merged with the capabilities of GIS provides a powerful cost-efficient mapping tool for studying regional scale (10s-100s km) trends in the environment. For this reason, many scientists, academics, and professionals studying the world's oceans utilize GIS to investigate their areas of interest and we are rapidly discovering how GIS can help conserve valuable populations and resources (Fedra and Feoli 1998; Dahdouh-Guebas 2002; Zharikov *et al.* 2005; Thanilachalam and

Ramachandran 2002; Andréfouët 2008; Rioja-Nieto and Sheppard 2008; Cassata and Collins 2008; Grober-Dunsmore *et al.* 2008b).

Mapping and geospatial analysis of benthic environments are multidisciplinary tasks that have become more accessible in recent years because of advances in technology and cost reductions in survey systems (Andrews 2003). Seafloor mapping has traditionally been conducted using remote sensing technologies because they are cost-efficient tools that can collect data over extensive areas. A variety of remote sensing technologies exist to gather benthic data, for instance, aerial photography, multispectral and hyperspectral satellite and airborne sensors, LiDAR, single and multibeam sonar, side-scan sonar, and interferometric sonar.

Geospatial mapping of the seafloor has been employed in a multitude of applications within the ocean sciences. Broad examples of seabed mapping applications are navigation and marking potential shipping hazards, selecting seafloor construction sites, mapping geophysical hazards in tectonically active zones, and designing dredge projects. Specific ecological examples of seabed mapping applications include relating bathymetry to trophic structures in fish assemblages (Arias-González *et al.* 2006), managing marine protected areas (Knight *et al.* 1997; Dahdouh-Guebas 2002; Thanilachalam and Ramachandran 2002; Moufaddal 2005), and studying relationships between infaunal populations and seafloor structures (Zajac *et al.* 2003; Zajac 2008).

In relation to coral reef environments, remote sensing systems can characterize inter-reef structural differences (Costa *et al.* 2009), intra-reef habitat diversity and zonations, and variations in biogeochemical budgets (Andréfouët *et al.* 2003; Purkis *et al.* 2008). Kendall and Miller (2008) state that coral reef ecosystems are attractive environments for benthic mapping projects for three key reasons:

1. *Coral reef ecosystems are patchy landscapes with diverse bottom types including sand, submerged vegetation, and hardbottom features; ecological interactions among these bottom types have begun to be explored using landscape ecology theory.*
2. *Bottom features are arranged and shaped predictably according to their geological, ecological, and environmental context, but their spatial properties have not been systematically quantified.*

3. *Coral reef ecosystems occur in shallow, optically clear waters, meaning landscape scale benthic maps, which are becoming increasingly available in many regions, can be produced from remote sensing or aerial photography.*

1.1 Statement of purpose

The aim of this project is to study structures and spatial patterns in reef ecosystems through the analysis of benthic habitat maps. The primary questions in this research project are the following: (1) Are reef structures mapped at three study sites the same or different with regard to reefscape patch relationships? (2) If inter- and intra-reef metrics indicate that the sites are the same, what are possible mechanisms that could explain the similarities? (3) If reefscape patch relationships are different, what sculpted the reefs into the structures and shapes that are observed? (4) According to the results, can satellite-derived habitat maps and morphometrics be used to predict spatial arrangements within reefal environments?

To answer these questions, the initial data processing involved the generation of benthic habitat maps. The two major stages of map production include classification of field data into habitat categories followed by discrimination of image data into those habitat categories (Mather 1997). GIS, satellite remote sensing, airborne LiDAR, and ground verification were used in concert to produce maps of three diverse coral reef ecosystems. The sites consisted of Vieques, Puerto Rico; Andavadoaka, Madagascar; and Saipan, Commonwealth of the Northern Mariana Islands. Spatial relationships between reefscape patches were explored by compiling a database of morphometrics (*e.g.* patch complexity, rugosity, exceedance probability) derived from each map, and subsequently analyzing those metrics in two- and three-dimensions.

1.2 Spatial patterns in coral reefs

Theoretical ecologists emphasize that ecosystems exhibit spatial self-organization, a phenomenon that begins with disordered initial conditions and results in large-scale ordered spatial patterns. Thus, understanding the initial conditions that can give rise to natural ecosystem engineering, as well as how patterns form through time, can aid in comprehending current ecosystem configurations, ecological stability, and diversity. Self-organized spatial patterns have been claimed to have important ecological consequences

for facilitating the persistence of otherwise nonpersistent interactions, the coexistence of competing species, pathogen persistence, as well as for predator searching efficiency and reproductive fitness (Rohani *et al.* 1997). One central question pertaining to these concepts is whether spatial patterns can be useful indicators of the proximity of a system to catastrophic change (Pascual and Guichard 2005).

Several studies (von Hardenberg *et al.* 2001; Lejeune *et al.* 2002; Gilad *et al.* 2004; Sleeman *et al.* 2005) suggest that regular pattern formation leads to resource optimization, which has positive consequences for productivity and diversity (Rietkerk and van de Koppel 2008). The potential application and relevance of regular pattern formation to global environmental change, ecosystem adaptation, and restoration involves transplanting organisms so that they reach a certain threshold density, to induce short-range facilitation, and arranging them spatially in a way to make optimal use of limiting resources (Sleeman *et al.* 2005; Rietkerk and van de Koppel 2008). Mimicking regular patterns in coral reefs is an intuitive strategy to aid ecosystem restoration because the patterns increase the interception of resources that flow past and spatially optimize their exploitation (Rietkerk and van de Koppel 2008).

An outstanding research question is whether a change in regular patterns can indicate loss or gain of resilience in real ecosystems, or even act as a warning signal for an abrupt loss of the patterns altogether (Rietkerk and van de Koppel 2008). Resilience, defined as the ability of an ecosystem to resist lasting change caused by disturbances, is partially a function of spatial heterogeneity in coral reefs (McClanahan *et al.* 2002). If a reef system is disturbed and environmental stressors are acting synergistically, heterogeneity can decrease and an ecological shift may occur. The shift is usually from a coral-dominated intricate structure to an algae-dominated homogeneous system. Further research is needed to better understand and predict regular pattern formation in coral reef ecosystems, and how this affects the response of the systems to disturbances and global environmental change (Nyström and Folke 2001).

The modern model of the ecosystem as a hierarchy with emergent properties is exemplified in reefs as massive structures formed by small colonial organisms, the self-similarity of those structures across large spatial scales, and the uniformity of function by diverse biological communities (Hatcher 1997). Repeating patterns in coral reefs are seen

from small-scale architectures of distinct colonies to large-scale reef distributions (Mistr and Bercovici 2003). One species of coral can grow in different spatial patterns depending on the geographic location of specific colonies (Mistr and Bercovici 2003). This observation suggests that environmental conditions, such as light and nutrient flux, play an important role in controlling colony configurations. Colonies and reef systems can develop regular patterns because they obstruct flow and intercept available resources, either by enhanced rugosity or by increased complexity of the path for the flow field (Mistr and Bercovici 2003). Graus and MacIntyre (1989) and Mistr and Bercovici (2003) modeled coral reef structure formation in response to unidirectional ocean currents and found that coral structures will align perpendicular to flow, propagating against flow direction. This coral growth behavior has also been documented in several observational studies (Chamberlain and Graus 1975; Done 1982; Sebens *et al.* 2003).

Reef systems generate spatial patterns in both horizontal and vertical zonations. Attenuation of light as it penetrates the water column and changes in flow regime are both suspected to contribute to changes in coral growth morphologies (massive, branching, platey) with depth (Graus and Macintyre 1989; Jackson 1991). These vertical spatial patterns along reef walls are well-documented, however, the scope of this study deems them unmeasurable because nadir-viewing satellite sensors impede the perception of vertically-aligned habitat components. Therefore, the vertical information utilized in this analysis was associated with seafloor depths, not changes in patterns down the vertical component of reef structures.

1.3 Landscape ecology concepts and spatial metrics

Landscape ecology traditionally has been limited to the study of terrestrial systems; however, the questions and methods defining the science are equally relevant for marine and coastal systems (Hinchey *et al.* 2008). Because advances in technology have enabled scientists to employ the principles of landscape ecology to marine ecosystems, investigations are becoming more pervasive in the literature (Paine and Levin 1981; Steele 1989; Robbins and Bell 1994; Irlandi *et al.* 1995; Zajac *et al.* 2003; Hewitt *et al.* 2004; Pittman *et al.* 2004; Crawford *et al.* 2005; Darcy and Eggleston 2005; Yang and Liu 2005; Zajac 2008; Hovel and Regan 2008; Grober-Dunsmore *et al.* 2008a;

Garza 2008; Bell *et al.* 2008; Hamylton and Spencer 2008). According to Hinchey *et al.* (2008), the overall impression of the state of the application of landscape methods to marine and coastal systems is that it is a rapidly-emerging field that holds great promise.

In landscape ecology, patterns and processes are quantified using patches to represent habitats in thematic maps. Spatial metrics, based on number, size, shape, and arrangement of patches are used to assess the nature and degree of spatial organization of landscapes (Walsh *et al.* 1998). Coral reef benthic habitat maps are one form of a thematic map, therefore the same principles and applications of spatial metrics can be applied to study patch relationships (Purkis *et al.* 2007).

An example of the application of landscape ecology to a marine system is a study by Purkis *et al.* (2005). The authors combined a satellite-derived habitat map with a bathymetric DEM to quantitatively study the geomorphology and habitat distribution of a modern carbonate ramp in the Arabian Gulf. An IKONOS image was classified into eight substrate classes using the “reef-up” approach of Purkis (2005), yielding an overall map accuracy of 81%. Purkis *et al.* (2005) found that neighborhood transitions in the study area were clearly probabilistic, not randomly distributed. For example, there was a high probability that sparse coral was found next to macro-algae, and sand was frequently neighboring seagrass. Similarly, there was a degree of correlation between classes and their occurrence at particular depth intervals. “Hard” carbonate facies (live and dead corals) were preferentially deeper than “soft” unconsolidated facies (algae and seagrass). In the same study, fractal behavior was investigated using boundary- and patch-based metrics. The results indicated scale invariance of patches over three orders of magnitude (10^3 m^2 to 10^5 m^2), meaning fractal behavior was present among substrate classes (Purkis *et al.* 2005).

Scale invariance is a feature of objects that do not change if length scales are multiplied by a common factor. In other words, scale invariant objects appear similar at all levels of magnification and can be described by power laws. A power law is any polynomial relationship that exhibits the property of scale invariance. Power law polynomial relationships must be between two quantities which are related proportionally; one quantity is the frequency of an event and the other is the size of the event.

Fractals are conceptual geometric objects that can be split into parts and each part is a reduced-size copy of the whole. Fractal shapes are too irregular to be described by Euclidean geometry, and so are described by self-similarity and power law scaling. Avnir *et al.* (1998) describe fractals as mathematical constructs characterized by a never-ending cascade of similar structural details that are revealed upon magnification on all scales. Thus, in a purely mathematical sense, a fractal object must have power law scaling over infinite orders of magnitude (Avnir *et al.* 1998). In reality, empirical investigations of power law scaling are limited on the lower bound by basic building block units (*e.g.* a pixel in a raster map) and on the upper bound by the size of the system (*e.g.* the entire map of a barrier reef system). These limitations compel us to interpret fractality as the adherence of a system to power law scaling over “several” orders of magnitude. Avnir *et al.* (1998) clarify that an acceptable number of orders of magnitude should be ≥ 3 to describe a system as fractal. Natural real-world objects that estimate mathematical fractals include coastlines, clouds, and snowflakes. In this study, the fractal behavior of reefscape patches is explored in an analogous manner to studies done by Rankey (2002) and Purkis *et al.* (2007).

Analyzing the property of scale invariance in reefscales using fractality is useful for predicting ecosystem behavior. If a predictable relationship between the frequency and size of habitat patches is found at observable scales, it can be used to interpolate the behavior of the system at unobservable scales. Satellite-derived reefscape maps can capture the upper bound of a system’s size, but certainly cannot capture the fine-scale sub-meter patterns within the system due to the limitation of the pixel. So, when aiming to link structure to function, a primary goal in the field of landscape ecology, the interpolation of area-frequency relationships to finer scales can facilitate a better understanding of ecosystem processes that would be otherwise elusive.

1.4 Development of high spatial resolution coral reef mapping

Benthic habitat mapping, of both geomorphological structure and biological cover, from the late-1970s to the late-1990s was carried out using aerial photography, high resolution multispectral airborne data, medium spatial resolution (10-30 m) multispectral satellite data (SPOT & Landsat), or a combination of these data (Mumby

and Harborne 1999). Aerial photographs provided higher spatial resolution than did satellites of that time, however, aerial photos contain distorted margins requiring rectification, and involve expensive surveys (Chauvaud *et al.* 1998). Although airborne platforms provide high spatial resolution, surveys are costly and cover limited area (Mumby *et al.* 1999). According to Andréfouët *et al.* (2003), it is now clear that for geomorphology and habitat-scale (10s–100s km) applications, SPOT and Landsat data are adequate for simple complexity mapping (3-6 classes), but for more complex objectives (7-13 classes) they are limited by their spatial and spectral resolution as well as their digitization rate of 8-bits (Mumby *et al.* 1998; Mumby and Edwards 2002; Hochberg and Atkinson 2003; Capolsini *et al.* 2003). It should be noted that aerial photos, multispectral airborne sensors, and medium spatial resolution satellites are extremely useful for certain applications, but in terms of mapping reefs at a regional scale to the habitat level, they each have limitations. Aerial photos are distorted and need to be rectified, multispectral airborne sensors are expensive to operate over a regional scale, and medium spatial resolution satellites are too coarse to capture the details of habitat shapes.

The 1999 launch of the IKONOS satellite and the 2001 launch of the QuickBird satellite provided coral reef scientists with enhanced mapping capabilities. IKONOS and QuickBird, both considered to be high spatial resolution satellites, have 4 m and 2.4 m length pixels respectively. Both of these satellites collect multispectral data across four bands in the blue, green, red, and near-infrared (Table 1) wavelengths, allowing comparisons to be made between them. QuickBird and IKONOS data can both be delivered with an 11-bit radiometric resolution, which is superior to former systems with 8-bit formats. When considering the enhanced radiometric resolution of 11-bits (2048 levels of tonal variation) over 8-bit systems (256 levels), target discrimination is improved by a factor of eight in the range of tone levels collected (Maeder *et al.* 2002). This improvement in radiometric resolution is critical for collecting data in low-light conditions typical of underwater environments (Maeder *et al.* 2002).

Numerous coral reef studies have analyzed the effectiveness of IKONOS data for mapping purposes, and many have utilized IKONOS imagery in shallow benthic habitat mapping applications since the satellite's inception. Mumby and Edwards (2002)

evaluated the accuracy of IKONOS data for mapping coral reef habitats in Turks and Caicos using supervised classifications; an acceptable overall accuracy of 64-74% was presented. They found that IKONOS data had limited abilities in identifying habitats spectrally due to the poor spectral resolution of the satellite, constraining their use to medium level mapping (~5-9 classes). Boundaries of patches were accurately delimited as a result of the satellite's high spatial resolution, suggesting that IKONOS imagery is well-suited for mapping at a geomorphological scale.

Maeder *et al.* (2002) mapped benthic cover in Roatán, Honduras using IKONOS imagery, *in situ* hyperspectral measurements, and the ISODATA (Iterative Self-Organizing Data) algorithm to generate an unsupervised classification. Maeder *et al.* (2002) extracted 5 classes at each of two sites, Half Moon Bay and Tabyana Bay, with overall accuracies of 90% and 89% respectively. The classifications were limited to the scale of general geophysical structures and biological communities, rather than species composition (Maeder *et al.* 2002).

Andréfouët *et al.* (2003) collected ten IKONOS images of coral reef sites distributed around the world and sought to clarify the potential of the data for coral reef habitat mapping. This international collaborative study considered sites that encompass the primary biogeographic coral regions of the world including bank reefs, fringing reefs, barrier reefs, and atolls. Andréfouët *et al.* (2003) applied unsupervised or supervised classifications depending upon available data and conditions for each site. Overall mapping accuracy was calculated to be 77% for 4-5 classes, 71% for 7-8 classes, 65% for 9-11 classes, and 53% for greater than 13 classes. This general linear trend of overall accuracy decreasing with increasing habitat complexity could be used to estimate the accuracy of a given site *a priori* (Andréfouët *et al.* 2003). The authors noted that if 80% accuracy is required for scientific or management applications, only 4-5 classes can be mapped with IKONOS, but if 70% accuracy is the threshold, up to 10 classes can be mapped.

Evaluations of IKONOS data between 2002 and 2003 (Mumby and Edwards 2002; Maeder *et al.* 2002; Palandro *et al.* 2003; Capolsini *et al.* 2003; Hochberg and Atkinson 2003) proved their capability to map coral reef ecosystems successfully.

Nevertheless, spectral limitations of IKONOS scenes restrict the number of distinguishable habitats to approximately 5-9 classes.

Upon clarification of the appropriate applications of IKONOS data, myriad research prospects unfolded such as change detection of coral bleaching events (Elvidge *et al.* 2004), algal biomass estimation (Andréfouët *et al.* 2004), spatial and temporal pattern analysis of coral assemblages (Purkis and Riegl 2005), and texture-based classification methods (Purkis *et al.* 2006), among many others (Mumby *et al.* 2004; Riegl and Purkis 2005; Purkis 2005; Wang *et al.* 2007; Wongprayoon *et al.* 2007; Vela *et al.* 2008; Rowlands *et al.* 2008).

Fewer studies involving coral reef mapping have been published using QuickBird data than IKONOS, however, the similarities between these satellite sensors, such as bit-depth and band width, enables users to apply analogous image processing techniques to yield comparable results (Rowlands *et al.* 2008). Mishra *et al.* (2006) and Benfield *et al.* (2007) independently assessed the ability of QuickBird imagery to map coral reef habitats.

Mishra *et al.* (2006) focused on the utility of QuickBird imagery for identifying and classifying tropical-marine benthic habitats after applying atmospheric and water column corrections to two scenes of Roatán, Honduras. Groundtruth points were used to evaluate the final classification, yielding an overall accuracy of 81%, which suggested that QuickBird data are well-suited for coral reef mapping.

Benfield *et al.* (2007) also proved that QuickBird data produce high-quality thematic maps by generating accuracies >80%, an acceptable threshold for inventory and baseline habitat mapping purposes within the marine environment.

1.5 Coupling thematic habitat maps with digital elevation models

Landscapes are composed of clusters, or patches, of interacting habitats that contain structure, function, and change (Urban *et al.* 1987). The extents of biological habitat patches and three-dimensional geomorphological features underlying biological cover can be analyzed in a GIS framework. Concurrently analyzing benthic cover data with bathymetric data provides a more realistic representation (vs. a 2-D map) of habitat complexity by taking the vertical relief component into account. Moreover, a growing

body of data suggests that the underlying geology and geomorphology of marine environments dictates the location of critical life habitat for many marine species (Wright and Heyman 2008; Walker *et al.* 2008).

Riegl *et al.* (2008) linked a digital elevation model to benthic cover transects to understand the status of coral reefs around Vieques, Puerto Rico and St. Croix, U.S. Virgin Islands. The main objectives accomplished in this study were to describe the geomorphology of the two reef systems, investigate community-level zonation, and compare the variability of assemblages between study sites.

A study by Hogrefe *et al.* (2008) involved coupling DEMs from land and sea, providing a great example of future applications of DEMs in coral reef management. Conceivably, a next step may be to combine terrestrial land-use maps and marine benthic habitat maps with a seamless land-sea DEM for quantifying anthropogenic inputs to downstream reef communities.

1.6 Utility of habitat maps: marine protected area design and modeling

Information extracted from habitat maps following GIS analysis can be used in conservation management and reserve design or provide input metrics for ecological models that predict coral reef community compositions (Garza-Pérez *et al.* 2004; Langmead and Sheppard 2004) and/or reef fish assemblages (Arias-González *et al.* 2006; Purkis *et al.* 2008; Grober-Dunsmore *et al.* 2008a; Grober-Dunsmore *et al.* 2008b; Pittman *et al.* 2009).

The size and spatial arrangement of habitat patches in a reefscape exert a strong influence on movements of many organisms, which in turn, can affect patterns of organism abundance and distribution (Grober-Dunsmore *et al.* 2007). Marine protected area effectiveness is contingent on understanding key ecological patterns and processes at appropriate spatial scales and may depend upon maintaining critical linkages among essential habitat patches to conserve reef fish communities (Grober-Dunsmore *et al.* 2007; Cassata and Collins 2008; Grober-Dunsmore *et al.* 2008a).

The utility of proxies for measuring biodiversity and species abundance in tropical marine environments is appealing for marine conservation and has recently been investigated using benthic cover maps. Examples of information that can be extracted

from these maps are habitat diversity (Mumby 2001) and beta diversity (Harborne *et al.* 2006), which is a measure of biodiversity. The concept that species diversity increases with increasing landscape heterogeneity has been established in terrestrial systems, yet applying this idea to marine ecosystems is a very recent venture in marine spatial planning. Maps of beta diversity can be incorporated into conservation planning by identifying areas with a high diversity of contrasting habitats at a given spatial scale (Harborne *et al.* 2006).

To date, relationships between habitat patterns are poorly understood in reef ecosystems and limited quantitatively-derived spatial information is available to incorporate into conservation planning. Hence, the goal of this project is to measure repeating spatial patterns at multiple scales and to explain the environmental mechanisms which have formed the observed patterns. This research is a step towards establishing a knowledge base of coral reef ecosystems, which is necessary for enacting management decisions in a spatial setting, particularly in marine protected areas. Terrestrial reserves are usually designed from a landscape ecology perspective; considering the successes in protecting natural areas on land, a similar perspective would be beneficial in reefscape management.

2. METHODS

2.1 Study Sites

Sites were chosen for investigation based primarily on the diversity of reefal structures and secondarily on the accessibility of satellite imagery, bathymetry, and groundtruth data. Upon meeting the desired requirements, three sites were chosen from data archives: Vieques, Saipan, and Andavadoaka. The latter site was significant in that the final map product was used in designing the Velondriake marine protected area (Figure 5), which is later discussed in detail. Each study site location is shown in Figure 1 and a detailed summary of data attributes is listed in Table 1.

Table 1: Study sites summary: data attributes (grey) and environmental characteristics (green).

	<i>Saipan, CNMI</i>	<i>Vieques, PR</i>	<i>Andavadoaka, MG</i>
Multispectral satellite imagery source	IKONOS (GeoEye)	IKONOS (GeoEye)	QuickBird (DigitalGlobe)
Spectral resolution (nm)	B1: Blue (445-516) B2: Green (506-595) B3: Red (632-698) B4: NIR (757-853)	B1: Blue (445-516) B2: Green (506-595) B3: Red (632-698) B4: NIR (757-853)	B1: Blue (450-520) B2: Green (520-600) B3: Red (630-690) B4: NIR (760-900)
Spatial resolution (m)	4	4	2.44
Radiometric resolution	8-bit (256 hues)	11-bit (2048 hues)	8-bit (256 hues)
Coordinate system	UTM	UTM	UTM
Datum	WGS84	WGS84	WGS84
Grid zone	55N	20N	38S
DEM source	LiDAR	LiDAR	Acoustic soundings
DEM resolution (m)	4	4	4
Area analyzed (km ²)	64.5	294.6	157.7
# of habitats mapped	13	8	13
# of habitats analyzed	10	8	10
MMU (m ²)	16	16	5.95 resampled to 16
MMU analyzation threshold (m ²)	64	64	64
Tidal phase/range	diurnal, 0.40 m	semi-diurnal, 0.46 m	semi-diurnal, 2.60 m
Current direction	W	W-NW	NE
Dominant wind direction/speed	E-NE trade winds avg = 15.0 knots	E-NE trade winds avg = 19.4 knots	SW avg = 7.6 knots
Location of maximum wave action	northern side of island and barrier reef crest	eastern point of island	southwest facing reefs
Storm frequency/type	tropical storms and typhoons = 3 every 5 years	tropical storms = 1 every 5 years hurricanes = 1 every 11 years	3-4 major cyclones per year (usually strike east coast, occasionally west coast)
Climate	tropical-marine rainy season Jul-Oct annual rainfall ≈ 80 in. (203.2 cm) avg air temp = 82°F (28°C)	tropical-marine rainy season Aug-Nov annual rainfall ≈ 45 in. (114.3 cm) avg air temp = 80°F (27°C)	monsoonal rainy season Nov-Apr annual rainfall ≈ 16 in. (41.8 cm) avg air temp = 76°F (24°C)
Land attached or isolated	attached	attached	attached
Holocene reef thickness	6 – 14 m	8 – 12 m	12.9 – 13.4 m
Reef system	well developed barrier reef, partially developed fringing reef, small patch reefs	Fringing reefs, backstepping system	well developed fringing reefs, large offshore isolated platforms
River inputs	3 rivers drain into the Tanapag, most rivers drain off the east coast	4 streams in the northeast, a few unnamed ephemeral creeks on the south coast	absent, closest river outlet is 100 km away

2.1.1 Vieques, Puerto Rico

Site Information

The island of Vieques (Figure 2) lies off the eastern coast of Puerto Rico, with central coordinates of 18°7' N, 65°25' W. Vieques (135 km²) was formerly controlled by the U.S. Navy for 60 years as a live munitions target range. In May 2001, authority was transferred from the Navy and a portion of the west end of the island was administered as the Vieques National Wildlife Refuge under the protection of the U.S. Fish and Wildlife Service. In May 2003, the eastern end of Vieques was added to the wildlife refuge making the total protected land area ~73 km². However, a 900-acre portion of the eastern component is considered contaminated from former bombing activities and is closed off. The Navy's presence for so many years left the surrounding marine ecosystems relatively unaffected by human influences because of limited coastal development and its associated runoff (Riegl *et al.* 2008). For this reason, scientific interests in the marine realm have followed the establishment of the refuge; mapping efforts have been conducted by NOAA's Biogeography Team in 2001 and Riegl *et al.* (2008).

Eight IKONOS multispectral scenes of Vieques were provided by NOAA and groundtruthing was funded and gathered by NCRI in June 2005. The groundtruth expedition involved spot-checks of benthic habitats, which were performed with a differential GPS along the southeast coast (Figure 3). LiDAR data were acquired for the coastal region of Vieques in 2001 by the U.S. Army Corps of Engineers and the Joint Airborne LiDAR Bathymetry Technical Centre of Expertise. These data were collected with 400 laser pulse soundings per second and to an extent of 2000 m offshore or to a depth of 30 m using the Scanning Hydrographic Operational Airborne LiDAR System. Appendix II-A shows the DEM derived from LiDAR points and Appendix I-A provides the final habitat map and key for Vieques.

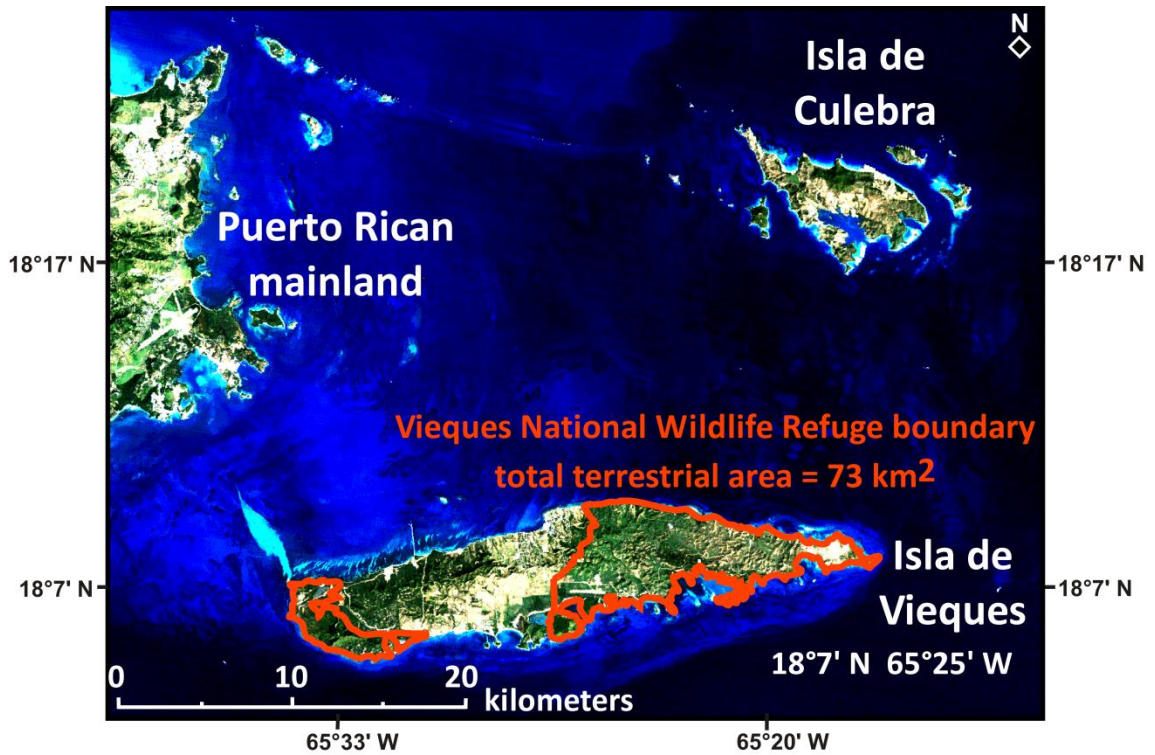


Figure 2: 1985 Landsat MSS image of Vieques with georeferenced red polygons showing the boundary of the Vieques National Wildlife Refuge.

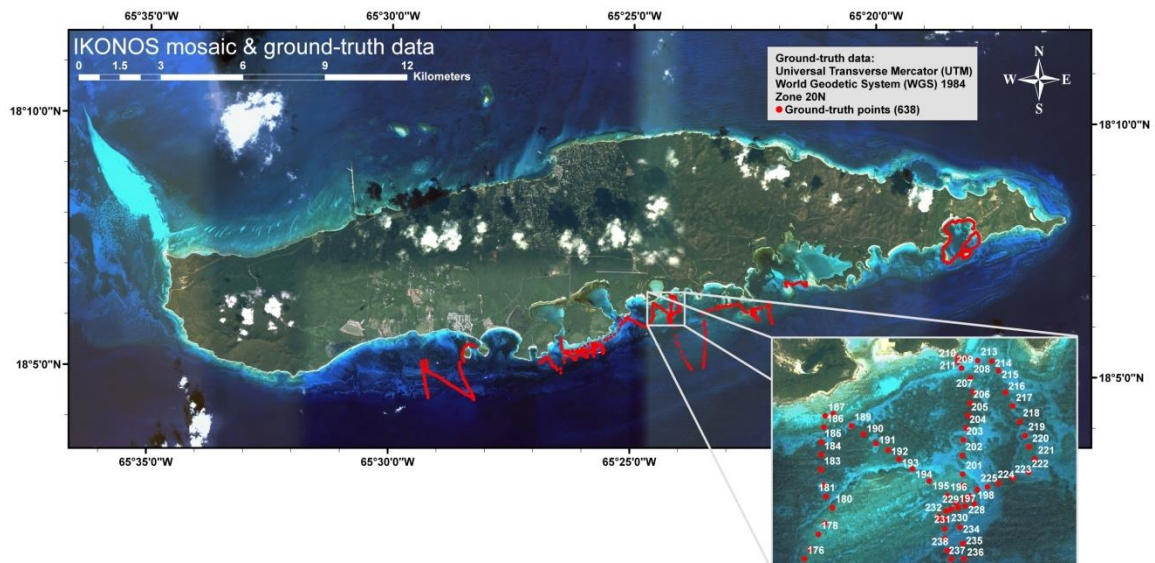


Figure 3: Geospatial representation of Vieques groundtruth points (red).

Geological Background

Vieques is an emergent formation positioned on the southeastern edge of the Puerto Rico-Hispaniola microplate, a stable block within the broad zone of strike-slip and oblique subduction between the North American and Caribbean plates (Byrne *et al.* 1985). The northern edge of the microplate is constrained by the Puerto Rico trench, while the southern edge of the microplate is bounded by the Muertos Trough (van Gestel *et al.* 1999). To the east, the Puerto Rico-Hispaniola microplate is bordered by the Anegada Passage fault zone and to the west the microplate ends near central Hispaniola (van Gestel *et al.* 1999).

Vieques is composed of Cretaceous to Eocene-aged intrusive rocks (Figure 4) that formed when Puerto Rico, Vieques, and the Virgin Islands were part of an active subduction zone (van Gestel *et al.* 1999). The igneous rocks were overlain by limestone creating the Puerto Rico-Virgin Islands platform between the Oligocene (30 Ma) and the early Pliocene (4 Ma) (van Gestel *et al.* 1999). This platform, a carbonate sedimentary structure built on arc basement, was then tilted and uplifted between the Pliocene and the Holocene, leading to the exposure of Puerto Rico, Vieques, and the Virgin Islands. As a result, the rocks of Vieques are composed of arc basement with carbonate sedimentary facies that have been eroded throughout the Holocene. These exposed rocks weathered to produce alluvium deposits along the coasts (Figure 4) with muddy bays supporting dense mangrove swamps.

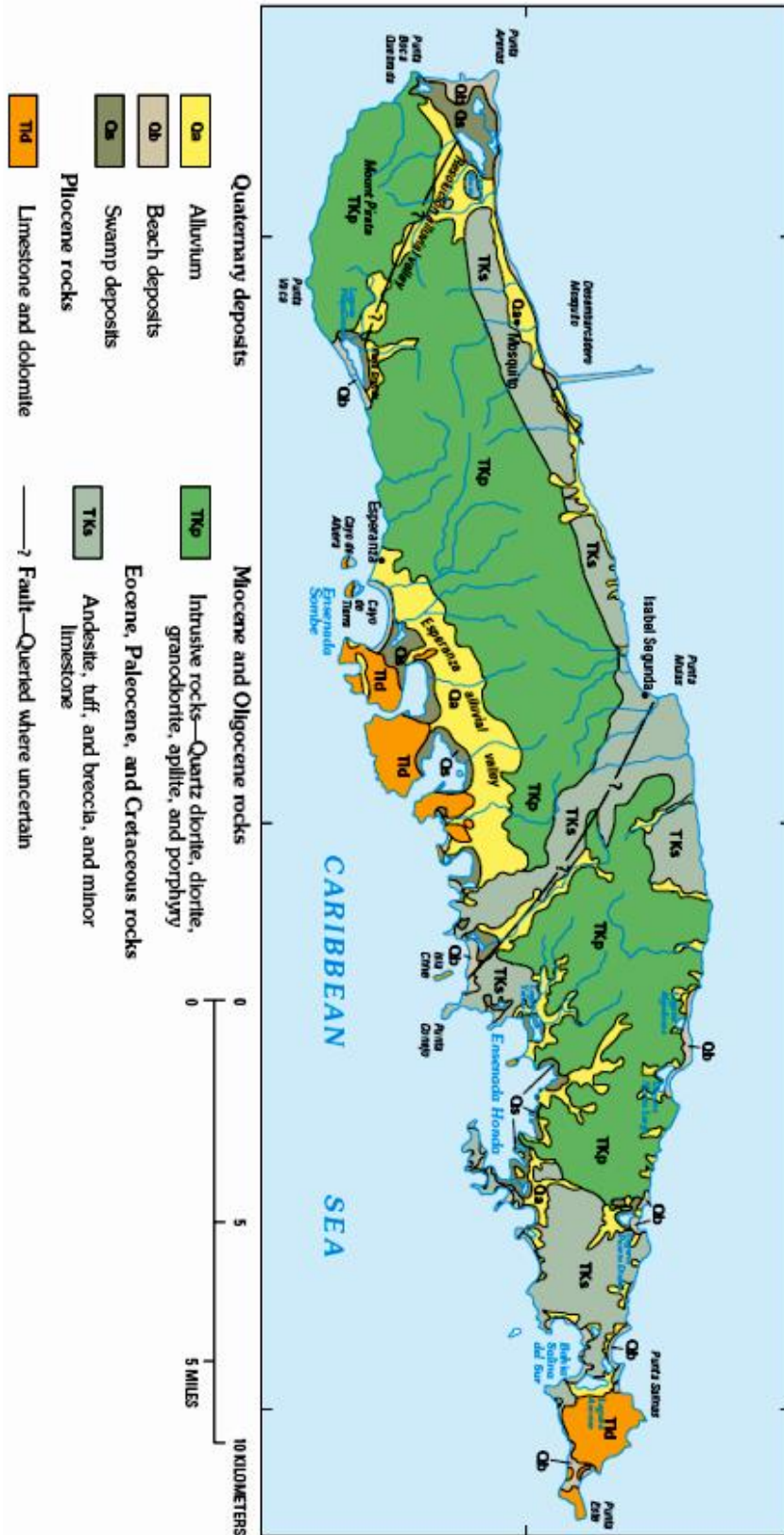


Figure 4: Vieques surficial geology map from Renken *et al.* (2002), modified from Briggs and Ackers (1965) and Learned *et al.* (1973).

Sea-level was the major driver in reef development around Vieques. Throughout the Holocene transgression, rising sea-level caused reef backstepping to generate three distinct reef zones along the southern coast including the shelf-edge reef, mid-shelf reef, and fringing reef (Riegl *et al.* 2008). However, along the northern coast, the shelf-edge reef is totally absent and the mid-shelf reef is only moderately developed in the northeast. The disparate reef profiles along the north and south coasts are the product of differing bathymetry (Riegl *et al.* 2008). As sea-level rose, the shelf-edge reefs (20 m deep) and the mid-shelf reefs (10 m deep) in the south initiated on steep slopes, while the flat shallow platform in the north was yet to be flooded. The discontinuous fringing reef (2-5 m deep) grew last and is clearly well-developed around headlands where runoff and sedimentation are lowest (Riegl *et al.* 2008). Between the three reef tracks of the south exist gently sloping platforms; the lower platform (flanked by the shelf-edge reef and the mid-shelf reef) is filled with unconsolidated sand sheets and the upper platform (flanked by the mid-shelf reef and the fringing reef) is partially covered by sand yet has exposed hardgrounds which provide suitable substrates for benthic sessile organisms. Seaward of the fringing reef of the north, the shallow platform is covered with a layer of unconsolidated sand that provides ideal conditions for vast seagrass beds to grow.

2.1.2 Andavadoaka, Madagascar

Site Information

Andavadoaka (Figure 5) is located on the southwest coast of Madagascar (22°4' S and 43°14' E). Blue Ventures, a UK-based NGO, commissioned Nova Southeastern University's (NSU) Remote Sensing Lab for the production of a marine habitat map to facilitate management of the Velondriake MPA.

Three geometrically corrected QuickBird images of the region were provided by Blue Ventures, as well as manta-tow data and diver surveys. Groundtruthing was funded by NSU's Remote Sensing Lab and conducted in 2008. A tethered video camera, differential GPS, and acoustic single-beam depth sounder, with an acquisition rate of 3 Hertz, were utilized to collect groundtruth data. The acoustic soundings were used to tune a model of spectral bathymetry (Figure 11); this process is further detailed in the data

processing section below. Appendix II-B shows the DEM derived from the acoustic soundings.

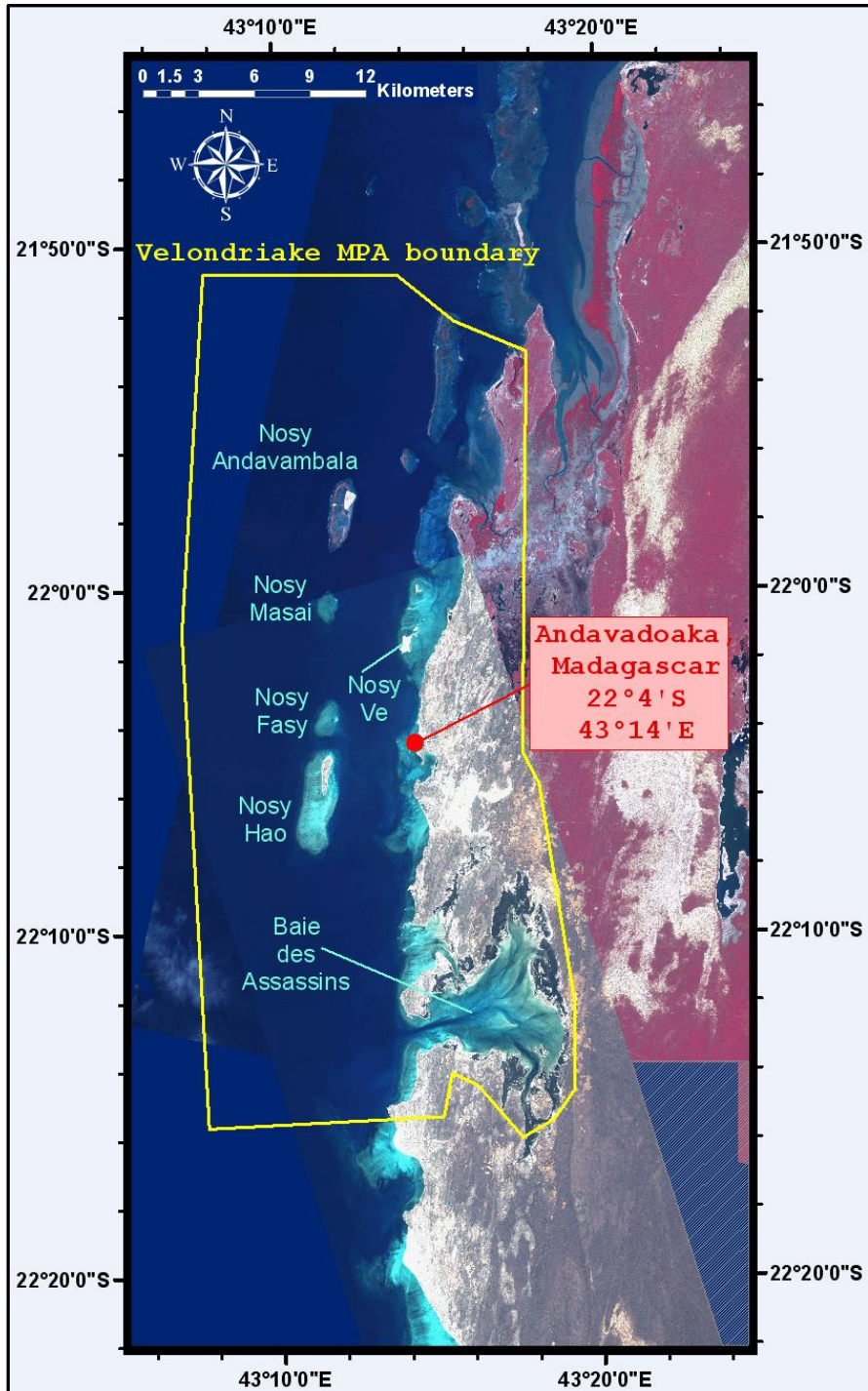


Figure 5: Andavadoaka region with the Velondriake MPA boundary shown. This figure consists of 2 images: a northern SPOT (Satellite Pour l'Observation de la Terre) scene and a southern QuickBird scene. In the SPOT scene (20 m spatial resolution), vegetation appears red because the satellite lacks a blue band, which results in a false color composite.

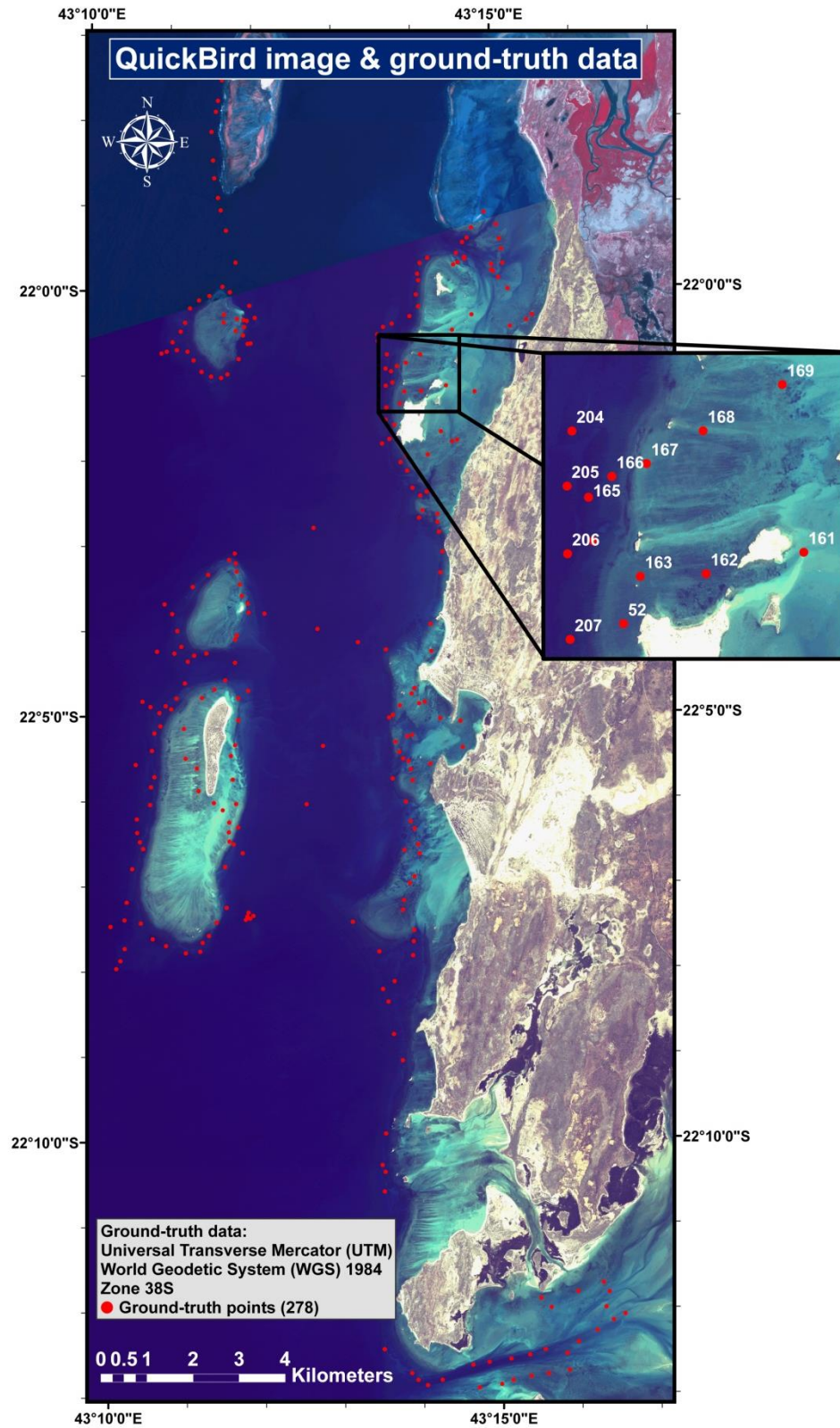


Figure 6: Andavadoaka QuickBird image with groundtruth points (red) plotted.

The collaboration between NCRI and Blue Ventures was an effort to map and inventory essential habitats in a region where marine conservationists required geospatial information to make decisions regarding the location of the Velondriake MPA (Figure 5). The success of the MPA provides a model of how a community-based organization can empower people to live sustainably. Effective ecosystem management requires not only that we recognize essential habitat types, but that we strive to maintain the functional linkages among habitats that underlie ecosystem health and integrity (Grober-Dunsmore *et al.* 2007). The purpose of the Velondriake MPA is to protect marine and coastal biodiversity, while promoting sustainable management of resources and economic development. The reserve, which spans 800 km² and benefits more than 10,000 people, protects coral reefs, mangroves, seagrass beds, baobab forests and other threatened habitats (Velondriake 2008). Population increase and commercially-exploited fisheries have threatened the livelihoods of the local Vezo people, who depend upon marine resources for food, transport, and trade. The Vezo, or “people of the sea”, have adopted sustainable fishing practices, such as no-take zones and seasonal restrictions for octopus, their main economic resource. With the help of conservationists, villagers are also implementing ecotourism businesses and developing mariculture for sea cucumbers, algae, and seaweed (Velondriake 2008).

The MPA was so successful that the president of Andavadoaka was honored with the J. Paul Getty Award for outstanding contributions to international conservation. Eight neighboring villages instituted their own protected areas for octopus in order to reap similar benefits and the national government of Madagascar used the project as a model to create similar seasonal closures across the country. The project is a proven example of how economic development can be balanced with conservation of natural resources (Velondriake 2008).

Appendix I-B shows the map and habitat key, both of which were produced for MPA management and for this study of reefscape spatial patterns. Partners involved with reserve design and implementation of conservation strategies were NCRI, Blue Ventures, Madagascar’s Institute of Marine Sciences, the Wildlife Conservation Society, and local Madagascan villages.

Geological Background

Madagascar is a large block of continental crust intermittently uplifted during the Permian Period (250 Ma) as a complex horst between two subsiding depressions within a system of N-NE trending fractures in the Indian Ocean floor (Kutina 1975).

Approximately 160 Ma the Indian subcontinent and Madagascar split from Gondwana. Between 80-100 Ma, Madagascar separated from the Indian subcontinent. The island is now part of a large plateau that is inclined westwards towards the Mozambique Channel (Rogers 1998).

The island's metamorphic and igneous core of intensely deformed granite and gneiss rises along a N-NE aligned linear dome of nearly 2700 meters high (Besairie 1964). The next younger rocks are the Mesozoic (Cretaceous) sedimentary rocks that lie on a belt nearly 150 km wide and run along the western coast about 100 km inland (Figure 7). During the Tertiary, another belt of limestone was deposited, appearing westward of the Mesozoic belt. The west coast of Madagascar is generally composed of unconsolidated sands with intermittent portions of alluvial and lake deposits as well as mangrove swamps (Figure 7). The southwest coast is dominated by vast sandy beaches and barrier islands (Velondriake 2008).

A great asymmetry exists between Madagascar's two coasts. On the east coast, the continental shelf is very narrow, dropping off to 100 meters in depth between 5-8 km from shore, leading to poor development of coral reefs and mangroves (Gabrie *et al.* 2000). The west coast has a much broader continental shelf, ranging from 50-100 km offshore, which is home to the majority of the country's coral reef formations and mangroves (Gabrie *et al.* 2000).

Andavadoaka's well developed fringing reefs are the northern end of a 350 km-long reef system, the third largest continuous reef system in the world (Velondriake 2008). The fringing reef system is separated from land by a shallow lagoon, a few hundred meters wide (Nadon *et al.* 2005).

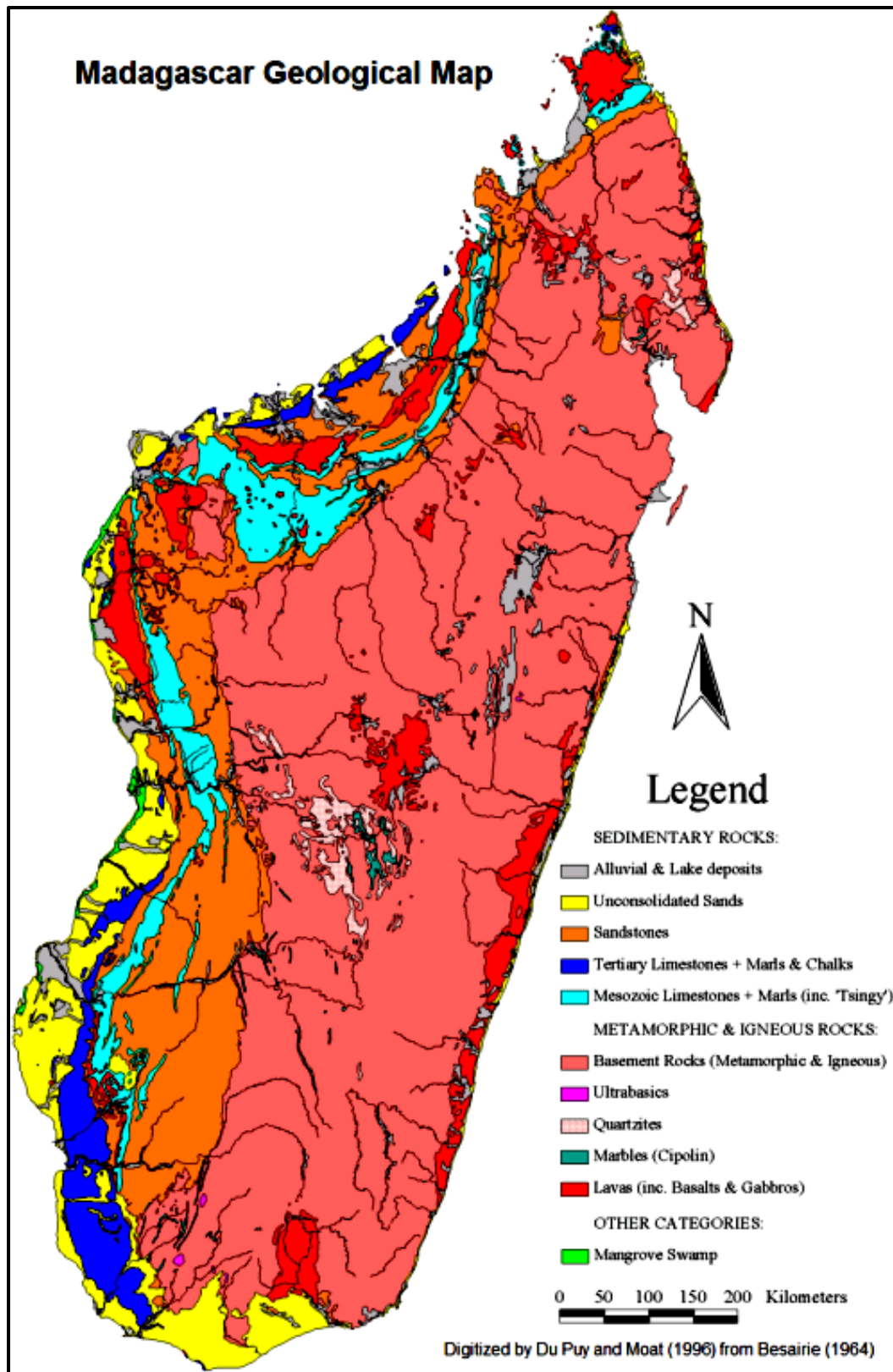


Figure 7: Madagascar surficial geology map digitized by Du Puy and Moat (1996) from Besairie (1964).

2.1.3 Saipan, Commonwealth of the Northern Mariana Islands

Site Information

Saipan (Figure 8), located north of Guam in the western Pacific, is the largest island and capitol of the U.S. Commonwealth of the Northern Mariana Islands (CNMI), a chain of 14 islands in the Mariana Archipelago. Saipan, located at 15°11'14" N, 145°44'45" E, has a coastline that spans 87 km in perimeter and a total land area of approximately 120 km². A large barrier reef system is located on the western side of the island, while the remaining coastline is surrounded by a narrow fringing reef. Saipan's coral reefs are considered to hold the highest biological diversity within the CNMI. As a result, seven marine conservation regions have been designated in coastal waters including: Mañagaha Marine Conservation Area (5 km²), Lighthouse Reef Trochus Reserve (1.1 km²), Laulau Bay Sea Cucumber Reserve (2 km²), Forbidden Island Marine Sanctuary (2.5 km²), Tank Beach Trochus Reserve (0.2 km²), and Bird Island Marine Sanctuary (1.5 km²). Saipan also protects a portion of land entitled Bird Island Wildlife Conservation Area (3.2 km²). Figure 8 shows the georeferenced boundary polygons of the island's MPAs and wildlife conservation area.

IKONOS images and LiDAR were provided for this site by NOAA and groundtruth data (Figure 9) were downloaded from the NOAA Biogeography Program's website for CNMI mapping (http://ccma.nos.noaa.gov/products/biogeography/us_pac_terr/htm/data.htm). Appendix I-C gives the final benthic habitat map and key produced for Saipan, in addition, the DEM derived from LiDAR is shown in Appendix II-C.

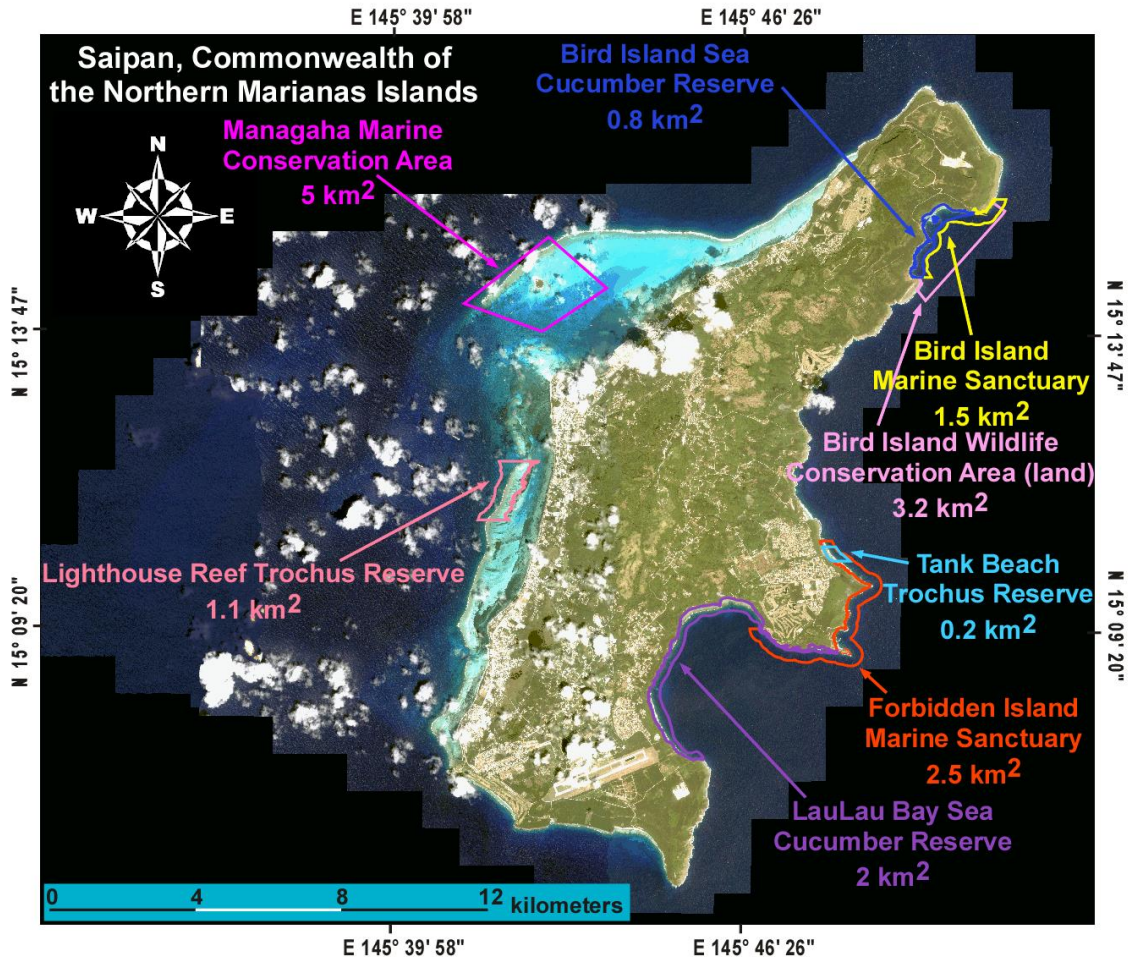


Figure 8: IKONOS mosaic of Saipan, CNMI. Georeferenced marine (7) and terrestrial (1) conservation boundary polygons are shown (MPA data downloaded from http://www.mpa.gov/helpful_resources/inventory.html).

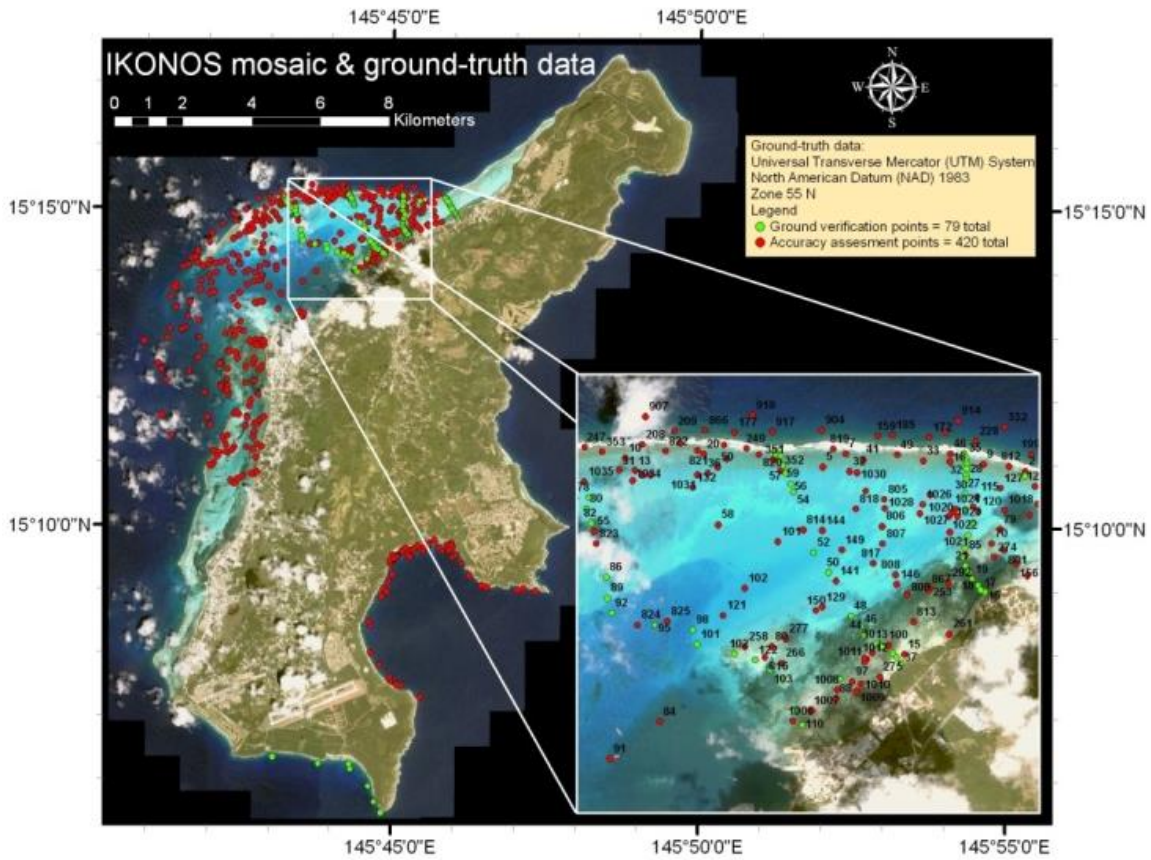


Figure 9: IKONOS mosaic of Saipan with groundtruth points (red and green) plotted.

Geological Background

In the western Pacific Ocean, the oceanic Pacific plate subducts below the oceanic Philippine Sea plate in a northwestward direction at a rate of 9 cm/yr forming the deep Mariana Trench and the Mariana Islands in a classic case of island arc volcanism. As the subducting slab is geothermally heated, loss of water induces partial melting of the overriding mantle and generates low-density magma that buoyantly rises through the lithosphere. The magma bursts through fractures in the seafloor, spewing pillow lava, which slowly accretes into distinct volcanoes for millions of years. When these oceanic volcanoes breach the sea-surface, islands are born along the arc system.

The Mariana Island arc system can be separated into two geologically defined regions: the younger northern island arc (≈ 5 Ma) and the older southern island arc (≈ 40 Ma), which boasts more developed reef systems. Saipan is among the southern islands (Rota, Tinian, and Farallon de Medinilla) and its extensive barrier reef system lies along the northwestern side of the island.

The oldest igneous rocks of Saipan (Figure 10), known as the Sankakuyama Formation, date back to the late Eocene age (41 Ma) and are composed of dacitic tuffs, breccias, and flow rocks (Riegl *et al.* 2008). These rocks represent a remnant volcanic cone that formed the base unit of Mount Achugao. Throughout the Eocene, two more igneous rock layers were laid down, including the andesitic tuff, breccia, and lava flows of the Hagman Formation and the marine transitional rocks, volcanogenic sediments, and andesitic breccias of the Densinyama Formation. The Fina-Sisu Formation of middle Miocene age (13 Ma), consisting of calcareous marine tuffs and andesitic flow rocks, was the last igneous layer to be deposited.

Following the cessation of the active volcanic period of Saipan, multiple limestone units (Figure 10) were constructed during sea-level fluctuations and local tectonic uplift events. The limestone stratigraphic sequence resting atop volcanic rocks began with the very old Tagpochau Limestone (Miocene), followed by the Mariana Limestone (Pliocene), the Tanapag Limestone (Pleistocene - Holocene), and alluvium deposits (Pleistocene - Holocene) derived from erosive weathering processes represent the youngest layer.

The Tanapag Limestone is a fringing reef that grew around Saipan during the Pleistocene and Holocene, which corresponds to the last major inter-glacial stage (Cloud 1959). After this reef-building period, the alluvium deposits formed the western coastal plain of Saipan. The modern reef began accreting 2.8 ka and likely began growing on the Mariana Limestone framework. According to Riegl *et al.* (2008), the disappearance of the Mariana Limestone under the Tanapag Lagoon is possibly due to a slumping event that occurred along the fault lines (SW-NE strike) of the west coast prior to modern reef growth. Therefore, the lagoonal rim (barrier reef) of Saipan is structurally controlled by the extent of the Mariana Limestone and the surficial fill within the lagoon is comprised of alluvium deposits (Figure 10).

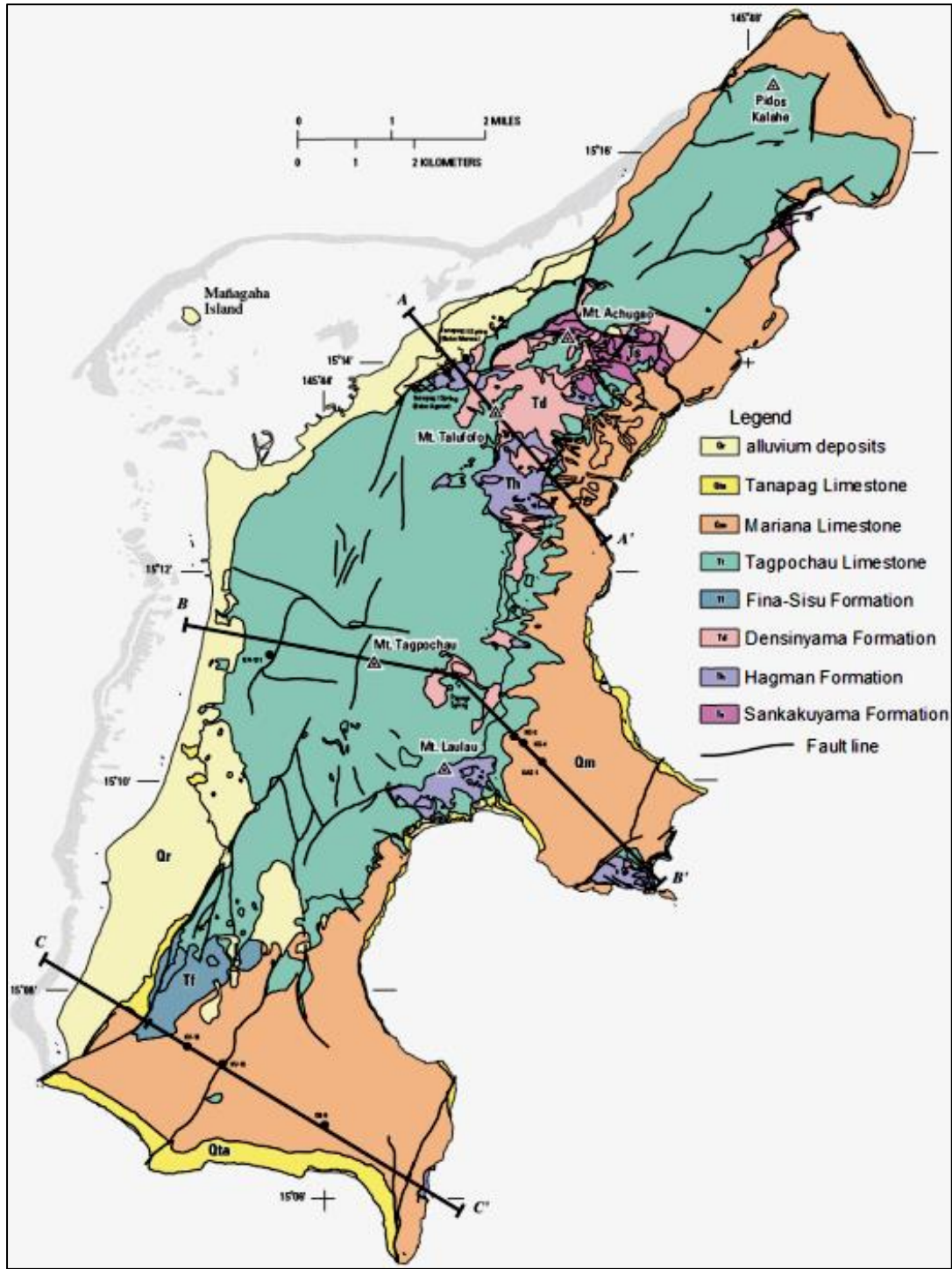


Figure 10: Saipan surficial geology map (USGS map modified from Cloud *et al.* (1956) and available: <http://pubs.usgs.gov/wri/wri034178/pdf/fig04a.pdf>). The grey reef outline is likely a continuation of the Mariana Limestone that slumped during a tectonic event and provided antecedent topography for the modern barrier reef to grow upon. The fault lines along the extent of the alluvium deposits would be the boundaries of the slumped block.

2.2 Data processing

Data were processed and analyzed using ENVI 4.5, ENVI Zoom 4.5, Global Mapper v9.03, Matlab 7.4, Canvas X, Excel 2007, and ArcGIS 9.2. Figure 12 is a diagram showing the progression from data collection to the final output product.

The sequence of data processing began with the generation of georeferenced mosaics for each of the three study sites using QuickBird and IKONOS images. Land features and clouds were masked using thresholds in the near-infrared band, while optically deep waters with no returning spectral reflectance were masked using image enhancement and digitization.

Sun glint was removed from the imagery when wave patterns posed significant problems by reflecting light directly towards the sensor's instantaneous-field-of-view. This sea surface roughness correction was applied using Matlab with the methodology from Hedley *et al.* (2005), a revision of Hochberg *et al.*'s (2003) technique. The correction algorithm assumes zero water-leaving radiance over optically deep waters in the NIR band and the relative amount of radiance reflected from the surface is only a function of geometry, independent of wavelength. Therefore, glint contribution is present in all bands, visible and NIR. By identifying deep water pixels with maximum and minimum values in the NIR band, the glint contribution was calculated and then subtracted from each visible band to produce a deglinted image.

Unsupervised spectral classifications were performed in ENVI using the ISODATA algorithm. This function calculates class means evenly distributed in the data space, then iteratively clusters the remaining pixels using minimum distance techniques. Each iteration recalculates means and reclassifies pixels with respect to the new means until the maximum number of iterations (set to 300) is reached.

A 3x3 pixel median filter (moving window) effectively reduced noise in the classifications before they were processed in Canvas X, an image editing and illustration program with GIS extensions.

Bathymetry was derived for Andavadoaka from *in situ* acoustic surveys. The ratio transform method described by Stumpf *et al.* (2003) was employed to estimate depth values for each pixel in the multispectral image. This non-linear log band ratio model was empirically tuned with the acoustic depth soundings to yield a DEM. Figure 11 gives the

relationship between the actual depth soundings (Z_{actual}) and pseudo-bathymetry (Z_{pseudo}). Pseudo-bathymetry is a unitless band ratio calculated from a multispectral image using the equation below, where b_1 = blue band, b_2 = green band.

$$Z_{\text{pseudo}} = \frac{\text{Log}(b_1)}{\text{Log}(b_2)}$$

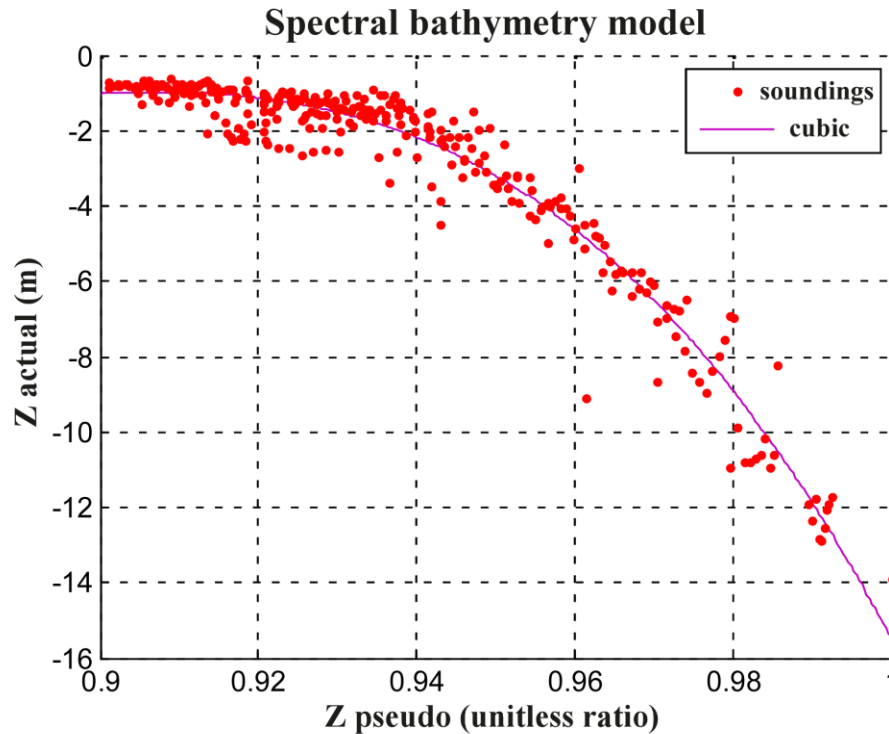


Figure 11: The Stumpf *et al.* (2003) model compared pixels in a pseudo-bathymetry image to *in situ* depth soundings located in the exact same geographical positions. Cubic regression was used to build an equation that was applied to every pixel in the image; the product of which was a DEM for Andavadoaka.

LiDAR surveys for Vieques and Saipan were interpolated in ArcGIS using the natural neighbor algorithm to output a DEM. Natural neighbor interpolation finds the closest subset of input samples to a query point and applies weights to them based on proportionate areas in order to interpolate a value (Sibson 1981).

Groundtruth points and DEMs were utilized in concert with mosaics and classification polygons to digitize ecological habitat classes into resultant thematic maps. During the digitization process, ambiguous deep features in mosaics were stretched using histogram enhancements, primarily in the blue band. Although light penetration through the water column is sufficient for deep (> 40 m) corals to survive, the amount of light

returning from such depths is insufficient for feature discrimination in satellite imagery. For this reason, habitats in shallow depths, where adequate light existed to discriminate bottom features, were mapped using satellite imagery. Deeper bottom features and patches of unknown composition were mapped using the digital elevations models. For example, a dark colored patch without groundtruth data may be visually perceived from a satellite image as an aggregate reef, but a DEM could confirm that the patch has no vertical relief. Thus, an aggregate reef is ruled out and the patch is assumed to be composed of seagrass or algae. Further investigation into the texture and boundary of the patch would confirm its vegetation composition for classification into the correct habitat category.

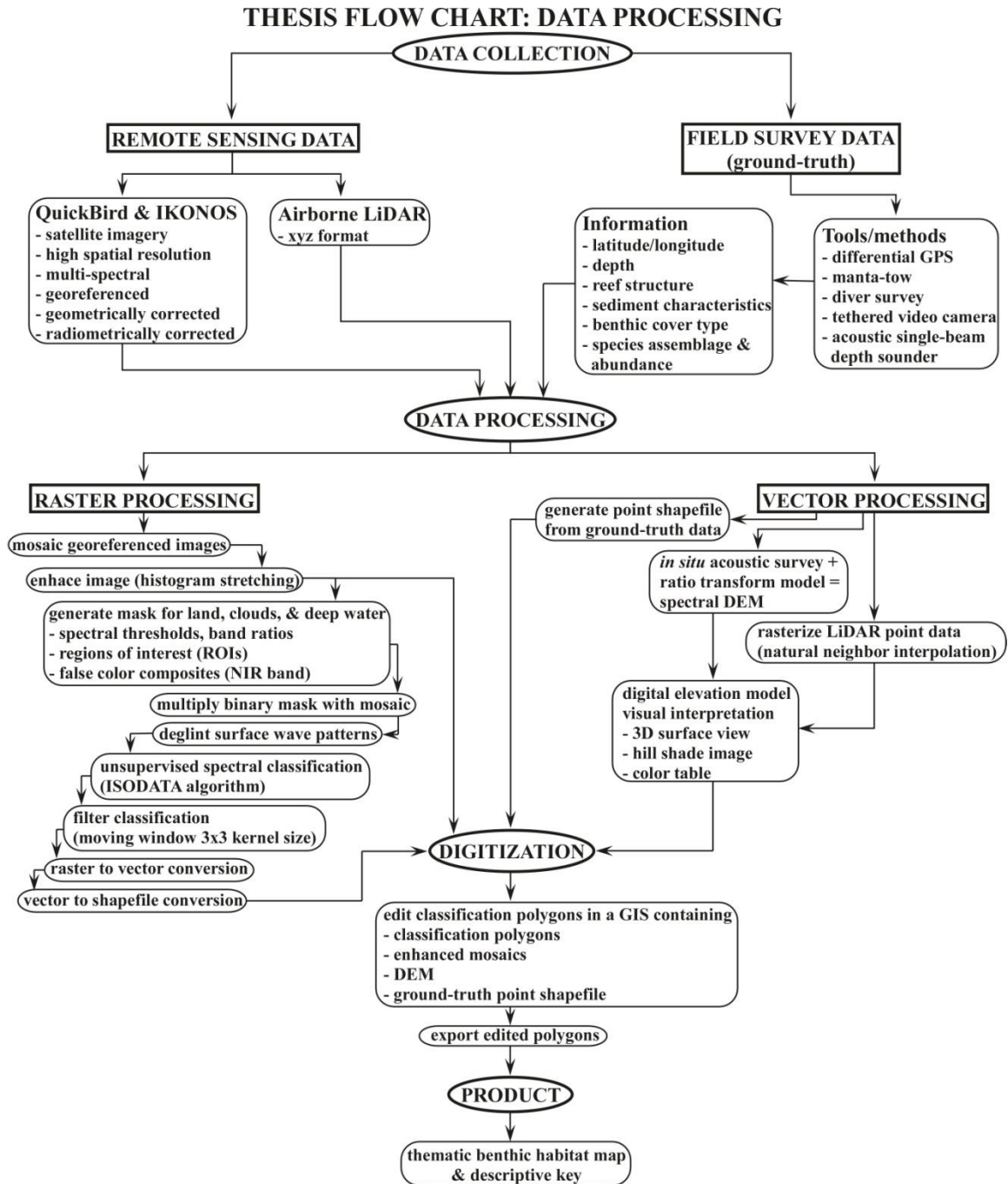


Figure 12: Flow chart showing the sequence of data processing techniques used to produce benthic habitat maps.

2.3 Morphometric calculations

A suite of morphometrics were calculated for polygons from each class in each benthic habitat map to assess patch characteristics, spatial patterns, and three-dimensional relationships. A database was compiled from these metrics and a subsequent analysis was completed to compare inter- and intra-reef characteristics.

The patch metrics calculated included: perimeter (m), area (m²), centroid (*i.e.* the geometric center of the patch) location (easting, northing), exceedance probability (*EP*), compactness, principle axes ratio (*PAR*), fractal dimension (*D_B*), and fractal span (*D_S*).

Exceedance probability (*EP*) was calculated for each patch using the following equation:

$$EP = \frac{m}{(n + 1)}$$

where *m* = the rank number from largest area to smallest area and *n* = the number of polygons. *EP* represents a cumulative probability $EP[X \geq x]$ that a given patch area *X* has an area equal to or larger than *x*. In other words, the data plotted on *EP* figures represent the probability (y-axis) that a given patch will be of area equal or greater than a given area (x-axis) (Rankey 2002).

Compactness was calculated to facilitate the analysis of systematic trends in the geometric shape of habitat patches. Compactness is the ratio of the perimeter of a circle, with equal area to a given polygon, to the perimeter of the polygon. Measures of compactness range from 0 to 1, with values closer to 0 representing elongate shapes and values closer to 1 representing circular shapes (Peura and Iivarinen 1997). The equation below gives the calculation of compactness, where $A = A_{circle} = \pi * r^2$ and *r* equals the radius of the circle.

$$compactness = \frac{P_{circle}}{P_{polygon}} = \frac{2\sqrt{A\pi}}{P_{polygon}}$$

The principle axes ratio (*PAR*) is a ratio of the longest segments of lines that cross each other orthogonally at the centroid of the patch (Purkis *et al.* 2007) and therefore those lines represent the directions with zero cross-correlation (Peura and Iivarinen 1997). The ratio of principle axes can be calculated from the covariance matrix (*C*) of a polygon contour. The lengths of the axes are equal to the eigenvalues (*i.e.* roots of the

eigenvectors) of the covariance matrix. These eigenvalues represent the maximum and minimum variance of the polygon contour and taking the ratio of these yields *PAR*. The actual calculation of eigenvectors and eigenvalues is not necessary. Values of *PAR* range from 0 to 1 in a similar manner to compactness values (Peura and Iivarinen 1997); with 0 corresponding to elongate shapes and 1 denoting circular shapes.

$$C = \begin{pmatrix} c_{xx} & c_{xy} \\ c_{yx} & c_{yy} \end{pmatrix}$$

$$PAR = \frac{c_{yy} + c_{xx} - \sqrt{(c_{yy} + c_{xx})^2 - 4(c_{xx}c_{yy} - c_{xy}^2)}}{c_{yy} + c_{xx} + \sqrt{(c_{yy} + c_{xx})^2 - 4(c_{xx}c_{yy} - c_{xy}^2)}}$$

The fractal dimension (D_B) of each polygon was calculated with the box-counting method (Turcotte 1989; Schlager 2004). Fractal dimension is a measure of shape complexity and ranges from 1 for simple shape boundaries to 2 for very intricate shape boundaries. Box-counting refers to an iterative process where a series of grids are systematically laid over an object and the number of boxes in the grid that intersect the object's boundary are counted. During each iteration, the grid becomes finer, the size of the boxes (side = δ) decreases, and the number (N) of boxes intersecting the boundary increases. If N increases proportionally to the reduction in δ (for ≥ 3 orders of magnitude), the relation is considered a power function and the boundary is inferred to be fractal (Purkis 2005). The box-counted fractal dimension is equal to the slope of the regression line in a bilogarithmic plot of N versus $1/\delta$.

The number of box-reduction *cycles* over which δ decreases in proportion to increasing N is referred to as the fractal span (D_S) (Purkis 2005). Fractal span is therefore the number of iterations completed that adhere to a power law and if a larger number of iterations are completed, the shape has a more complex boundary. Therefore, fractal span (D_S) is also a measure of shape complexity and it was calculated for every patch in each reefscape. Fractal span frequencies, totaled by habitat, were used to calculate the cumulative percent of fractal span integers ranging from 1 through 8.

Neighborhood transitions were computed for every pixel in the thematic maps. The first step of this process was to rasterize the habitat vectors and mirror the edges of

the raster maps to incorporate border pixels into calculations. Each pixel has eight neighboring pixels to be considered as transitions. The second step was to calculate transition frequency matrices (TFMs) which gave the raw counts of transitions between pixels (*e.g.* how many times sand pixels were next to reef pixels) and excluded self-similar transitions (*e.g.* how many times sand pixels were next to sand pixels). The third step was to use the TFMs to calculate transition probability matrices (TPMs) which gave the probabilities of transitions instead of raw numbers. The fourth step was to normalize the TPMs which yielded relative transition matrices (RTMs). The resultant embedded RTMs were consolidated from a square matrix with mirrored transitions into partial triangular matrices with total transitions, and then multiplied by 100 to give the final habitat transition percentages (*e.g.* the percent of sand pixels adjacent to reef pixels).

Three-dimensional metrics comprised centroid depth, mean depth of the patch, mean habitat depth, and rugosity (*i.e.* surface to planar ratio). Centroid depth corresponded to a single pixel depth value taken directly from a DEM. Whereas, the mean depth of a patch was equal to the average depth taken from all the DEM pixels subtended by each polygon.

Rugosity was calculated for every patch by taking the ratio of patch surface area to planimetric area. Surface areas were produced by utilizing the DEMs to compute a triangulated irregular network (TIN) for every patch. The DEMs x, y, z, coordinates were plotted in 3-D space as nodes that were connected with lines arranged as triangles. The resultant TIN was a digital data structure that partitioned a surface into a set of contiguous, nonoverlapping triangles; the triangular areas were subsequently summed to yield a total surface area for a specific patch, which was then divided by the planimetric area to yield patch rugosity.

3. RESULTS

A total reef ecosystem area of 516.8 km² was visually interpreted and mapped to a minimum mapping unit of 16 m² (1 pixel) for IKONOS images and 5.95 m² (1 pixel) for QuickBird images. The QuickBird map was resampled in ENVI to 16 m² pixels in order to correspond to the spatial resolution of the IKONOS maps. The total number of analyzed patches across all sites summed to 51,856 and the minimum mapping unit threshold for analysis was 64 m² (4 pixels). Patches composed of less than 4 pixels were excluded from calculations because they failed to capture the geometric properties of a “patch”.

Habitat areas were summed and divided by site areas to derive habitat percentages (Figure 13). Subsequently, consolidated benthic classes were summed separately from unconsolidated benthic classes to compare the percent of hard bottom features to sediment-covered bottom features (Figure 14). Habitat percentage (Figure 13) calculations revealed that sand and reef classes consistently represented large proportions of all maps (Appendix I). Saipan was mainly composed of sand and reef, which together equaled 74% of the reefscape. Vieques was largely divided into 4 main classes that totaled 87% of the reefscape including: sand, reef, sparse seagrass, and dense seagrass. Andavadoaka was also primarily composed of 4 classes that totaled 80% of the reefscape, but they differed from Vieques and included: sand, reef, sparse algae, and dense algae.

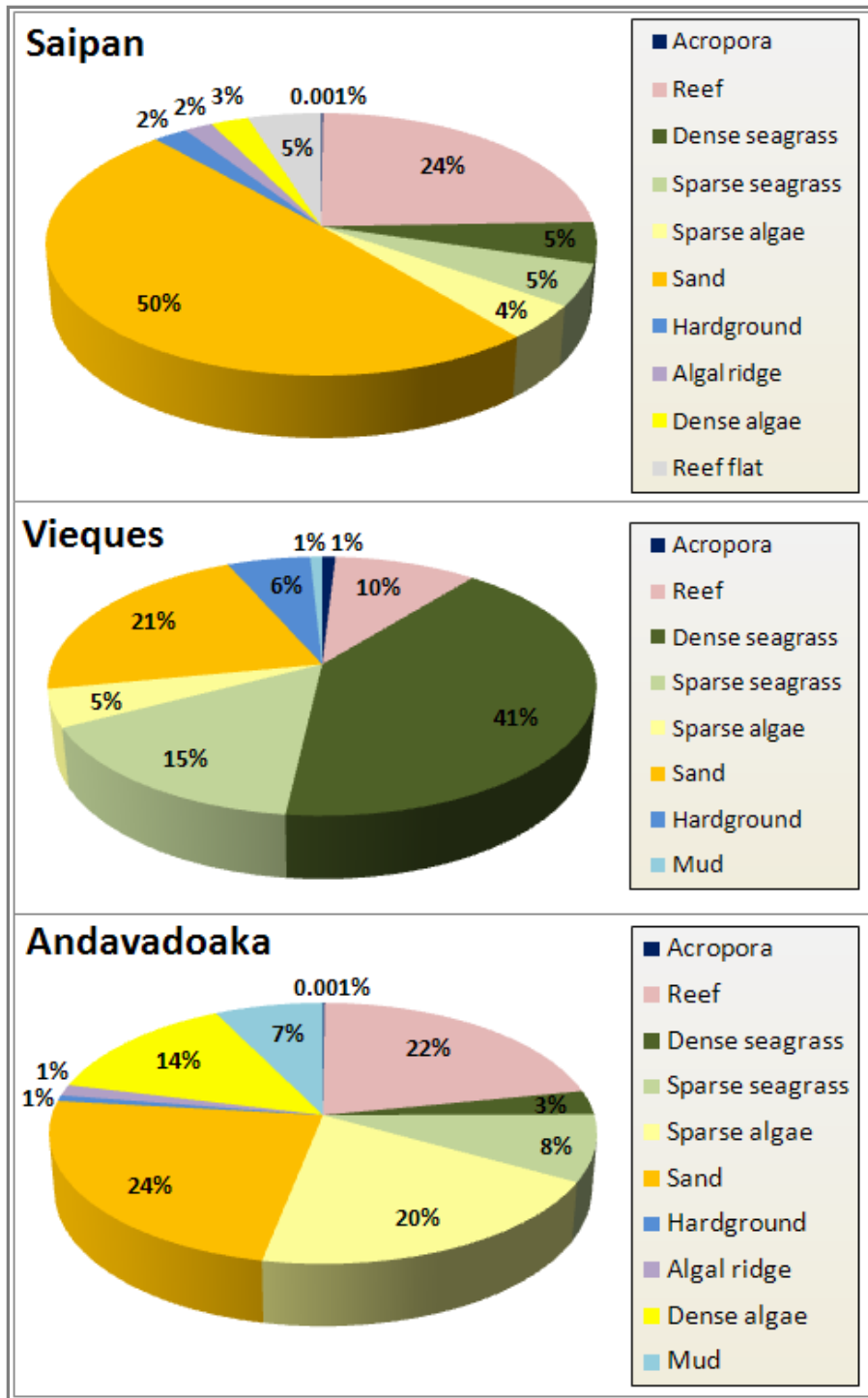


Figure 13: Habitat percentages of total mapped areas showing the most prevalent benthic cover classes: aggregate reef, seagrass, algae, and sand.

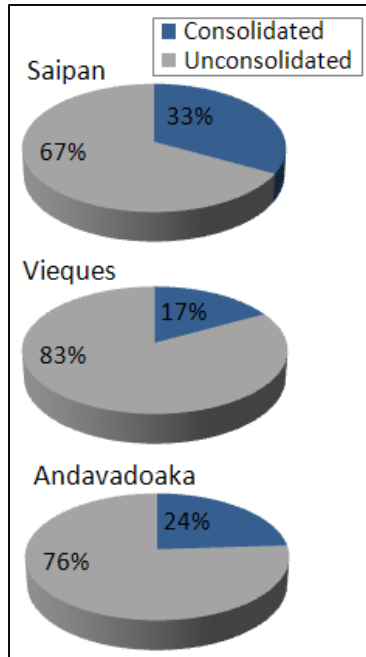


Figure 14: Comparison of hard, consolidated (Σ *Acropora*, reef, hardground, reef flat, algal ridge) benthic class percentages versus soft, unconsolidated (Σ sand, sparse seagrass, dense seagrass, sparse algae, dense algae, mud) benthic class percentages.

The centroid depth for each polygon, calculated from the DEMs, was averaged by class to yield mean habitat depths (Figure 15). Habitat depths plotted by site (Figure 15) gave insight regarding the deviation of polygons from the mean class depth. Vieques is notably different from Saipan and Andavadoaka in that the majority of the classes have large standard deviations from their mean depths. Overall, most habitats exhibited conformity to a specific depth range with only a few meters in deviation, but some habitats displayed extremely large deviations in distribution by depth. Notable deviations included: Vieques reef, sand, sparse seagrass, dense seagrass, and sparse algae as well as Saipan reef and sand.

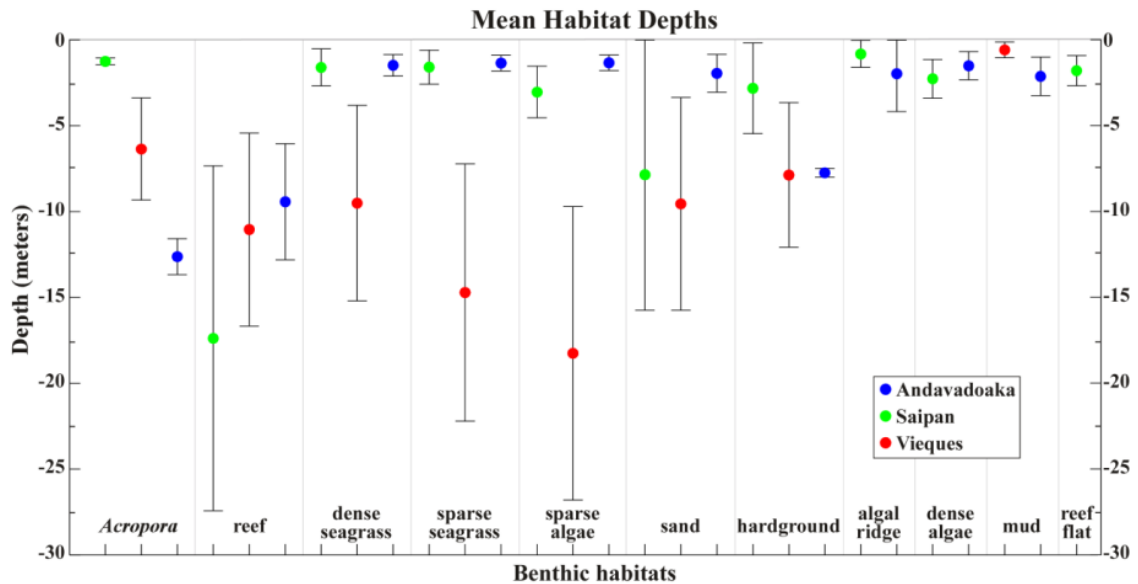


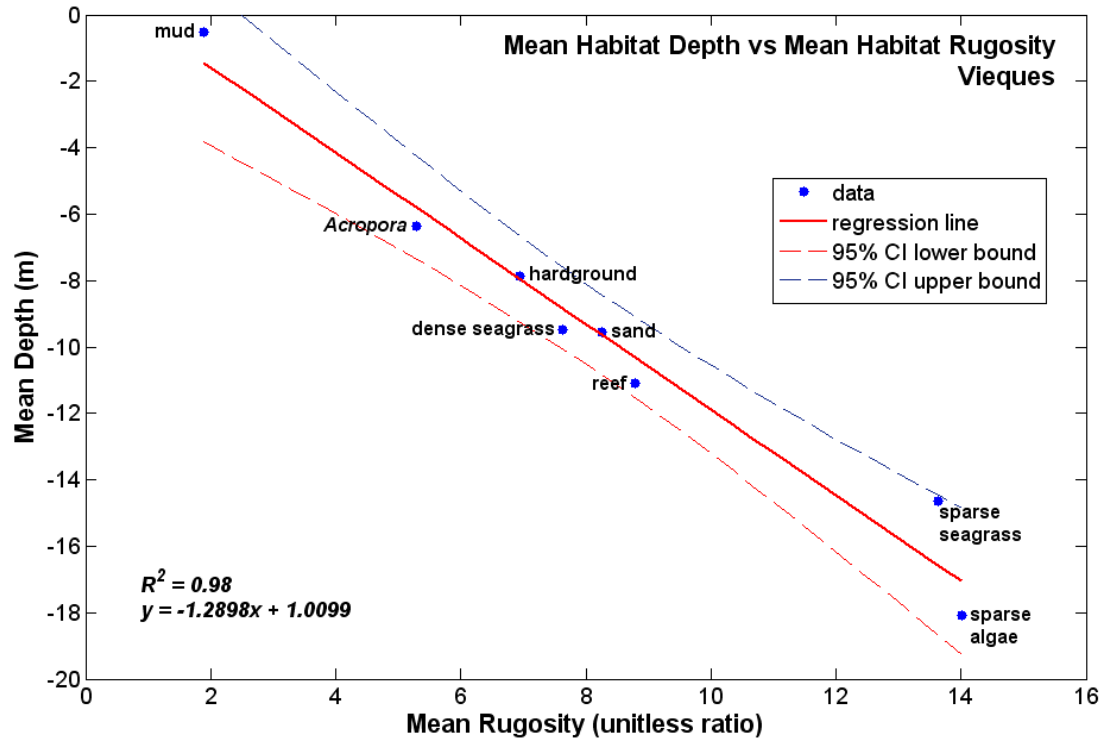
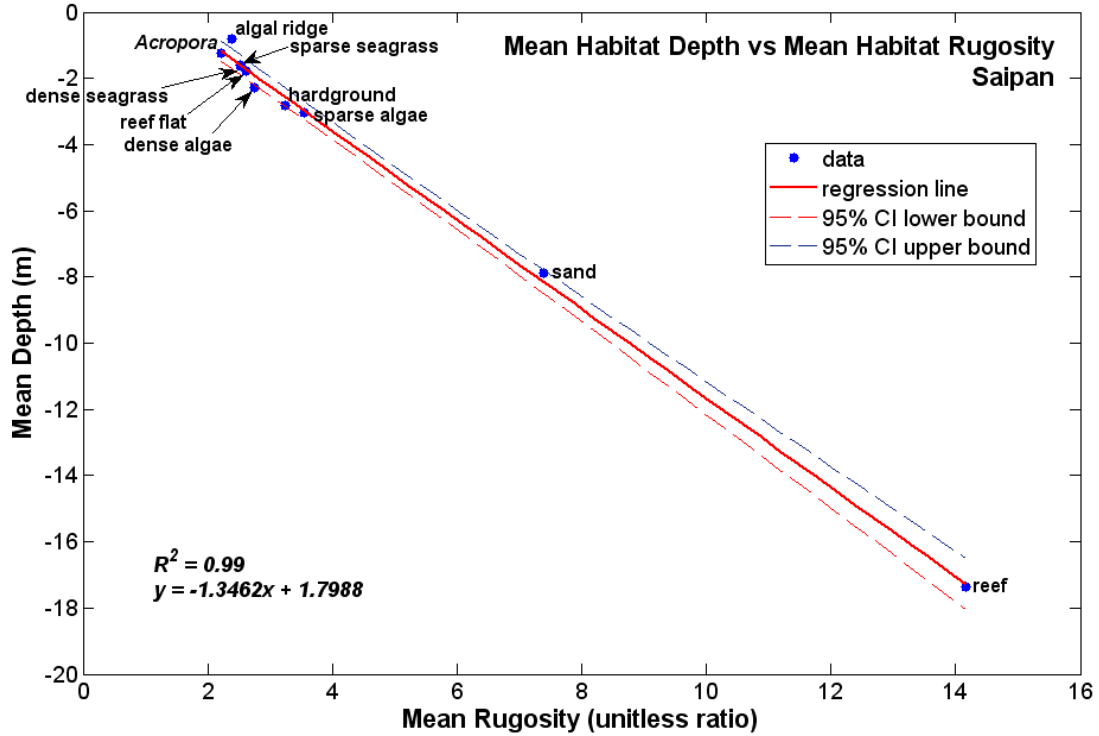
Figure 15: Depth profile with mean habitat depths and error bars representing +/- 1 standard deviation.

Calculating a measure of topographic complexity (*i.e.* rugosity) across the reefscales provided essential information pertaining to the depth distribution of highly rugose habitats versus habitats with insignificant topographic variability (Figure 16). Rugosity was averaged for habitat classes and plotted against their mean depths (Figure 16). Linear regressions between depth and rugosity produced strong correlations (all R^2 values ≥ 0.96).

Regression parameters for depth versus rugosity graphs for each site were statistically similar and their errors are presented below in Table 2. These data show overlapping 95% confidence intervals for all three slopes, implying that the increase in rugosity with increasing depth is very similar for each reefscape. The y-intercept ranges also overlap and can therefore be thought of as statistically similar. Although the change in rugosity with depth remained constant between sites, the sequence of habitats along the regression is not identical. Saipan and Andavadoaka gave similar results with the majority of habitats being constrained to shallower depths with low rugosity values; the depth regimes for these two sites are likely comparable because they are fringing and barrier reef systems, whereas Vieques has a reef system with three terraces.

Table 2: Regression errors for Figure 16 plots of depth vs. rugosity.

Site	Slope (m)	Slope: 95% CI	Y-Intercept
Saipan	-1.3462 +/- 0.0573	-1.4034 to -1.2889	1.7988 +/- 0.3222
Vieques	-1.2898 +/- 0.2453	-1.5351 to -1.0444	1.0099 +/- 2.2380
Andava	-1.5894 +/- 0.3507	-1.9401 to -1.2386	2.4712 +/- 1.6816



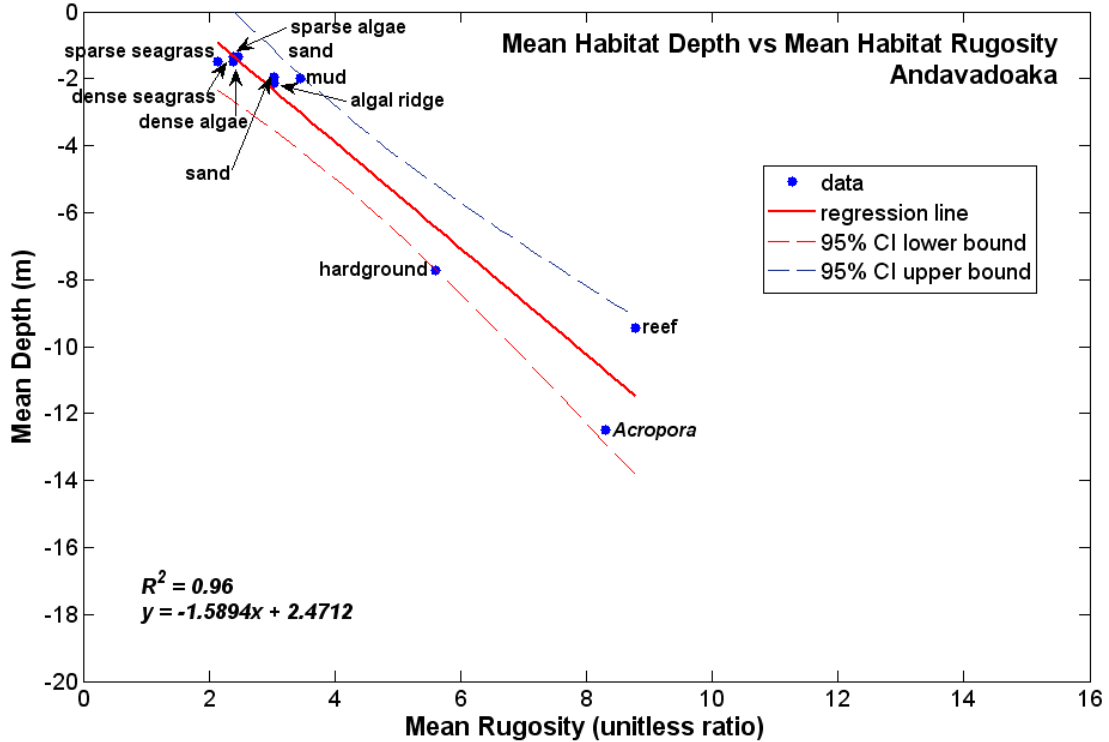


Figure 16: Mean habitat depth (averaged from mean patch depths) versus mean habitat rugosity (averaged from patch rugosities) graphed by site. Andavadoaka depths were derived from a spectral model (Figure 11) that was accurate to a depth of approximately 16 m, hence the lack of any data deeper than this threshold.

Transition matrices (Figure 17) were calculated to explore the juxtaposition of habitat classes and to quantitatively describe the observed spatial arrangements of classes in the reefscape. When considering these matrices, self-to-self transitions (*e.g.* sand pixel adjacent to sand pixel) were excluded because they were always the highest percentage and provided no information regarding pixel neighbors.

Neighborhood transitions (Figure 17) were summarized into RTMs for enhanced visual comprehension. These matrices show adjacency percentages for pixels from each habitat; thus each matrix sums to 100. Each value is the percent of transitions between the horizontal habitat class and the vertical habitat class. For illustration, the Vieques RTM shows that dense seagrass was adjacent to sparse seagrass 44.8% of the time. Habitat transitions that were similar across all three sites were the following: sand/sparse algae (V:2.7%, A:19.5%, S:5.7%), sand/sparse seagrass (V:16.7%, A:11.4%, S:8%), and dense seagrass/sparse seagrass (V:44.8%, A:11.2%, S:17.9%). These classes were very commonly found adjacent to each other, which is to be expected because macro-algae

and seagrasses both grow on sand. Dense seagrass was frequently the core of a given seagrass patch and therefore was naturally surrounded on the periphery by sparse seagrass.

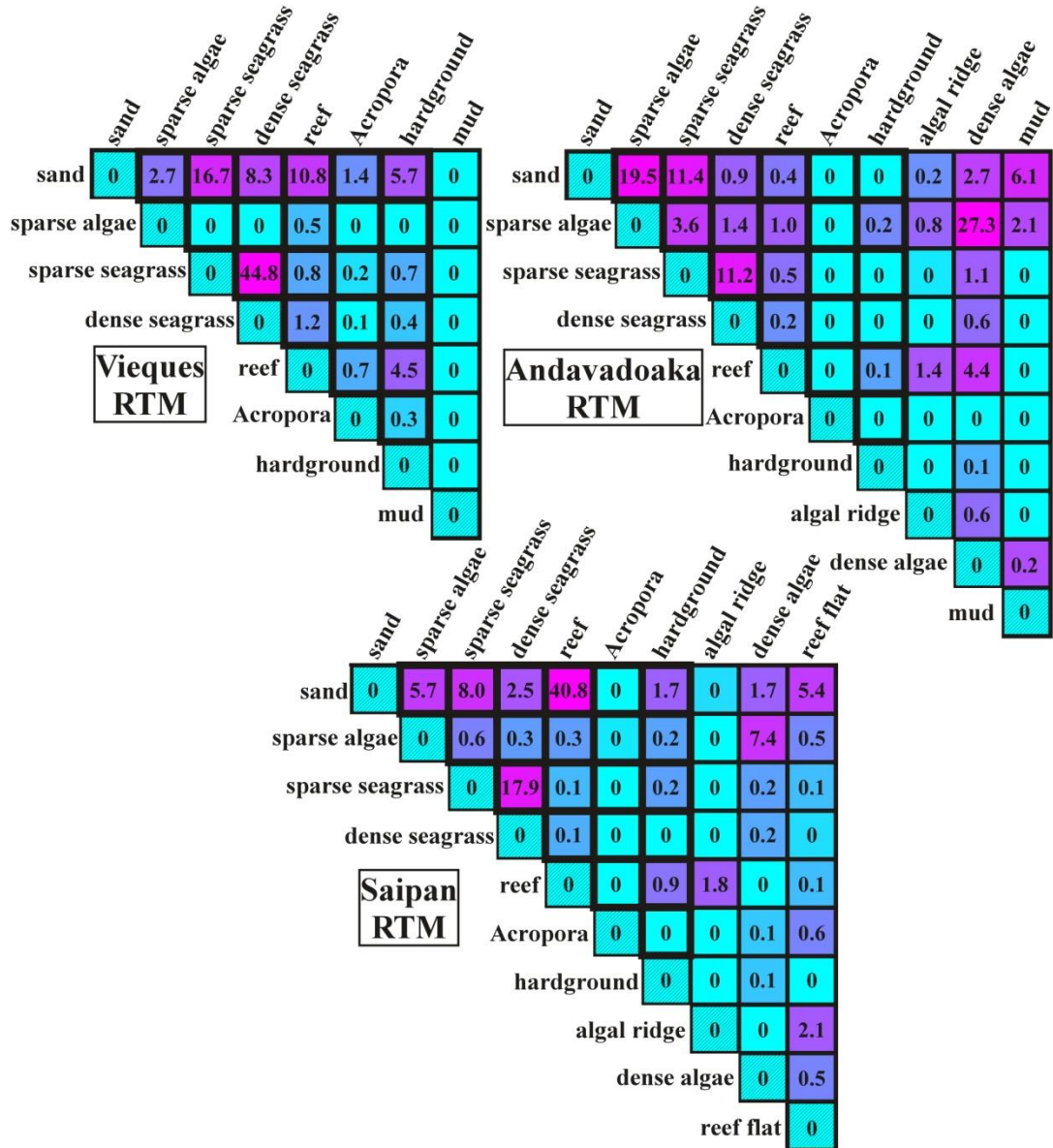


Figure 17: Embedded relative transition matrices (RTMs). The portion of each matrix outlined in bold highlights habitat transitions present at all 3 reef sites. Magenta colors represent high adjacency percentages and turquoise represents low percentages.

Correlations (R^2 values) between RTMs were calculated to investigate the statistical significance of similarities between sites (Table 3). The purpose of calculating these R^2 values was to investigate how similar the *arrangements* of habitats were between sites and to see whether or not probabilities of juxtaposition were constant. Considering

the disparate geological histories of these reefal environments and their geographical distributions (Indian, Pacific, and Atlantic Oceans), the results of habitat neighborhood transitions were quite interesting. Statistically significant correlations were found between Andavadoaka/Vieques and Saipan/Vieques, meaning that these systems were frequently composed of habitats that were arranged in a spatially comparable regime.

Comparisons were made between neighborhood transitions that were consistent across all sites (Table 3 – I), unconsolidated classes (Table 3 – II), consolidated classes (Table 3 – III), and transitions between unconsolidated and consolidated classes (Table 3 – IV).

Vieques and Saipan showed the strongest correlations with an overall $R^2 = 0.55$ and p -value = 0.01. Prevalent transitions between habitats that existed only in Vieques and Saipan included: sand/reef (V:10.8%, S:40.8%) and sand/dense seagrass (V:8.3%, S:2.5%)

Table 3: Coefficient of determination values (R^2) calculated from embedded relative transition matrices. Statistically significant correlations with p -values ≤ 0.05 have been highlighted in grey.

I. Transitions that were *similar across all sites* (sand, sparse algae, sparse seagrass, dense seagrass, reef, *Acropora*, hardground)

	Vieques	Andava	Saipan
Vieques	1	0.50	0.55
Andava	-	1	0.24
Saipan	-	-	1

II. Transitions between *unconsolidated* classes that were similar across all sites (sand, sparse algae, sparse seagrass, dense seagrass)

	Vieques	Andava	Saipan
Vieques	1	0.27	0.96
Andava	-	1	0.53
Saipan	-	-	1

III. Transitions between *consolidated* classes that were similar across all sites (reef, *Acropora*, hardground)

	Vieques	Andava	Saipan
Vieques	1	0.99	0.99
Andava	-	1	0.99
Saipan	-	-	1

IV. Transitions between *consolidated and unconsolidated* classes

	Vieques	Andava	Saipan
Vieques	1	0.17	0.89
Andava	-	1	0.21
Saipan	-	-	1

Exceedance probability versus patch area was graphed bilogarithmically by site (Figure 18) with the outputs from linear regressions compiled into Table 4. Analyzing patch areas using exceedance probabilities for each study site (Figure 18) revealed markedly similar results. Linear regressions (all R^2 values ≥ 0.99) for all polygons by site yielded analogous trends with slopes equal to the following: Vieques $m = -0.60$, Andavadoaka $m = -0.70$, and Saipan $m = -0.72$. A shallower slope in the regression line would indicate a group of polygons with a wide range of areas and comparable abundance. On the contrary, a steep slope represents a set of polygons with a more condensed range of patch areas that have a broad range of abundance probabilities.

For all sites, the probability of finding a small patch with an area of 64 m^2 was approximately equal to 1, meaning the analyzed minimum mapping unit was the most common patch size (Figure 18). The probability of encountering a 1 km^2 ($=10^5 \text{ m}^2$ on x-axis) patch was about 0.01 for each site, whereas the likelihood of finding a very large patch (10 km^2 or 10^7 m^2) was between 0.001 and 0.0001.

To explore each map in more detail, exceedance probabilities were determined by habitat (Figure 19) with regression outputs also summarized in Table 4. Vieques had 8 habitats analyzed and when they were plotted in *EP* graphs, 6 of them showed the repeating pattern of having the shallowest slope (reef, *Acropora*, sand, mud, dense seagrass). The remaining two habitats (hardground, sparse seagrass) had slopes that

corresponded precisely with the other sites plotted (Andavadoaka hardground excluded because $N = 4$ polygons). Also, when observing EP by site (Figure 18) Vieques had a shallower slope than Andavadoaka and Saipan, which had almost identical slopes. The agreement in slope values between Andavadoaka and Saipan was persistent throughout the EP by habitat plots, 7 graphs matched closely. These observations showed clear similarities between two sites with Vieques being dissimilar when probabilities were separated by habitat.

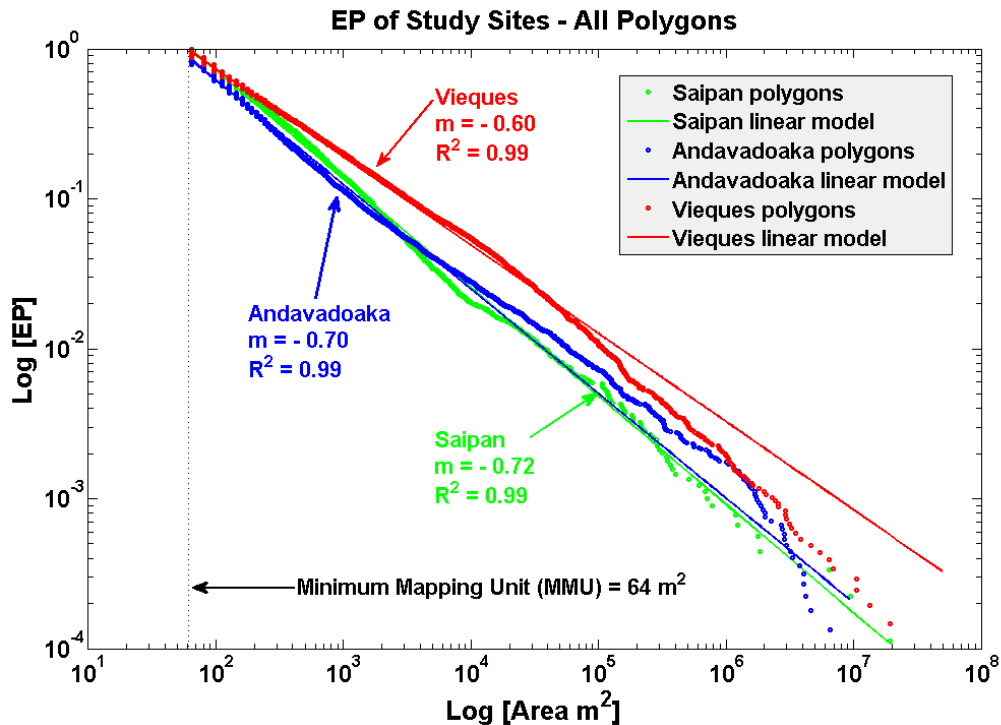


Figure 18: Exceedance probability graphed by site. All polygons from each study site were ranked in EP calculations. The minimum mapping unit threshold (dashed vertical line on plot) for analysis was 64 m^2 , which equals the area of 4 pixels.

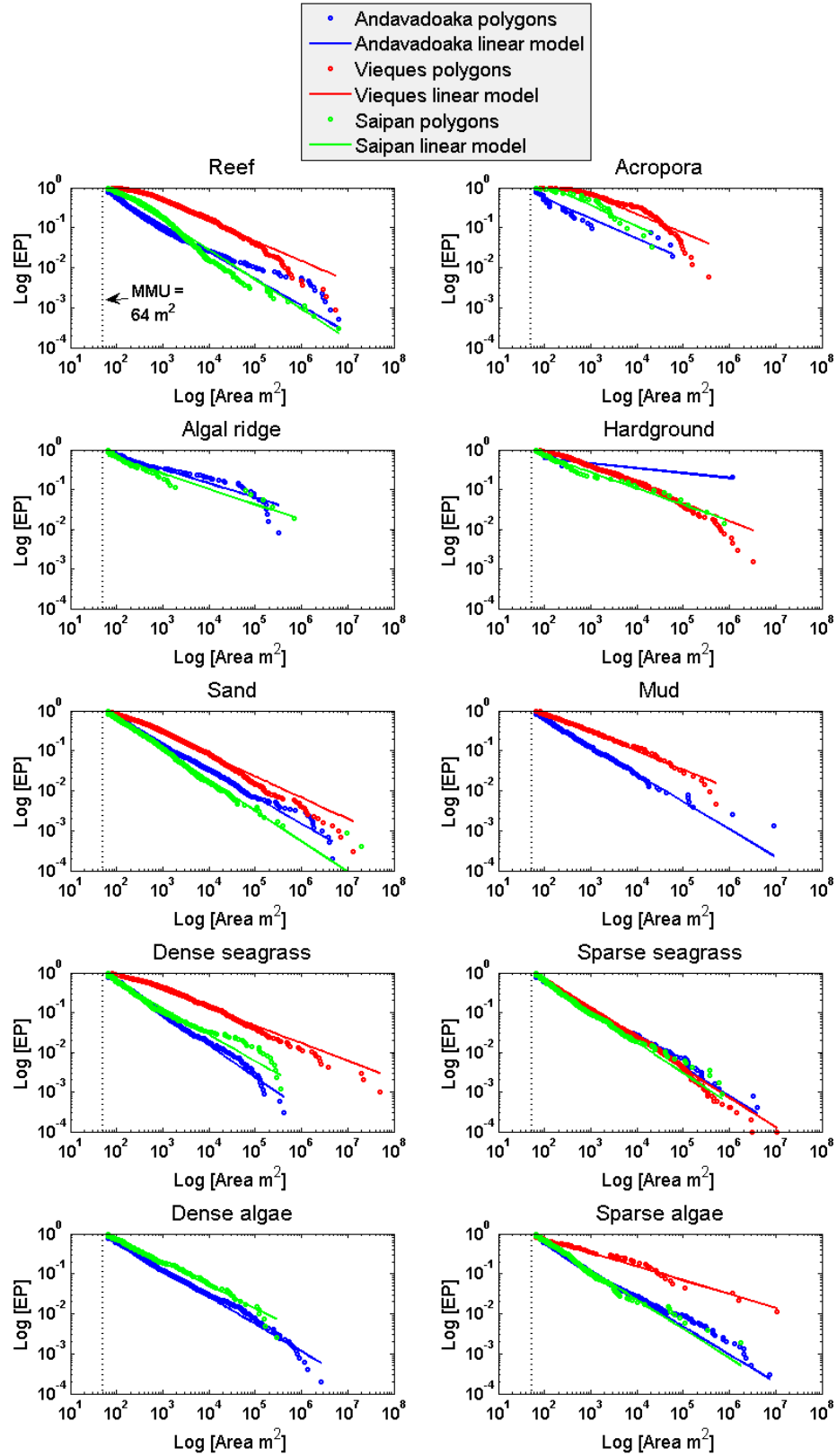


Figure 19: Exceedance probability graphed by habitat. Polygons from each habitat were ranked in *EP* calculations. MMU analysis threshold shown as dashed line on each plot.

Table 4: Summary of data plotted in exceedance probability graphs for each habitat and for each site. Linear regression in log-log space was used to calculate the slope (m), y-intercept (b), coefficient of determination (R^2), and fractal dimension (D_B). The slope of the regression line plus the Euclidean dimension (=2) is equal to the fractal dimension (D_B). The equation of a line in log-log plots, with base e , is expressed by the following:

$$\log(F(x)) = m \cdot \log(x) + b$$

which simplifies to: $F(x) = (x^m)(e^b)$ and in this case $EP = (Area^m)(e^b)$

$$D_B = m + 2$$

HABITAT	SITE	NUMBER OF POLYGONS (N)	SLOPE (m)	Y-INTERCEPT (b)	COEFFICIENT OF DETERMINATION (R^2)	FRACTAL DIMENSION (D_B)
reef	Andava	2,182	-0.67	2.53	0.98	1.33
	Saipan	3,524	-0.74	3.27	0.98	1.26
	Vieques	1,078	-0.49	2.62	0.98	1.51
Acropora	Andava	52	-0.50	1.69	0.95	1.50
	Saipan	30	-0.53	2.67	0.93	1.47
	Vieques	169	-0.47	2.78	0.93	1.53
algal ridge	Andava	123	-0.36	1.37	0.96	1.64
	Saipan	53	-0.39	1.30	0.96	1.61
hardground	Andava	4	-0.12	0.08	0.92	1.88
	Saipan	72	-0.41	1.50	0.99	1.59
	Vieques	669	-0.45	2.10	0.98	1.55
sand	Andava	4,123	-0.66	2.61	0.99	1.34
	Saipan	2,335	-0.77	3.11	0.99	1.23
	Vieques	3,074	-0.53	2.35	0.99	1.47
mud	Andava	768	-0.69	2.71	0.99	1.31
	Vieques	215	-0.47	2.04	0.99	1.53
dense seagrass	Andava	3,526	-0.80	3.22	0.99	1.20
	Saipan	861	-0.67	2.56	0.99	1.33
	Vieques	983	-0.44	2.08	0.99	1.56
sparse seagrass	Andava	2,562	-0.72	2.84	0.99	1.28
	Saipan	1,154	-0.77	3.05	0.99	1.23
	Vieques	14,244	-0.74	2.99	0.99	1.26
dense algae	Andava	5,073	-0.68	2.68	0.99	1.32
	Saipan	400	-0.57	2.32	0.99	1.43
sparse algae	Andava	3,973	-0.70	2.75	0.99	1.30
	Saipan	519	-0.73	2.94	0.99	1.27
	Vieques	90	-0.35	1.34	0.99	1.65
ALL HABITATS COMBINED	Andava	22,386	-0.70	2.74	0.99	1.30
	Saipan	8,948	-0.72	3.01	0.99	1.28
	Vieques	20,522	-0.59	2.41	0.99	1.41

Compactness values near 0 represent elongate shapes while values near 1 represent circular shapes. Trends in semi-log plots (Figure 20) of compactness versus patch area revealed that smaller patches tended to be more round, whereas larger patches tended to be more elongate.

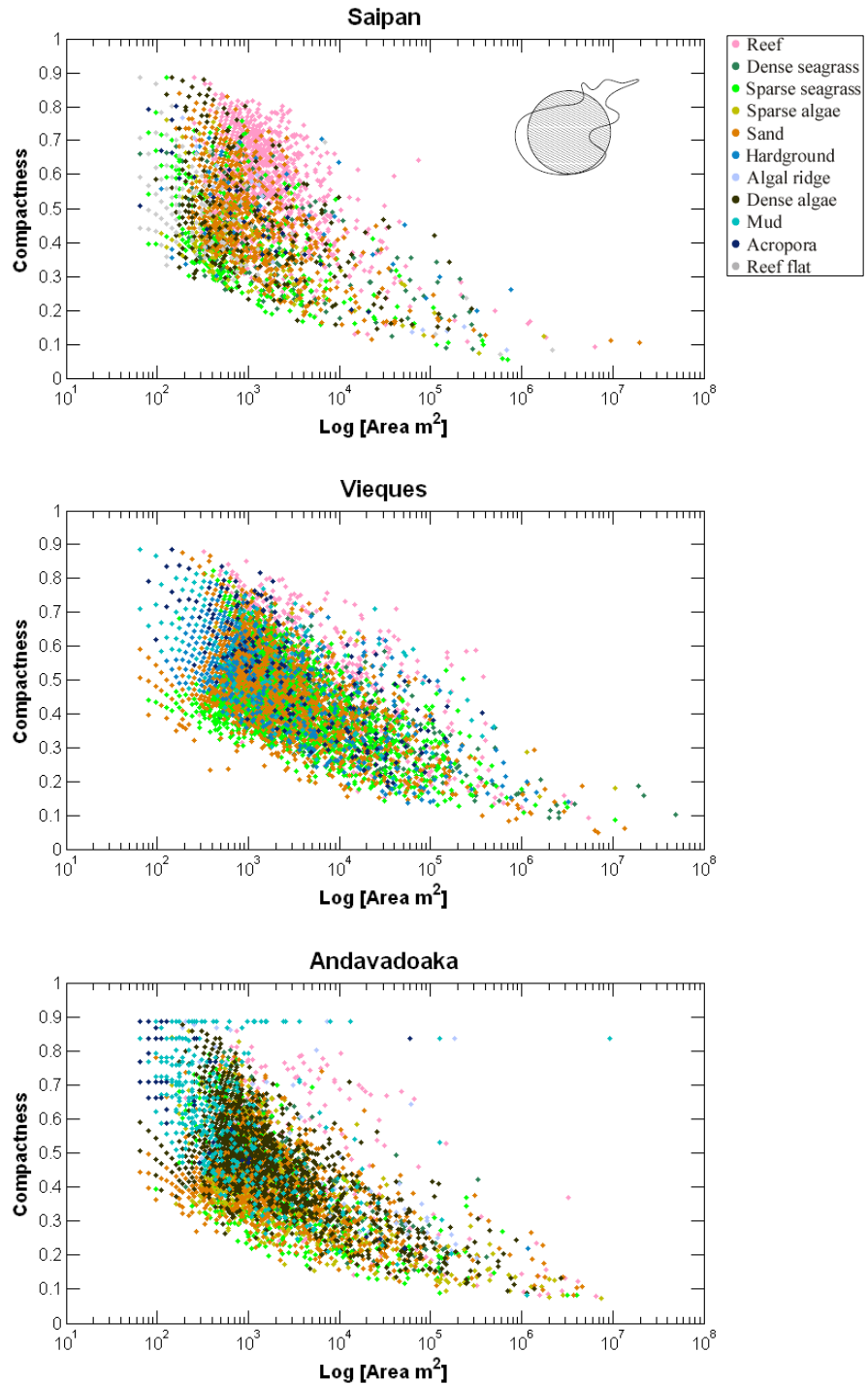


Figure 20: Semi-log plots showing the relationship between compactness and patch area. Number of polygons = Saipan 8,948; Vieques 20,522; Andavadoaka 22,386.

Principle axes ratios have the same range as compactness with values near 0 representing elongate shapes and values near 1 representing circular shapes. Semi-log plots (Figure 21) of *PAR* versus patch area display a vague relationship. Therefore, compactness (Figure 20) seems to be a more robust metric than *PAR* for measuring elongation and circularity of patch shapes. For this reason, compactness was used to investigate fractal dimension (Figure 22).

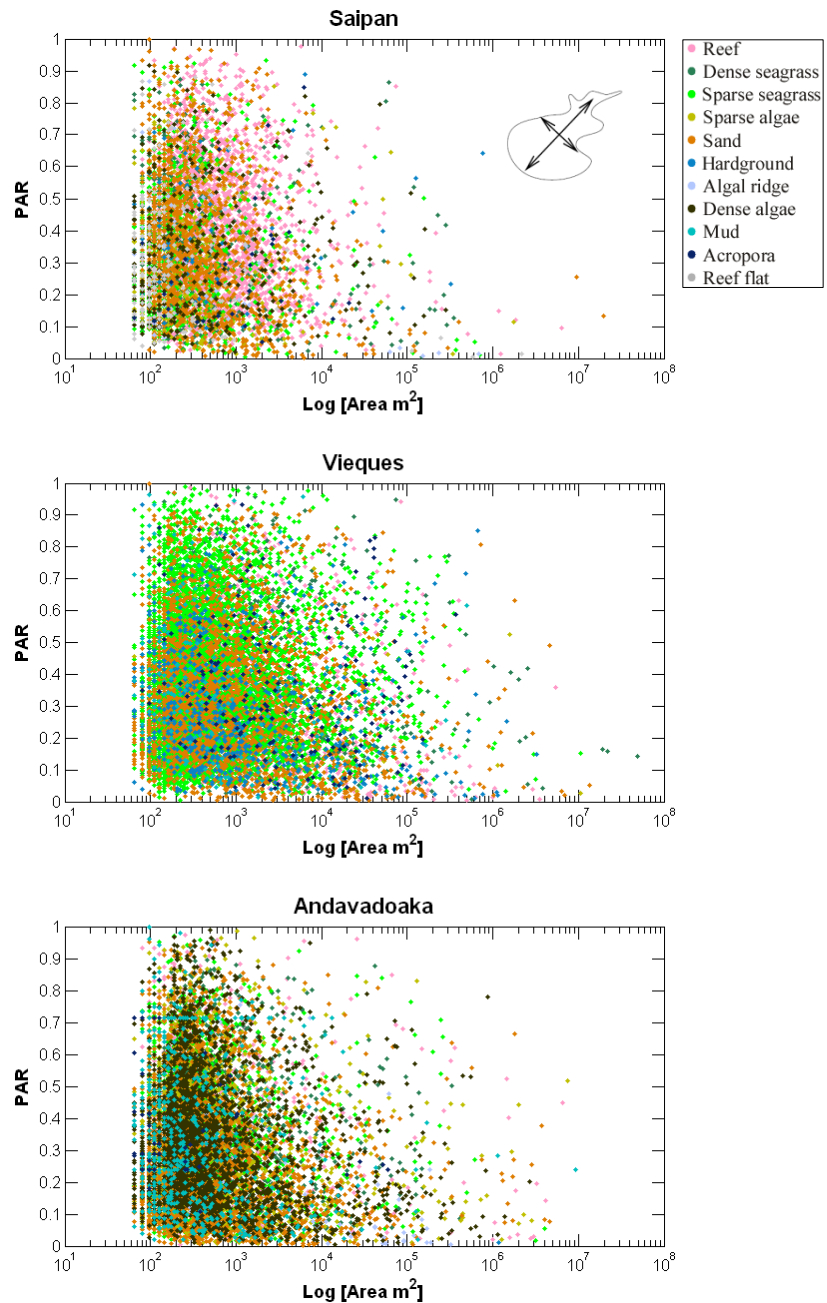


Figure 21: Semi-log plots showing the relationship between principle axes ratio (*PAR*) and area. Number of polygons = Saipan 8,948; Vieques 20,522; Andavadoaka 22,386.

The fractal dimension (D_B), a measure of shape complexity, ranges from 1 for simple shape boundaries to 2 for very intricate shape boundaries. When plotted against compactness, fractal dimension (Figure 22) illustrated an increase in shape complexity with an increase in shape circularity for all sites. Therefore, more thin elongate habitat patches have a tendency to exhibit more simple boundaries.

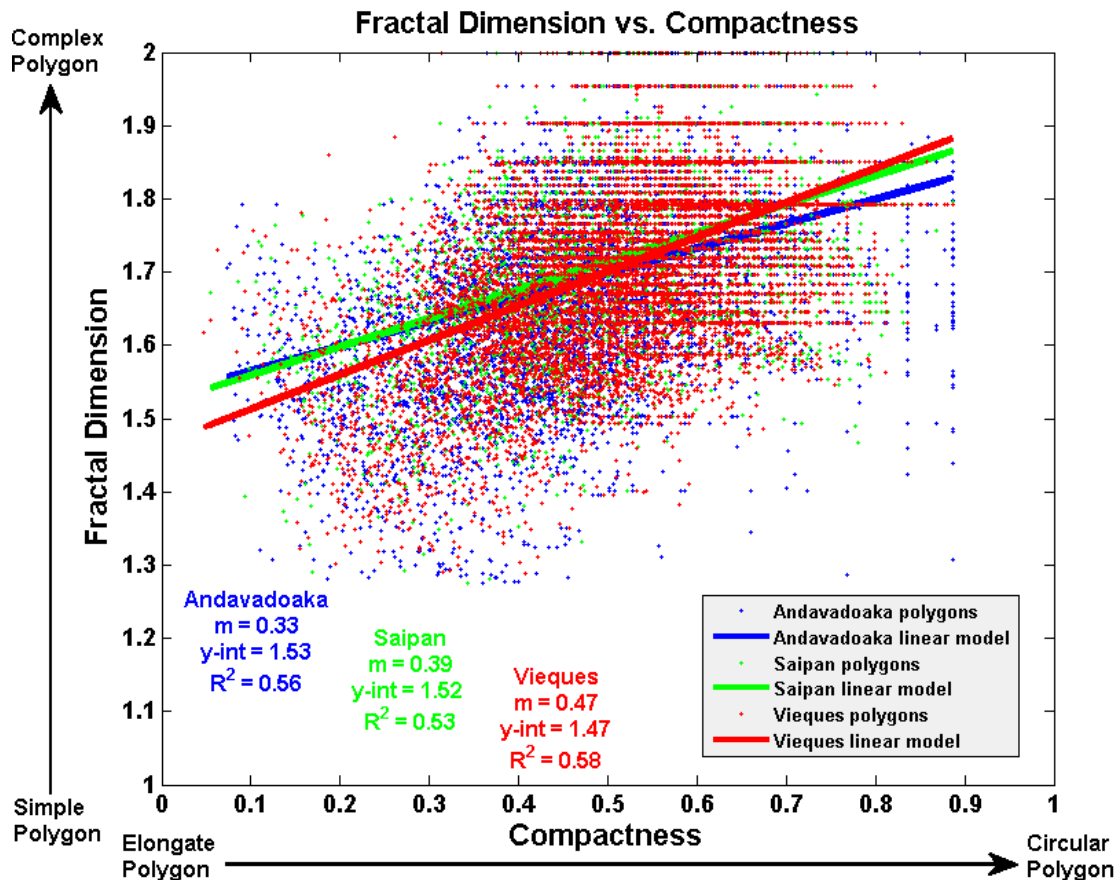


Figure 22: Graphical representation of the fractal dimension versus compactness values calculated for each polygon (Andavadoaka $N = 22,129$; Saipan $N = 8,876$; Vieques $N = 20,384$). Linear regression slopes, intercepts, and R^2 values are shown on the graph.

Cumulative percentage (Figure 23) represents the percent of a habitat class which is composed of patches with a given fractal span. Results from plotting the cumulative percentage of fractal span were extraordinarily similar for all study sites (Figure 23). Trajectories showed that 70-80% of each reefscape consisted of patches with simple geometric boundaries ($D_S \leq 3$). Approximately 90% of each map was made up of polygons with $D_S \leq 4$. The graphs in Figure 23 level-off after $D_S = 4$, indicating that the remaining 10% of each reefscape was composed of intricate polygons ($5 \leq D_S \leq 8$).

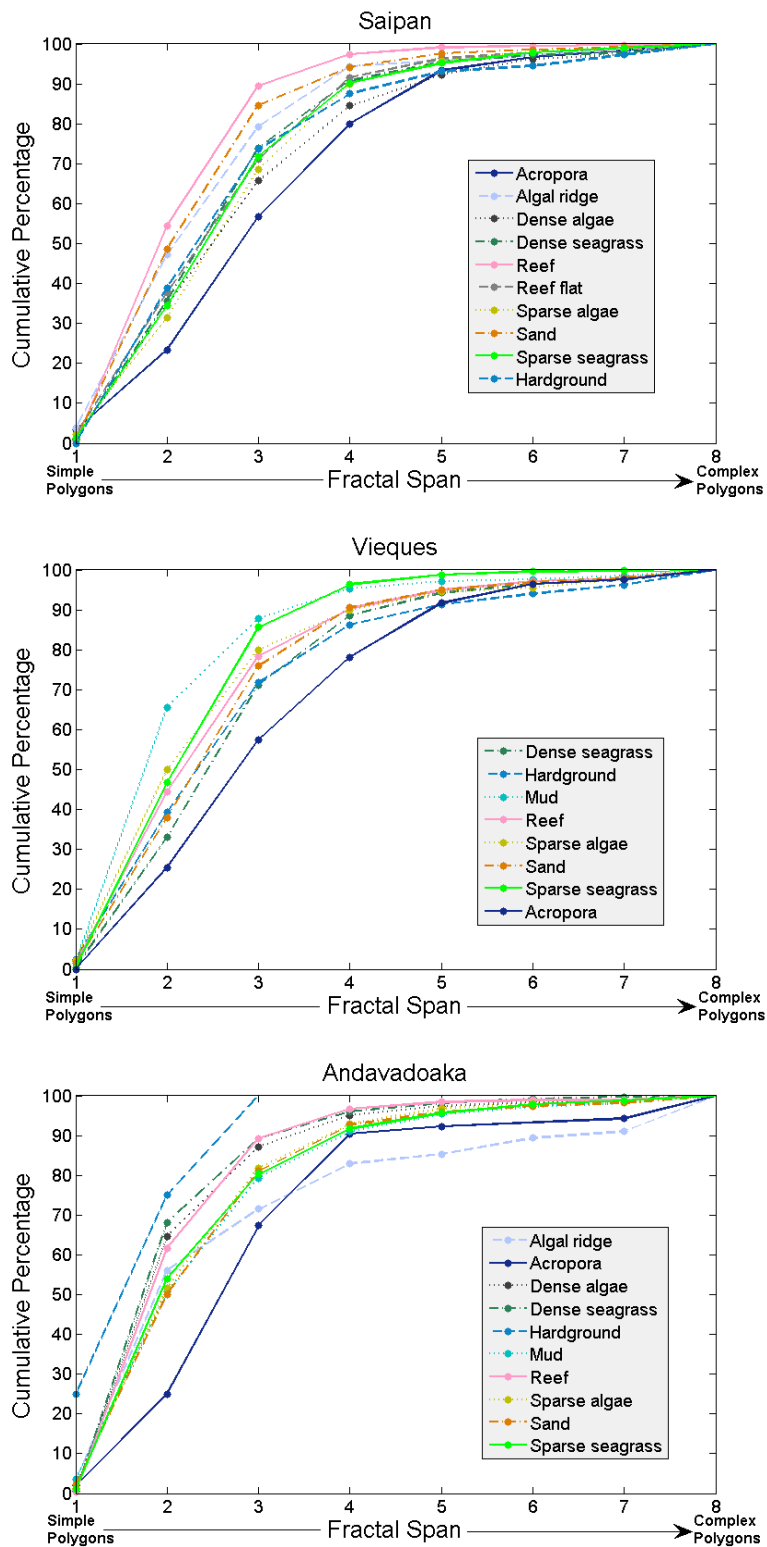


Figure 23: Cumulative percentage versus fractal span for all habitats. Fractal span (D_S), a measure of patch complexity, is equal to the number of box-counting iterations completed that adhere to a power law. Polygons with a low fractal span have simple boundaries and as fractal span increases, the polygonal boundary becomes more intricate.

4. DISCUSSION

4.1 Habitat class percentages

The difference between Vieques (Appendix I-A), where seagrass made up more than half of the area studied, and Andavadoaka (Appendix I-B), where macro-algae was a huge component, can be explained by accommodation space and substrate composition. Here, accommodation space is referred to in a submerged aquatic vegetation sense and does not refer to available water column space for vertical coral growth. In the case of Vieques, there lies an essentially unlimited vast expanse of shallow unconsolidated sands to the north of the island that provide ideal conditions for seagrass beds to grow. Whereas in Andavadoaka, accommodation space for submerged aquatic vegetation is limited by the extent of the backreef. Not only does this constrain seagrass bed expansion, but the actual substrate within the backreef also provides a growth advantage for macro-algae over seagrass because it contains rubble intermixed with sand. Rubble is suitable for macro-algae species to inhabit due to their holdfast adaptations, but seagrasses have root systems and can only thrive in sand or mud. Hence, the observed gradient that exists leeward of the reef crest in Andavadoaka; rubble decreases in abundance and consequently the habitat arrangement shifts from algal-dominated to seagrass-dominated (Appendix I-B).

4.2 Mean habitat depth and rugosity

Vieques is distinctively different from Saipan and Andavadoaka with regards to habitat arrangements by depth. This observation is rooted in the variation in reef structures: Vieques is the only backstepping reef system, whereas the other sites are fringing and barrier reef systems. Backstepping systems naturally form benthic habitats in extremely variable depths due to the sequence of platforms created during transgression intervals. In comparison, fringing and barrier reef systems naturally create backreef regions which confine the majority of the mapped habitats to shallower depths with only slight deviations from mean depths.

Saipan's large depth range deviations for reef (7 - 28 m) and sand (0 - 17 m) are explained by the geological history of the island. The previously mentioned tectonic slumping event that occurred along the western side of Saipan left behind benthic

structures that were in an ideal position for colonization. Coral colonies grew atop this surface and the remainder of the deep bank was filled with sand sheets that were apparently unable to support the development of seagrass and macro-algae beds. The Saipan LiDAR DEM (Appendix II-C) best illustrates the position of the deep bank (green) surrounding the shallow fringing and barrier reef systems (red - yellow).

Shallow topographically simple classes (Figure 16) which are similar for Saipan and Andavadoaka include: the algal ridges, sparse algae, dense algae, sparse seagrass, and dense seagrass. The algal ridges are directly beneath the corridor of maximum wave action and are raised structures but have low rugosity. High incoming wave energy in this habitat generally inhibits coral colonization and facilitates the growth of encrusting coralline algae, limiting changes in vertical relief across the raised crest. Algae and seagrass classes, whether sparse or dense, all display similar characteristics in that they formed through colonization of vast sand sheets located close to shorelines or through colonization of rubble patches with intermixed sand pockets in the backreef. In any case, these habitats have very low relief and lie in shallow waters in Saipan and Andavadoaka.

As mentioned before, Vieques was the only backstepping system evaluated. Accordingly, the rugosity and depth relationship (Figure 16) was different from the other two sites and it showed much more separation, rather than shallow clumping, between habitats along the rugosity regression line.

All study sites displayed the general trend of shallow classes being non-rugose and deep classes being rugose. Interestingly, the increase in depth with increasing rugosity was consistent between sites (Saipan $m = -1.3$; Vieques $m = -1.3$; Andavadoaka $m = -1.6$), but the sequence of habitats along this gradient was not consistent. This implied that rugosity was not controlled by habitat type, meaning that rugosity increased with depth no matter what habitat was positioned on the seafloor surface. A possible mechanism for explaining this reefscape behavior is the weathering of coastal landforms coupled with reef ecosystem growth and its accompanying affects on hydrodynamic processes. Perhaps erosion, runoff, and sedimentation provide enough infill to seafloor features adjacent to the coastline (with this effect decreasing as depth increases) to reduce rugosity in shallow habitats. At the same time, the growth of reef systems is known to change local hydrodynamics and favor the deposition of sand and rubble within the

backreef (*e.g.* Saipan & Andavadoaka) or in between linear reefs (*e.g.* Vieques). These effects, plus the influence of environmental conditions and antecedent topography on the spatial arrangement of reef-building organisms, result in the reef habitat class being deeper with high vertical relief. This observation was shown to exist for all three sites (Figure 16).

4.3 Neighborhood transitions

The particularly large percent of sand pixels next to reef pixels in Saipan was a product of the deep western bank discussed earlier; this vast bank area encompassed strictly those two classes and represented a large portion of the mapped area (Appendix 1-C). Another reason for this observed 40.8% adjacency is that the interior of Saipan's Tanapag Lagoon is composed primarily of patch reefs surrounded by uncolonized sand. In comparison, Vieques' linear and patch reefs were generally neighboring sand (10.8%), attributable to the halo effect. Bare sand halos, a product of fish (parrot and surgeon fish) and urchin (*Diadema*) herbivory, surround reef structures and separate them from seagrass beds (Levitan and Genovese 1989). In addition, the Saipan reefs also tended to border hardgrounds (4.5%) that always rest directly landward of the reefs because they represent the terminal phase of a shallowing-upward sequence (Moore 2001), meaning the transgression/backstepping in Vieques. A transgression sequence was absent in Saipan because the barrier and fringing reefs initiated on the Mariana Limestone, promoting lagoonal development instead of hardground development.

In Andavadoaka, a notable transition between sparse algae/sparse seagrass (3.6%) was absent in the other two sites (V:0%, S:0.6%). This can be recognized qualitatively as the sequence of habitats leeward of algal ridges, which begins with dense algae followed by sparse algae, and then shifts to sparse seagrass and lastly dense seagrass. This spatial gradient, observed throughout the mapped region of Andavadoaka, was discussed previously and can be related to the preferential growth of macro-algae with holdfasts (*e.g.* *Sargassum sp.*) on sand mixed with rubble versus the preference of seagrasses with roots (*e.g.* *Thalassodendron ciliatum*, *Syringodium isoetifolium*, and *Thalassia testudinum*) to grow in well-sorted sands.

4.4 Exceedance probability

The *EP* results demonstrated that a predictable relationship between patch frequency and patch size existed over 5 orders of magnitude for all three sites. The general trend found here (Figures 18 & 19) demonstrates that small patches are much more likely to occur in reefscape compared to larger patches, which are less frequently observed. The decay of prevalence with increasing area is constant and therefore easily quantified (Table 4). A strongly correlated linear relationship between these parameters, that persists for ≥ 3 orders of magnitude, is interpreted as evidence of fractal behavior and adherence to a power law, a function that describes proportional, rather than constant, changes in y relative to x (Purkis *et al.* 2005). When fractal dimension is the same across ≥ 3 orders of magnitude, the reefscape can also be considered scale invariant.

A question of particular interest is how can these exceedance probability results be useful in the management of MPAs? If habitat patch areas have frequency trends, we can predict how many patches of a given size will be present in certain reef environments. The size of an MPA affects the number of habitat patches within the MPA boundaries, so questions about specific habitat patches of defined areas can be solved.

The essential goals of MPAs are to protect biodiversity, maintain ecological interactions within a community, and sustain fished species as well as their habitats. They need to be located across representative habitats and biogeographic regions to assure that the diversity of habitats and taxa are protected (WHOI Seminar 2001). Rare or threatened species are often identified as the reason behind implementing an MPA and special attention is usually given to areas thought to be diversity hotspots, critical or rare habitats, or spawning grounds where one or more targeted species congregate (WHOI Seminar 2001). Many scientists argue that MPAs should be large and numerous, forming an expansive network of no-take zones that are managed for pollution sources and policed by law enforcement officials.

So, how big should MPAs be? Most studies addressing this question suggest that MPAs should be as large as possible. One reason for this is because studies that have examined the relationship between area and species diversity indicate that, as on land, diversity increases with area (WHOI Seminar 2001). Thus, the larger the MPA, the greater the number of species protected. Another reason for creating a large MPA is to

protect a greater representation of the habitats that an individual uses during its lifetime. Fish often shift among habitat types as they grow because they require different resources (*i.e.* different kinds of food and habitats for reproduction). If these habitats are not near or within an MPA, fish may not encounter the MPA or must leave the MPA as their resource and habitat needs change (WHOI Seminar 2001). Large MPAs are also critical for species whose larvae disperse only short distances. The bigger the MPA, the more likely larval dispersal will be within the MPA, allowing these protected populations to be self-replenishing. Recent studies of larval dispersal distances suggest that MPAs on the order of 5 to 10 kilometers would encompass the dispersal distances for some species whose larvae disperse relatively short distances (WHOI Seminar 2001).

How many MPAs should there be? There are several reasons why the answer to this question is "many". One reason is because it is unlikely that all representative habitats (and associated species) in a region will be included within any one MPA (WHOI Seminar 2001). Thus, for adequate habitat and biogeographic representation, many MPAs will be necessary. In addition, because most marine species produce offspring that are potentially dispersed great distances (10-100s km) by currents, few MPAs will be large enough for protected populations to be self-replenishing (WHOI Seminar 2001). Instead, protected populations are reliant on recruitment of young born elsewhere in distant populations. If these parental sources are not protected, then replenishment of the populations within MPAs can be jeopardized. Networks of MPAs are larval sources that can replenish not only protected populations, but also unprotected populations outside MPAs. Therefore, another reason for allocating protected space across a network of many, broadly distributed MPAs is to broaden the range of populations that will benefit from recruitment of larvae produced within MPAs (WHOI Seminar 2001).

What if an MPA is partly designed to protect critical habitat for a given species and managers decide to increase the amount of habitat in which the species can thrive? Here, the map extent of the Vieques (294.6 km²) study site is considered as a hypothetical MPA. An example of one managed critical habitat within the MPA could be seagrass beds where manatees graze on vegetation. Biological studies within the MPA may show

that local manatees prefer to congregate and forage in very dense seagrass meadows approximately 100-120 m² in size.

If the MPA is 294.6 km² and incorporates 983 mapped dense seagrass patches all together, how much larger does the MPA need to be in order to double the 100-120 m² sized dense seagrass patches? Exceedance probability results (Figures 18, 19 & Table 4) from this study can be used to calculate the answer because a predictable relationship exists between patch size and its frequency of occurrence.

The number, or tally, of 100-120 m² dense seagrass patches within the MPA can be solved for using the information and equations in Table 4. To begin, *EPs* must be calculated:

$$EP = (Area^m) * (e^b)$$

$$100 \text{ m}^2 \text{ patches: } EP = (100 \text{ m}^2)^{-0.44} * e^{2.08} = 1.0552$$

$$120 \text{ m}^2 \text{ patches: } EP = (120 \text{ m}^2)^{-0.44} * e^{2.08} = 0.9738$$

Exceedance probability is the likelihood of encountering a patch of a given size or larger. So, subtracting these *EP* values gives the probability (*P*) of encountering a dense seagrass patch between or equal to those areas (100 m² ≤ patches ≤ 120 m²).

$$P = 1.0552 - 0.9738 = 0.0814$$

The total number of dense seagrass patches mapped in the MPA equals 983. So, what is the total number of dense seagrass patches within the defined critical area range that exist inside the MPA?

$$(P) * (\text{total patches}) = \text{critical dense seagrass patches}$$

$$(0.0814) * (983) = 80$$

If managers need to double that amount to augment manatee habitats, they need 160 critical dense seagrass patches to be included in their MPA. Assuming areas adjacent to the MPA are similar environments, how much larger does the MPA need to be to incorporate this number of patches?

$$\text{MPA extension} = \frac{(294.6 \text{ km}^2) * (160 \text{ patches})}{983 \text{ patches}} = 47.9 \text{ km}^2$$

$$\text{Total MPA size needed} = 294.6 \text{ km}^2 + 47.9 \text{ km}^2 = 342.5 \text{ km}^2$$

Thus, the MPA needs to be 342.5 km² to incorporate the desired amount of critical manatee habitat. But, what if the resource managers determine that funds only allow them to expand their MPA by 20 km² instead of 47.9 km²? The financially affordable MPA size equals:

$$294.6 \text{ km}^2 + 20 \text{ km}^2 = 314.6 \text{ km}^2$$

Accordingly, how many critical seagrass patches will this 20 km² expansion incorporate?

$$\# \text{ of critical patches} = \frac{(20 \text{ km}^2) * (983 \text{ patches})}{294.6 \text{ km}^2} = 67$$

Instead of the desired 160 patches, there will be 67 included in the MPA expansion; this information tells managers there is a need to plan for supplemental conservation of manatee habitat. Calculating an number of predicted habitat patches that will be included when planning an MPA expansion can also be helpful to planners when they are making decisions regarding resource allocations. Marine spatial planning requires specific questions and answers and decisions are frequently made locally, which is likely why few assessments of coral reef ecosystems using landscape ecology metrics have been used to understand predictable relationships across multiple reefscales. If we could predict spatial planning outcomes on a more general scale, across many regions, perhaps management efforts could be more collaborative and reef systems with similar habitat arrangements could be compared to produce more positive results from conservation efforts.

4.5 Compactness and principle axes ratio

Exceedance probability demonstrated that each reefscape displayed the property of scale invariance in terms of area-frequency relationships (Figures 18 & 19). Compactness and *PAR* were plotted against the natural logarithm of patch area to investigate whether or not the shape of patches was also scale invariant (Figures 20 & 21). The results indicated that patch shape was a less predictable measure than exceedance probability. However, there is a general trend (Figures 20 & 21) that showed smaller patches to have a propensity for circularity and larger patches to have a propensity for elongation.

Patches $\leq 0.001 \text{ km}^2$ ($= 10^3 \text{ m}^2$) in size exhibited every possible geometric shape, which could represent a lack of environmental forcing at such scales. As patch size increased (0.001 km^2 to 1 km^2) there was a moderate abundance of elongate shapes, which could possibly be explained by directional environmental forces that act over these scales, such as currents and wave fields (Purkis *et al.* 2007). Linear morphologies among patches of similar scale have previously been shown to be the result of hydrodynamic flow, more specifically wave power (Hamylton and Spencer 2008). Patches $> 1 \text{ km}^2$ ($= 10^6 \text{ m}^2$) in area were extremely linear in geometry for all three study sites. This observation may be a space-limiting issue because at these large scales the constraint of the antecedent topography or continental shelf size emerge as key factors affecting habitat configurations.

For example, in Saipan the largest elongate shapes were among the reef, sand, and reef flat classes. Considering that these habitat categories made up 79% (Figure 13) of the mapped reefscape (Appendix I-C), the role of the Mariana Limestone in controlling the overall design of the system is revealed. The linearity of the Mariana Limestone ridge (Figure 10) was mimicked by carbonate-accreting reef organisms, which in turn created the adjacent linear reef flat landward of the reef crest. Leeward of these linear units rest lagoonal spaces filled with sand deposits that follow the order of ecosystem-scale elongation.

Andavadoaka and Vieques have similar constraints on patch geometry at a large scale, yet the overall control is a product of linear continental shelves instead of a tectonically slumped bank like in Saipan. The Madagascan continental shelf along the southwestern coast is approximately 50 km wide (east-west direction), but the region of seafloor with depths shallow enough to support a coral reef ecosystem is about 10 km wide; this shelf constrains the size and shape of the reefscape. The mapped region of Andavadoaka (Appendix I-B) is 50 km long (north-south direction) and similar reef systems extend along 350 km of coastline. The habitat classes with the largest elongated patches in Andavadoaka include reef, sand, and sparse algae; together they comprise 66% (Figure 13) of the map, which suggests an elongated trend on the ecosystem-scale.

The island of Vieques is a linear-shaped block bound by oceanic trenches and troughs and therefore its surrounding shelf takes on the same form as the island itself. In

the map of Vieques (Appendix I-A), the largest elongated patches were reef, sand, and dense seagrass. These classes equaled a total of 72% (Figure 13) of the reefscape and they quantitatively captured the overall shelf/island linearity.

When comparing these patch shape patterns among various reef environments, a larger sample of benthic habitat maps would certainly provide more robust statistics. If more circular reef systems without attached landmasses, such as isolated atolls or shoals, were analyzed with metrics, the results could provide insight on whether or not these shape relationships hold for a larger assortment of reef structures.

4.6 Fractal dimension and fractal span

Ecosystem disturbance regimes are a mechanism that explains the prevalence of a large percent of habitat patches with simple boundaries, described by fractal dimension (Figure 22) and fractal span (Figure 23), as well as small sizes (Figures 18 & 19), described by *EP*. The sequence of ecological succession following a highly destructive disturbance begins with first stages of recovery described by patches with low organism abundance, low shape complexity, small size, and poor interspersion. Later stages of ecological succession are characterized by higher values in all these patch descriptors. The three sites considered here have similar disturbance regimes due to a high frequency of occurrence of tropical storms, typhoons, and hurricanes (Table 1). These reef systems each lie in a major cyclone zone (Figure 24) and the probability of a major storm causing a disturbance is at least 1 in every 5 years for all sites. The last major hurricanes to hit Vieques were Hugo (category 4) in 1989, Marilyn (cat 2) in 1995, and George (cat 2) in 1998. Saipan's most recent major typhoons were Paka (cat 5) in 1997, Pongsona (cat 4) in 2002, Chaba (cat 2) in 2004, Nabi (cat 5) in 2005, and Kong-rey (cat 3) in 2007. In Andavadoaka, the recent major cyclones were Geralda (tropical storm) in 1994, Leon-Eline (tropical storm) in 2000, Gafilo (cat 1) and Elita (cat 1) in 2004, and Fanele (cat 2) in 2009.

If cyclone disturbances inhibit certain assemblages from attaining spatial dominance, early successional stages are maintained. These natural and cyclical events may be the underlying cause of the ecological spatial patterns quantified in this study.

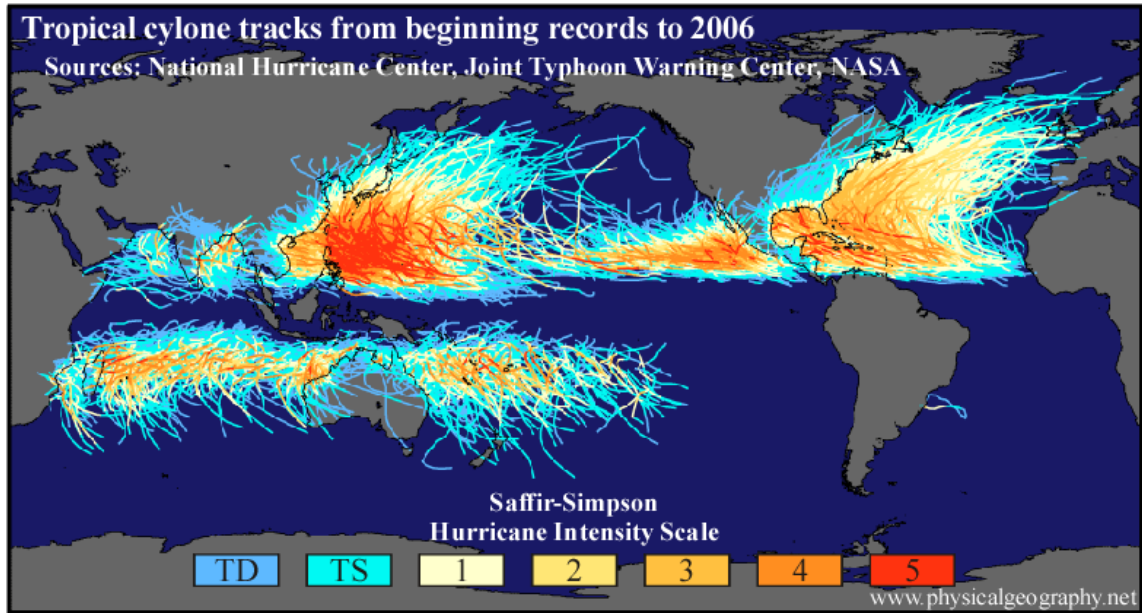


Figure 24: Worldwide geographic distribution of tropical cyclone paths indicating that all study sites are frequently disturbed by major storm events.

Purkis *et al.* (2007) found similar patterns suggesting early successional stages among modern reefs, but the study regions were all located in known cyclone paths in the Pacific Ocean. A spatial analysis, similar to this study, of reef systems which are unaffected by the destructive forces of cyclones (or other major disturbance regimes) could provide interesting data on stages of ecological succession. Perhaps those reefs would illustrate environmental characteristics of systems that have progressed to much later successional stages. Regions of interest for benthic habitat mapping that would help answer this question include reef ecosystems in the Red Sea, Arabian Gulf, Sulawesi, Malaysia, and Brazil; all of these places are spared from the geographical influence of tropical cyclones (Figure 24). In another view, an appealing long-term change detection mapping effort would be to examine a reef ecosystem with consecutive high spatial resolution images from before and after a cyclone disturbance to observe spatial changes among habitats, recovery time, and successional stages.

4.7 Error analysis

Classifying pixels in satellite imagery using an unsupervised method (*i.e.* ISODATA), as was the case in this mapping project, inherently produces errors. The manual digitization process was performed to reduce classification errors by relying on groundtruth data and human interpretations of benthic substrates. Accuracy assessments are ideal for all thematic maps and they are usually achieved by splitting the groundtruth data in half, using 50% of the points to create the map and 50% of the points to assess the map's accuracy. Another method is to generate the map from one set of data and then return to the study location to collect a second round of groundtruth data, which would be used to assess accuracy. In this research project, 100% of the groundtruth points were used to create the maps, instead of separating them for an accuracy assessment. The goal was to produce more accurate maps with all the available data incorporated. This approach was employed for two reasons: (1) logistically it was not feasible to return to the sites and collect a second round of groundtruth data (2) there were a limited number of points collected during field surveys, therefore it was beneficial to utilize all of them during digitization. Consequently, a subjective interpretation is that each map is approximately 75-80% accurate.

A question must follow, how might classification errors affect the metric calculations and analyses? If a small quantity of habitat patches were incorrectly identified, the results would be influenced to some extent. Possible concerns arise when habitats were analyzed separately, however, results that were related to all polygons or all sites would not be significantly affected. The reason being, habitat boundaries were very easily mapped from contrasting colors in the images, but if groundtruth points were not located within a patch boundary, occasionally it was difficult to identify substrate composition, leading to classification errors. Results from habitat percentages, depths, rugosities, and neighborhood transitions were examined by habitat, and thus may have been influenced more by classification errors. The results from *EP*, compactness, *PAR*, fractal dimension, and fractal span were all considered by site or for all polygons combined, so even if some polygons were misidentified, overall patch areas and shapes would not have been affected.

4.8 Summary: quantified spatial patterns and future research

The geological histories of the three sites within this study were extremely diverse. Tectonic slumping of a Pleistocene surface on a volcanic arc island created antecedent topography in Saipan, a broad continental shelf with barrier islands controlled the system in Andavadoaka, and sea-level driven backstepping shelf reefs categorized the Vieques system. Even with these distinct backgrounds, metric analyses indicated strong similarities between sites. The unifying theme behind these similarities is that each study site possessed comparable “linear templates” upon which the reef systems initiated and developed. This suggests that spatial patterns in reef ecosystems are somewhat controlled by antecedent topography, but once a “template” is in place, the systems develop in an equivalent manner due to environmental conditions and biological influences.

Habitat percentages (Figure 13) revealed that $\geq 74\%$ of each map was composed of 2-4 classes, sand, reef, seagrass, and algae. Also, the ratio of unconsolidated to consolidated (Figure 14) benthic substrates was relatively equivalent. For these reasons, perhaps fine mapping of habitat classes (*e.g.* ≥ 5 categories) is unnecessary for certain applications and relevant information, such as successional stage, could be extracted from maps with fewer classification groups, thereby decreasing the required time it takes to edit and digitize polygons.

The depth and rugosity (Figure 16) analyses showed the general trend of shallow classes being non-rugose and deep classes being rugose. The slope, or change in rugosity with increasing depth, was statistically similar between sites, implying that analogous environmental influences are controlling vertical relief.

Neighborhood transition outcomes (Figure 17 & Table 3) showed promise for predicting the juxtaposition of habitats and transition tallies can also be useful in investigating ecological dynamics through time from a snap-shot image (*e.g.* Purkis and Riegl 2005).

A noteworthy goal of deriving these neighborhood relationships and computing spatial metrics is to construct a classification method that will automatically and objectively map coral reef ecosystems and eliminate manual subjective visual interpretation of satellite images. Perhaps an automated technique for reefscape scale mapping will come to fruition. The concept has already been established in the fields of

remotely sensing forests and agricultural fields. Intuitively, advances in remote sensing capabilities develop from land-based research prior to being applied to marine environments due to water column hindrances.

The idea of automated habitat mapping based on spectral signatures does seem plausible as sensor technology advances, correction algorithms (atmospheric, sea-surface, water column) become more robust, and optical measurements of the spectral signatures of reefal components are accumulated. Yet, whether the automation will be based on spatial statistics and/or spectra is presently unknown because further research needs to be done at the reefscape scale.

When considering neighborhood transition probabilities as inputs for an automated mapping method, a legitimate sample of reefs would have to be mapped to very high accuracy ($\geq 90\%$). If neighborhood probabilities were calculated for every sample, emergent statistical rules could begin to be applied during classifications. Eventually, when acceptable significant statistics are derived from every type of reef system, the rules could be incorporated into supervised classifications using hierarchical classification trees to supplement spectral signatures of seafloor features.

Classification trees are used to predict the membership of objects to classes. Therefore, if insufficient mapping funds or few groundtruth data are available, these rules could help generate more accurate maps by including neighborhood probabilities. To provide an example, statistical rules derived from all the sampled barrier reef systems could be used to help map a specific unknown barrier reef. An unknown dark patch in the barrier reef without ground verification could be assigned to an appropriate habitat class based on probabilities from the hierarchical classification tree.

Separating reef ecosystem neighborhood probabilities by general reef structure (*e.g.* fringing reef statistics vs. isolated platform statistics) would produce more robust rules to incorporate into hierarchical classification trees, rather than lumping all statistics into one set of rules for all reef systems. In order to accomplish such a task, a substantially large sample size for every type of reef system would be necessary and as more reef environments are mapped at the reefscape scale, we continue to approach a large enough sample of habitat maps to generate reliable neighborhood statistics.

Exceedance probability results from studying patch size and frequency of occurrence (Figures 18, 19 & Table 4) demonstrated that a predictable relationship existed; small patches were very common and large patches were rare. This adherence to a power law across 5 orders of magnitude implied that these reefscape mosaics displayed fractal behavior and were therefore scale invariant. This information is valuable because a predictable relationship between the frequency and size of habitat patches found at observable scales can be used to interpolate the behavior of the system at unobservable finer scales. Also, when exceedance probabilities are broken down by habitat (critical dense seagrass meadows example), the data can help managers predict the number of habitat patches that will be included when designing or expanding an MPA.

Patch geometry investigations (Figures 20 & 21) showed a common trend with smaller polygons possessing circular boundaries and larger polygons having linear or elongate boundaries. These shape metrics provided information about the scale of hydrodynamic directional forcing, as well as the scale at which the size of continental shelves interact with habitat configurations.

Patch shape complexities (Figures 22 & 23) confirmed that 90% of each map was composed of geometrically simple patches and 10% was made up of very intricate complex shapes. Considering that the first stages of recovery from major disturbances are described by patches with low shape complexity and small size, these ecosystems seem to be in the beginning phases of ecological succession, likely from cyclone impacts.

Taking the compilation of metrics into account, the question remaining is can satellite-derived habitat maps and morphometrics be used to predict spatial arrangements within reefal environments? Because the results were so comparable between sites, spatial prediction seems very plausible. Not only does this have implications for automated habitat mapping techniques, but there are positive implications for MPA conservation planning and management.

The era of single-species management is over. Overexploitation of fisheries, habitat destruction, sedimentation, pollution, and warming ocean temperatures are among the many reasons why coral reef ecosystems are collapsing around the world. Few people would argue that reefs are not in dire need of aid. Adapting landscape ecology principles to the marine environment to manage systems holistically, instead of individual

commercially important species, is crucial for the survival of coral reefs. Furthermore, to solve these environmental issues on regional scales, cooperative and coordinated management of resources among agencies is urgently needed.

5. CONCLUSION

This study combined a multitude of data sources, allowing a unique in-depth analysis of coral reef GIS databases and map products in an effort to better understand ecological patterns. Any one of the study sites could have rightfully been analyzed by itself, therefore the entire collection of information was quite extensive and exciting to work with.

Coral reef mapping has only been implemented relatively recently. There has been an increase in remote sensing applications targeting reef environments, which reflects the growing concern about drastic and negative changes occurring on reefs over the past three decades due to anthropogenic and natural stressors (Andréfouët *et al.* 2003). Advances in technology, accuracy (Lim *et al.* 2009), and the speed at which physical aspects of marine and coastal areas can be mapped have greatly increased (Wright and Heyman 2008). But, with only 5-10% of the world's seafloor mapped with the resolution of similar studies on land, benthic marine mapping still represents a persistent gap in our knowledge (Wright and Heyman 2008). Furthermore, image processing techniques and mapping methodologies are currently still being investigated in the marine realm and as a result, there is a current lack of standardization in mapping marine benthos. Although there is a growing establishment of scientists working on applications of landscape ecology principles to marine studies, few coral reef scientists have examined spatial patterns across entire reefscapes with an ecosystem-based view. The necessity to solve coral reef environmental issues on a regional scale is evident and future research should focus on producing ecosystem assessments that can be applied in management strategies.

REFERENCES

- Andréfouët S (2008) Coral reef habitat mapping using remote sensing: a user vs. producer perspective - implications for research, management, and capacity building. *Journal of Spatial Science* 53, 1:113-129.
- Andréfouët S, Kramer P, Torres-Pulliza D, Joyce K, Hochberg E, Garza-Pérez R, Mumby P, Riegl B, Yamano H, White W, Zubia M, Brock J, Phinn S, Naseer A, Hatcher B, Muller-Karger F (2003) Multi-site evaluation of IKONOS data for classification of tropical coral reef environments. *Remote Sensing of Environment* 88:128-143.
- Andréfouët S, Zubia M, and Payri C (2004) Mapping and biomass estimation of the invasive brown algae *Turbinaria ornata* (Turner) J. Agardh and *Sargassum mangarevense* (Grunow) Setchell on heterogeneous Tahitian coral reefs using 4-meter resolution IKONOS satellite data. *Coral Reefs* 23:26-38.
- Andrews B (2003) Techniques for spatial analysis and visualization of benthic mapping data. SAIC Report No.623 for NOAA Coastal Services Center. Available: www.csc.noaa.gov/benthic/mapping/pdf/spatial.pdf.
- Arias-González J, Done T, Page C, Cheal A, Kininmonth S, and Garza-Pérez J (2006) Towards a reefscape ecology: relating biomass and trophic structure of fish assemblages to habitat at Davies Reef, Australia. *Marine Ecology Progress Series* 320:29-41.
- Avnir D, Biham O, Lidar D, and Malcai O (1998) Is the geometry of nature fractal? *Science* 279:5347.
- Besairie H (1964) Geological Map of Madagascar. Tananarive: Service Géologique de Madagascar.
- Bell S, Fonseca M, and Kenworthy W (2008) Dynamics of a subtropical seagrass landscape; links between disturbance and mobile seed banks. *Landscape Ecology* 23:67-74.
- Benfield S, Guzman H, Mair J, and Young J (2007) Mapping the distribution of coral reefs and associated sublittoral habitats in Pacific Panama: a comparison of optical satellite sensors and classification methodologies. *International Journal of Remote Sensing* 28, 22:5047-5070.
- Briggs R, and Ackers J (1965) Hydrogeologic map of Puerto Rico and adjacent islands: U.S. Geological Survey Hydrologic Investigations Atlas HA-197, 1 sheet, scale 1:240,000.
- Byrne D, Suarez G, and McCann W (1985) Muertos trough subduction - microplate tectonics in the northern Caribbean? *Nature* 317: 420-421.

- Capolsini P, Andréfouët S, Rion C, and Payri C (2003) A comparison of Landsat ETM+, SPOT HRV, IKONOS, ASTER, and airborne MASTER data for coral reef habitat mapping in South Pacific islands. *Canadian Journal of Remote Sensing* 29, 2:187-200.
- Cassata L, and Collins L (2008) Coral reef communities, habitats, and substrates in and near sanctuary zones of Ningaloo Marine Park. *Journal of Coastal Research* 24, 1:139-151.
- Chamberlain J, and Graus R (1975) Water flow and hydromechanical adaptations of branched reef corals. *Bulletin of Marine Science* 25, 1:112-125.
- Chauvaud S, Bouchon C, and Manière (1998) Remote sensing techniques adapted to high resolution mapping of tropical coastal marine ecosystems (coral reefs, seagrass beds and mangrove). *International Journal of Remote Sensing* 19, 18:3625-3639.
- Cloud P (1959) Geology of Saipan, Mariana Islands, Part 4 Submarine topography and shoal water ecology. US Geological Survey Professional Paper 280-K p.361-445.
- Cloud P, Schmidt R, and Burke H (1956) Geology of Saipan, Mariana Islands, Part 1 General geology. US Geological Survey Professional Paper 280-A p.1-126.
- Costa B, Battista T, and Pittman S (2009) Comparative evaluation of airborne LiDAR and ship-based multibeam SoNAR bathymetry and intensity for mapping coral reef ecosystems. *Remote Sensing of Environment* 113:1082-1100.
- Crawford T, Commito J, and Brorwik A (2005) Fractal characterization of *Mytilus edulis* L. spatial structure in intertidal landscapes using GIS methods. *Landscape Ecology* 21:1033-1044.
- Dahdough-Guebas F (2002) The use of remote sensing and GIS in the sustainable management of tropical coastal ecosystems. *Environment, Development, and Sustainability* 4:93-112.
- Darcy M, and Eggleston D (2005) Do habitat corridors influence animal dispersal and colonization in estuarine systems? *Landscape Ecology* 20:841-855.
- Done T (1982) Patterns of distribution of coral communities across the central GBR. *Coral Reefs* 1:95-107.
- Du Puy D, and Moat J (1996) A refined classification of the primary vegetation of Madagascar based on the underlying geology: using GIS to map its distribution and to assess its conservation status. In: W.R. Lourenço (editor). *Proceedings of the International Symposium on the Biogeography of Madagascar* p.205--218, + 3 maps.

- Elvidge C, Dietz J, Berkelmans R, Andréfouët S, Skirving W, Strong A, and Tuttle B (2004) Satellite observation of Keppel Islands (Great Barrier Reef) 2002 coral bleaching using IKONOS data. *Coral Reefs* 23:123-132.
- Fedra K, and Feoli E (1998) GIS technology and spatial analysis in coastal zone management. *EEZ Technology* Ed. 3:171-179.
- Gabrié C, Vasseur P, Randriamiarana H, Maharavo J, and Mara E (2000) Coral reefs of the Indian Ocean: the coral reefs of Madagascar. Oxford University Press, New York p.411-444.
- Garza C (2008) Relating spatial scale to patterns of polychaete species diversity in coastal estuaries of the Western United States. *Landscape Ecology* 23:107-121.
- Garza-Pérez J, Lehmann A, and Arias-González J (2004) Spatial prediction of coral reef habitats: integrating ecology with spatial modeling and remote sensing. *Marine Ecology Progress Series* 269:141-152.
- Gilad E, von Hardenberg J, Provenzale A, Schachak M, and Meron E (2004) Ecosystem engineers: from pattern formation to habitat creation. *Physical Review Letters* 93:098105.
- Graus R, and Macintyre I (1989) The zonation patterns of Caribbean coral reefs as controlled by wave and light energy input, bathymetric setting and reef morphology: computer simulation experiments. *Coral Reefs* 8:9-18.
- Grober-Dunsmore R, Frazer T, Lindberg W, and Beets J (2007) Reef fish and habitat relationships in a Caribbean seascape: the importance of reef context. *Coral Reefs* 26:201-216.
- Grober-Dunsmore R, Frazer T, Beets J, Lindberg W, Zwick P, and Funicelli N (2008a) Influence of landscape structure on reef fish assemblages. *Landscape Ecology* 23:37-53.
- Grober-Dunsmore R, Hale J, Beets J, Frazer T, Funicelli N, and Zwick P (2008b) Applying landscape ecology principles to the design and management of marine reserves. Florida Integrated Science Center (FISC), Biological Resources Division, U.S. Geological Survey (USGS). Available: http://fl.biology.usgs.gov/posters/Coral_and_Marine/Mngmt_of_Marine_Reserves/mngmt_of_marine_reserves.html.
- Hamylton S, and Spencer T (2008) An investigation of seagrass patterns at Alphonse Atoll, Seychelles: linking structure to function in marine landscapes. Proceedings from the 11th International Coral Reef Symposium, Ft. Lauderdale, Florida 7-11 July 2008, Session 17.

- Harborne A, Mumby P, Zychaluk K, Hedley J, and Blackwell P (2006) Modeling the beta diversity of coral reefs. *Ecology* 87, 11:2871-2881.
- Hatcher B (1997) Coral reef ecosystems: how much greater is the whole than the sum of the parts? *Coral Reefs* 16, 1:S77-S91.
- Hedley J, Harborne A, and Mumby P (2005) Simple and robust removal of sun glint for mapping shallow-water benthos. *International Journal of Remote Sensing* 26, 10:2107-2112.
- Hewitt J, Thrush S, Legendre P, Funnell G, Ellis J, and Morrison M (2004) Mapping of marine soft-sediment communities: integrated sampling for ecological interpretation. *Ecological Applications* 14:1203-1216.
- Hinchey E, Nicholson M, Zajac R, and Irlandi E (2008) Preface: Marine and coastal applications in landscape ecology. *Landscape Ecology* 23:1-5.
- Hochberg E, Andréfouët S, and Tyler M (2003) Sea surface correction of high spatial resolution IKONOS images to improve bottom mapping in near-shore environments. *IEEE Transactions on Geosciences and Remote Sensing* 41:1724-1729.
- Hochberg E, and Atkinson M (2003) Capabilities of remote sensors to classify coral, algae, and sand as pure and mixed spectra. *Remote Sensing of Environment* 85:174-189.
- Hogrefe K, Wright D, and Hochberg E (2008) Derivation and integration of shallow-water bathymetry: implications for coastal terrain modeling and subsequent analyses. *Marine Geodesy* 31, 4:299 - 317.
- Hovel K, and Regan H (2008) Using an individual-based model to examine the roles of habitat fragmentation and behavior on predator-prey relationships in seagrass landscapes. *Landscape Ecology* 23:75-89.
- Irlandi E, Ambrose W, and Orlando B (1995) Landscape ecology and the marine environment; how spatial configuration of seagrass habitat influences growth and survival of the bay scallop. *Oikos* 72, 3:307-313.
- Jackson J (1991) Adaptation and diversity of reef corals. *BioScience* 41, 7:475-482.
- Kendall M, and Miller T (2008) The influence of thematic and spatial resolution on maps of a coral reef ecosystem. *Marine Geodesy* 31:75-102.
- Kennedy D, and Woodroffe C (2002) Fringing reef growth and morphology: a review. *Earth-Science Reviews* 57, 3-4: 255-277.

- Knight D, LeDrew E, and Holden H (1997) Mapping submerged corals in Fiji from remote sensing and *in situ* measurements: applications for integrated coastal management. *Ocean & Coastal Management* 34, 2:153-170.
- Kutina J (1975) Tectonic development and metallogeny of Madagascar with reference to the fracture pattern of the Indian Ocean. *Geological Society of America Bulletin* 86, 4:582-592.
- Langmead O, and Sheppard C (2004) Coral reef community dynamics and disturbance: a simulation model. *Ecological Modelling* 175:271-290.
- Learned R, Grove G, and Boissen R (1973) A geochemical reconnaissance of the island of Vieques, Puerto Rico: U.S. Geological Survey Open-File Report, unnumbered, 78 p. 2 pls.
- Lejeune O, Tlidi M, and Coueron P (2002) Localized vegetation patches: a self-organized response to resource scarcity. *Physical Review E* 66:010901.
- Levitan D, and Genovese S (1989) Substratum-dependent predator-prey dynamics: patch reefs as refuges from gastropod predation. *Journal of Experimental Biology* 130:111-118.
- Lim A, Hedley J, LeDrew E, Mumby P, and Roelfsema C (2009) The effects of ecologically determined spatial complexity on the classification accuracy of simulated coral reef images. *Remote Sensing of Environment* 113:965-978.
- Maeder J, Narumalani S, Rundquist D, Perk R, Schalles J, Hutchins K, and Keck J (2002) Classifying and mapping general coral reef structure using IKONOS data. *Photogrammetric Engineering and Remote Sensing* 68, 12:1297-1305.
- Mather P (1997) *Computer processing of remotely sensed images*. Wiley, Chichester.
- McClanahan T, Polunin N, and Done T (2002) Ecological states and the resilience of coral reefs. *Conservation Ecology* 6, 2:18 [online]. Available: <http://www.consecol.org/vol6/iss2/art18/>
- Mishra D, Narumalani S, Rundquist D, and Lawson M (2006) Benthic habitat mapping in tropical marine environments using QuickBird multispectral data. *Photogrammetric Engineering and Remote Sensing* 72, 9:1037-1048.
- Mistr S, and Bercovici D (2003) A theoretical model of pattern formation in coral reefs. *Ecosystems* 6, 1:61-74.
- Moore C (2001) *Developments in Sedimentology vol.55: carbonate reservoirs - porosity evolution and diagenesis in a sequence stratigraphic framework*. Elsevier, Amsterdam.

- Moufaddal W (2005) Use of satellite imagery as environmental impact assessment tool: a case study from the NW Egyptian Red Sea coastal zone. *Environmental Monitoring and Assessment* 107:427-452.
- Mumby P (2001) Beta and habitat diversity in marine systems: a new approach to measurement, scaling and interpretation. *Oecologia* 128:274-280.
- Mumby P, Clark C, Green E, and Edwards A (1998) Benefits of water column correction and contextual editing for mapping coral reefs. *International Journal of Remote Sensing* 19:203-210.
- Mumby P, and Edwards A (2002) Mapping marine environments with IKONOS imagery: enhanced spatial resolution can deliver greater thematic accuracy. *Remote Sensing of Environment* 82:248-257.
- Mumby P, Green E, Edwards A, and Clark C (1999) The cost-effectiveness of remote sensing for tropical coastal resources assessment and management. *Journal of Environmental Management* 3:157-166.
- Mumby P, and Harborne A (1999) Development of a systematic classification scheme of marine habitats to facilitate regional management of Caribbean coral reefs. *Biological Conservation* 88, 2:155-163.
- Mumby P, Skirving W, Strong A, Hardy J, LeDrew E, Hochberg E, Stumpf R, and David L (2004) Remote sensing of coral reefs and their physical environment. *Marine Pollution Bulletin* 48, 3-4:219-228.
- Nadon M, Griffiths D, and Doherty E (2005) The coral reefs of Andavadoaka, southwest Madagascar. Blue Ventures report. London, UK p.29.
- Nyström M, and Folke C (2001) Spatial resilience of coral reefs. *Ecosystems* 4:406-417.
- Paine R, and Levin S (1981) Intertidal landscapes: disturbance and the dynamics of pattern. *Ecological Monographs* 51, 2:145-178.
- Palandro D, Andréfouët S, Dustan P, and Muller-Karger F (2003) Change detection in coral reef communities using IKONOS satellite sensor imagery and historic aerial photographs. *International Journal of Remote Sensing* 24, 4:873-878.
- Pascual M, and Guichard F (2005) Criticality and disturbance in spatial ecological systems. *Trends in Ecology & Evolution* 20, 2:88-95.
- Peura M, and Iivarinen J (1997) Efficiency of simple shape descriptors. *Advances in visual form analysis*. Singapore, World Scientific, p.443-451.

- Pittman S, Costa B, and Battista T (2009) Using lidar bathymetry and boosted regression trees to predict the diversity and abundance of fish and corals. *Journal of Coastal Research* 53:27-38.
- Pittman S, McAlpine C, and Pittman K (2004) Linking fish and prawns to their environment: a hierarchical landscape approach. *Marine Ecology Progress Series* 283:233-254.
- Purkis S (2005) A “reef-up” approach to classifying coral habitats from IKONOS imagery. *IEEE Transactions on Geoscience and Remote Sensing* 43, 6:1375-1390.
- Purkis S, Graham N, and Riegl B (2008) Predictability of reef fish diversity and abundance using remote sensing data in Diego Garcia (Chagos Archipelago). *Coral Reefs* 27:167-178.
- Purkis S, Kohler K, Riegl B, and Rohmann S (2007) The statistics of natural shapes in modern coral reef landscapes. *The Journal of Geology* 115: 493-508.
- Purkis S, Myint S, and Riegl B (2006) Enhanced detection of the coral *Acropora cervicornis* from satellite imagery using a textural operator. *Remote Sensing of Environment* 101:82-94.
- Purkis S, and Riegl B (2005) Spatial and temporal dynamics of Arabian Gulf coral assemblages quantified from remote-sensing and *in situ* monitoring data. *Marine Ecology Progress Series* 287:99-113.
- Purkis S, Riegl B, and Andréfouët S (2005) Remote sensing of geomorphology and facies patterns on a modern carbonate ramp (Arabian Gulf, Dubai, U.A.E.). *Journal of Sedimentary Research* 75:861-876.
- Rankey E (2002) Spatial patterns of sediment accumulation on a Holocene carbonate tidal flat, Northwest Andros Island, Bahamas. *Journal of Sedimentary Research* 72, 5:591-601.
- Renken R, Ward W, Gill I, Gomez-Gomez F, and Rodriguez-Martinez J (2002) Geology and hydrogeology of the Caribbean Islands aquifer system of the Commonwealth of Puerto Rico and the U.S. Virgin Islands. U.S. Geological Survey Professional Paper 1419.
- Riegl B, Moyer R, Walker B, Kohler K, Gilliam D, and Dodge R (2008) A tale of germs, storms, and bombs: geomorphology and coral assemblage structure at Vieques (Puerto Rico) compared to St. Croix (U.S. Virgin Islands). *Journal of Coastal Research* 24, 4:1008-1021.

- Riegl B, and Purkis S (2005) Detection of shallow subtidal corals from IKONOS satellite and QTC View (50, 200 kHz) single-beam sonar data (Arabian Gulf; Dubai, UAE). *Remote Sensing of Environment* 95, 1:96-114.
- Riegl B, Purkis S, Houk P, Cabrera G, and Dodge R (2008) Coral Reefs of the USA: Geologic setting and geomorphology of coral reefs in the Mariana Islands (Guam and Commonwealth of the Northern Mariana Islands). Springer, p.691-718.
- Rietkerk M, and van de Koppel J (2008) Regular pattern formation in real ecosystems. *Trends in Ecology & Evolution* 23, 3:169-175.
- Rioja-Nieto R, and Sheppard C (2008) Effects of management strategies on the landscape ecology of a Marine Protected Area. *Ocean & Coastal Management* 51:397-404.
- Robbins B, and Bell S (1994) Seagrass landscapes: a terrestrial approach to the marine environment. *Trends in Ecology & Evolution* 9, 8:301-304.
- Rogers B (1998) Karst and caves of Madagascar. Available: <http://www.sgp.org.pl/gw/hd/madaga.htm>.
- Rohani P, Lewis T, Grünbaum D, and Ruxton G (1997) Spatial self-organization in ecology: pretty patterns or robust reality? *Trends in Ecology & Evolution* 12, 2:70-74.
- Rowlands G, Purkis S, and Riegl B (2008) The 2005 coral-bleaching event Roatán (Honduras): Use of pseudo-invariant features (PIFs) in satellite assessments. *Journal of Spatial Science* 53, 1:99-112.
- Schlager W (2004) Fractal nature of stratigraphic sequences. *Geology* 32, 3:185-188.
- Sebens K, Helmuth B, Carrington E, and Agius B (2003) Effects of water flow on growth and energetic of the scleractinian coral *Agaricia tenuifolia* in Belize. *Coral Reefs* 22:35-47.
- Sibson R (1981) A brief description of natural neighbor interpolation. *Interpolating multivariate data*. John Wiley & Sons, New York p. 21-36.
- Sleeman J, Boggs G, Radford B, and Kendrick G (2005) Using agent-based models to aid reef restoration: enhancing coral cover and topographic complexity through the spatial arrangement of coral transplants. *Restoration Ecology* 13, 4:685-694.
- Stallins J (2006) Geomorphology and ecology: unifying themes for complex systems in biogeomorphology. *Geomorphology* 77:207-216.
- Steele J (1989) The ocean 'landscape'. *Landscape Ecology* 3, 3/4:185-192.

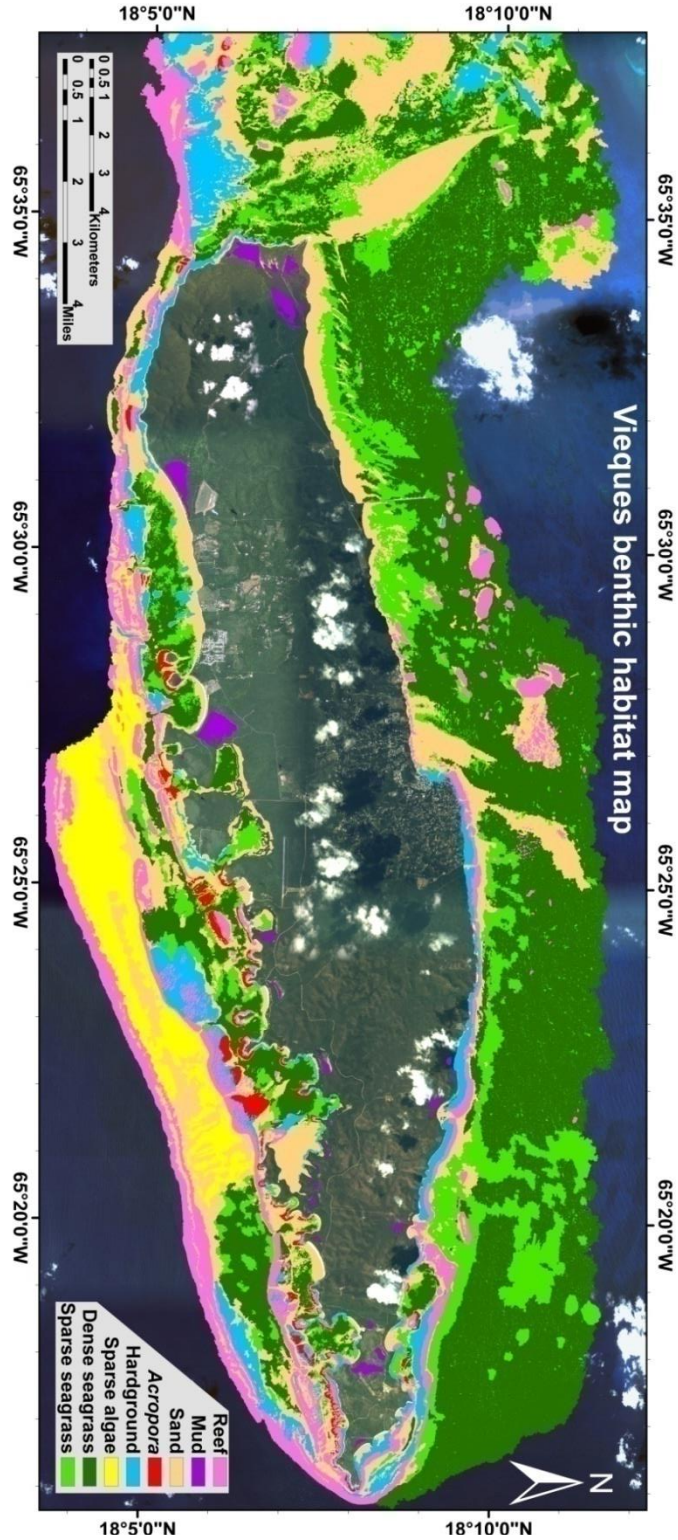
- Stumpf R, Holderied K, and Sinclair M (2003) Determination of water depth with high-resolution satellite imagery over variable bottom types. *Limnology and Oceanography* 48:547-556.
- Thanilachalam M, and Ramachandran S (2002) Management of coral reefs in Gulf of Mannar using remote sensing and GIS techniques – with reference to coastal geomorphology and land use. *Map Asia 2002, Asian Conference on GIS, GPS, Aerial Photography and Remote Sensing*. Bangkok, Thailand, Aug 7-9. Available: <http://www.gisdevelopment.net/application/nrm/coastal/mnm/nrmmm008.htm>.
- Turcotte D (1989) Fractals in geology and geophysics. *Pure and Applied Geophysics* 131, 1-2:171-196.
- Urban D, O'Neill R, and Shugart H (1987) Landscape ecology: a hierarchical approach can help scientists understand spatial patterns. *Bioscience* 37, 2:119-127.
- van Gestel J, Mann P, Grindlay N, and Dolan J (1999) Three-phase tectonic evolution of the northern margin of Puerto Rico as inferred from an integration of seismic reflection, well, and outcrop data. *Marine Geology* 161, 2-4: 257-286.
- Vela A, Pasqualini V, Leoni V, Djelouli A, Langar H, Pergent G, Pergent-Martini C, Ferrat L, Ridha M, and Djabou H (2008) Use of SPOT 5 and IKONOS imagery for mapping biocenoses in a Tunisian coastal lagoon (Mediterranean Sea). *Estuarine, Coastal and Shelf Science* 79, 4:591-598.
- Velondriake MPA (2008) Blue Ventures. Available: <http://www.livewiththesea.org/ecology/marine.htm>.
- von Hardenberg J, Meron E, Schachak M, and Zarmi Y (2001) Diversity of vegetation patterns and desertification. *Physical Review Letters* 87:198101.
- Walker B, Riegl B, and Dodge R (2008) Mapping coral reef habitats in Southeast Florida using a combined technique approach. *Journal of Coastal Research* 24, 5:1138-1150.
- Walsh S, Butler D, and Malanson G (1998) An overview of scale, pattern, process relationships in geomorphology: a remote sensing and GIS perspective. *Geomorphology* 21:183-205.
- Wang Y, Chen Y, Li J (2007) Mapping coral reef benthic cover with fused IKONOS imagery. *Proceedings from Geoinformatics 2007: Remotely Sensed Data and Information*, 25 May, Nanjing, China.
- WHOI Seminar (2001) Marine protected areas: finding a balance between conservation and fisheries management. Adapted from symposium lectures in: "Fisheries, Oceanography and Society, Marine Protected Areas: Design and Implementation for Conservation and Fisheries Restoration," presented by the Ocean Life Institute of the

- Woods Hole Oceanographic Institution on August 27-29, 2001. Available:
<http://www.fathom.com/course/21701790/index.html>.
- Wongprayoon S, Vieira C, Leach J (2007) Spatial accuracy assessment for coral reef classifications. Anais XIII Simpósio Brasileiro de Sensoriamento Remoto, Florianópolis, Brasil, 21-26 April, INPE p.6273-6281.
- Wright D, and Heyman W (2008) Marine and coastal GIS for geomorphology, habitat mapping, and marine reserves. *Marine Geodesy* 31, 4: *in press*.
- Yang X, and Liu Z (2005) Quantifying landscape pattern and its change in an estuarine watershed using satellite imagery and landscape metrics. *International Journal of Remote Sensing* 26, 23:5297-5323.
- Zajac R (2008) Challenges in marine, soft-sediment benthoscape ecology. *Landscape Ecology* 23:7-18.
- Zajac R, Lewis R, Poppe L, Twichell D, Vozarik J, and DiGiacomo-Cohen M (2003) Responses of infaunal populations to benthoscape patch structure and the potential importance of transition zones. *Limnology & Oceanography* 48:829-842.
- Zharikov Y, Skilleter G, Loneragan N, Taranto T, and Cameron B (2005) Mapping and characterizing subtropical estuarine landscapes using aerial photography and GIS for potential application in wildlife conservation and management. *Biological Conservation* 125:87-100.

APPENDICES

Appendix I: Benthic habitat maps and keys

A. Vieques



Acropora

Dense thickets of dead *Acropora palmata* stumps interspersed with occasional living colonies. In deeper water, many *A. palmata* skeletons remain in life position, while others have been reduced to rubble and provide in-fill to the framework. In the shallow high-energy coastal zones, dead *A. palmata* stumps and rubble are present in semi-circular formations surrounding headlands.



Reef

Rugose hardground with sparse (2-5%) live coral cover composed primarily of *S. siderea*, *Diploria sp.*, *M. annularis*, and *C. natans*. Present but at low abundance are *A. palmata*, *A. cervicornis*, and *A. prolifera*. Gorgonian cover is high. Coralline algae and turf algae dominate the substrate available for coral settlement as well as cover dead coral colonies.



Hardground

Sandy hardgrounds with dense gorgonian cover and sparse macro-algae assemblages which consist of *Halimeda sp.*, *Udotea sp.*, *Turbinaria sp.*, *Penicillus sp.*, and *Styopodium zonale*.



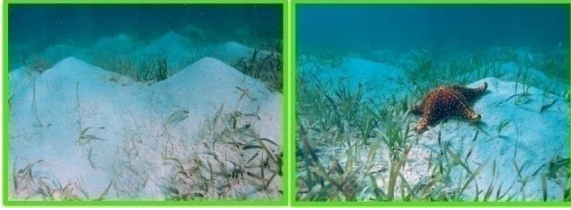
Dense seagrass

Sand sheets densely colonized (50-100% cover) by primarily *Thalassia testudinum* and secondarily by *Syringodium filiforme*. Intermittent algae (*Halimeda sp.*, *Udotea sp.*, *Turbinaria sp.*, *Penicillus sp.*, and *Styopodium zonale*) is associated with these seagrass meadows.



Sparse seagrass

As for dense seagrass, but low to medium density (0-50%) cover. This sparse seagrass assemblage typically characterizes the periphery of dense meadows.



Sparse algae

Coarse rippled unconsolidated sand sheets with sparse turf and macro-algae cover.



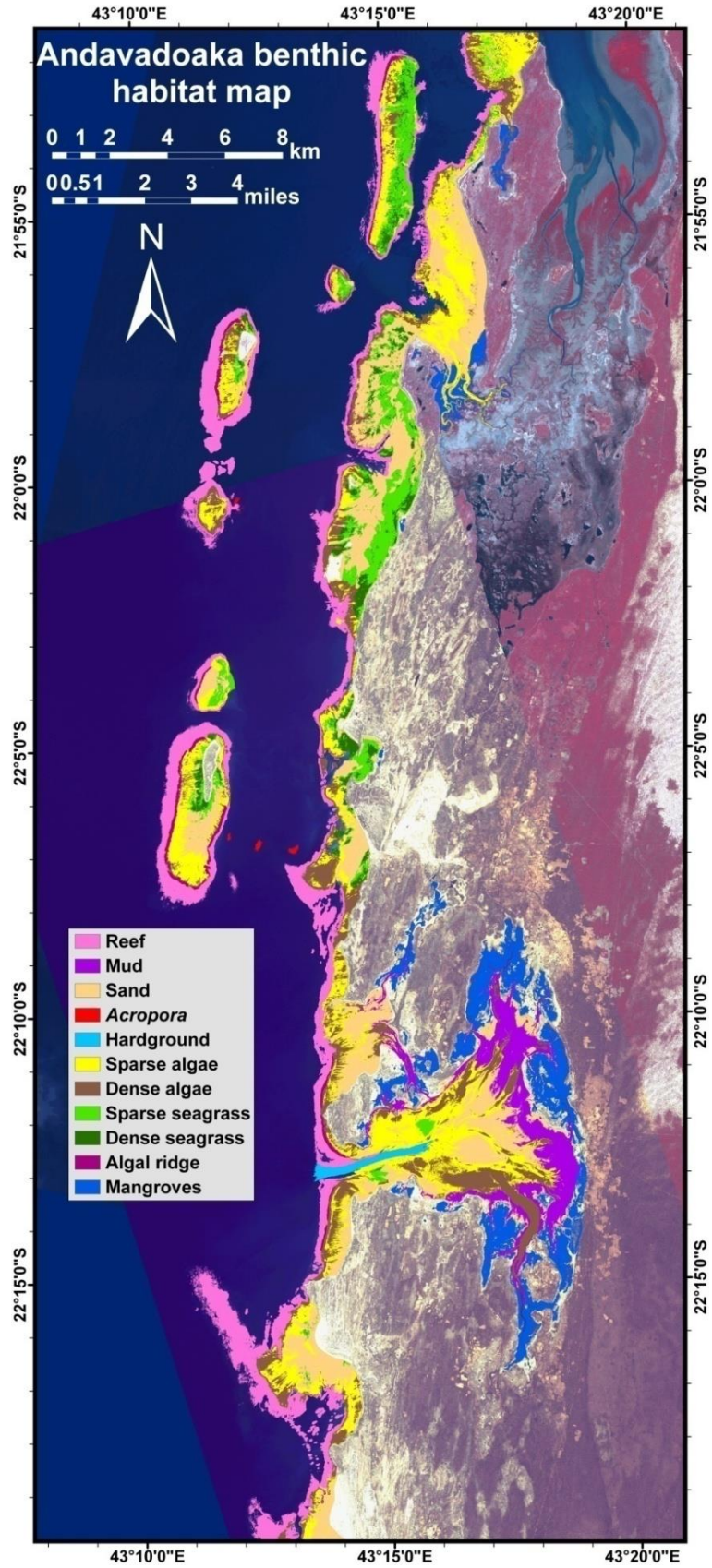
Sand

Bare carbonate skeletal sands, typically rippled.



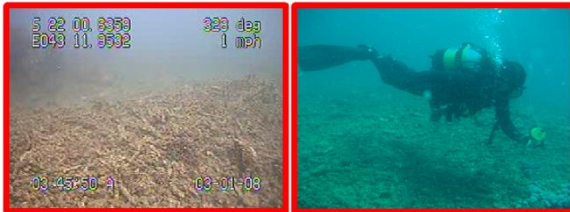
Mud

Highly enclosed mangrove-fringed muddy embayments.



Acropora

Isolated mounds of semi-consolidated *Acropora* rubble. Mounds are up to a hundred meters in diameter rising 10's of meters above a sandy seabed and composed entirely of dead *Acropora* fingers. The rubble flanks slope steeply due to cementation and are presumed stable. Both a red-algal crust and turfing algae are abundant. Occasional isolated fist-sized colonies of regenerating *Acropora* were observed. Settlement by massive corals is notably absent. The mounds are exclusively found on the leeward side of the offshore reefs, but separated by several hundred meters from the true reef slope.



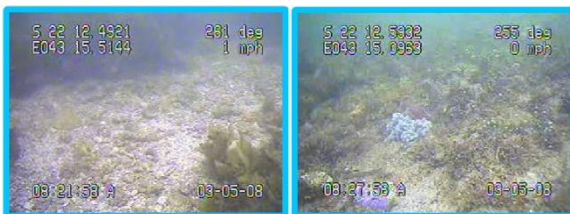
Reef

Mostly dead eroded coral framework, which provides several meters of relief above a seabed of unconsolidated sand, with 5-30% live coral cover, turf algae, and sponges. Sporadic and isolated patches of dense macro-algae atop the framework were occasionally encountered. Live stony corals are particularly prevalent in association with spur-and-groove morphology. Sub-meter patches of live coral cover exceeding 50% were rarely encountered.



Hardground

Scoured channel-beds with soft corals and algae. These channels have high velocity tidal flow capable of removing unconsolidated sediment and scouring the seabed. The result is a flat bare low-relief hardground which provides settlement opportunity for an assemblage of soft corals and well-rooted patches of *Sargassum*. The soft coral *Xenia* dominates this habitat class.



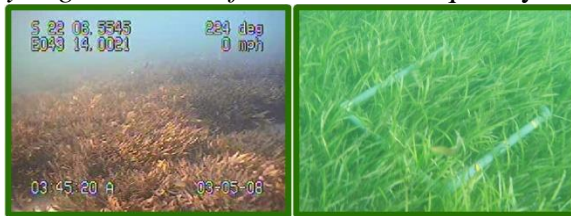
Algal ridge

An elevated margin bounding the seaward periphery of reef flats. This slightly raised structure is built by actively growing calcareous algae. Powerful wave energy during high tides and sub-aerial exposure during low tides inhibit the colonization of coral communities along these algal ridges.



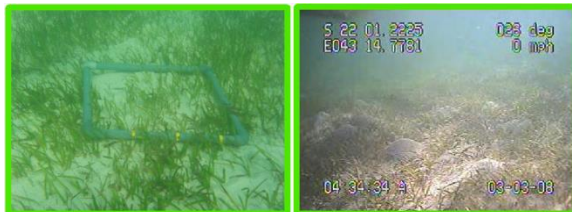
Dense seagrass

Seagrass meadows with 50-100% cover. Shoot density can exceed 100 per m². Dominant species is *Thalassodendron ciliatum*, with sub-dominance by *Thalassia testudinum*. *Syringodium isoetifolium* was infrequently observed in association with *Thalassia*.



Sparse seagrass

Seagrass patches with 10-50% cover consisting of a mixture of *Syringodium isoetifolium*, *Thalassia testudinum*, and *Thalassodendron ciliatum*. Patches are typically found atop sand and attain diameters of several meters.



Dense algae

Macro-algal cover, typically *Sargassum*, between 50-100% with expansive sand and coral rubble patches. The *Sargassum* forms dense meadows, growing up to a meter tall.



Sparse algae

Macro-algal cover between 10-50% with meter-sized patches of coral rubble and unconsolidated sand between algal growth. Rubble patches typically provide hard substrate onto which a sparse *Sargassum*-dominated algal assemblage adhere.



Sand

Shallow seafloor characterized by unconsolidated carbonate sand sheets. This class dominates the flats of offshore islands, as well as the shallows of coastal fringing reefs and the interior of mangrove-dominated embayments.



Mangroves

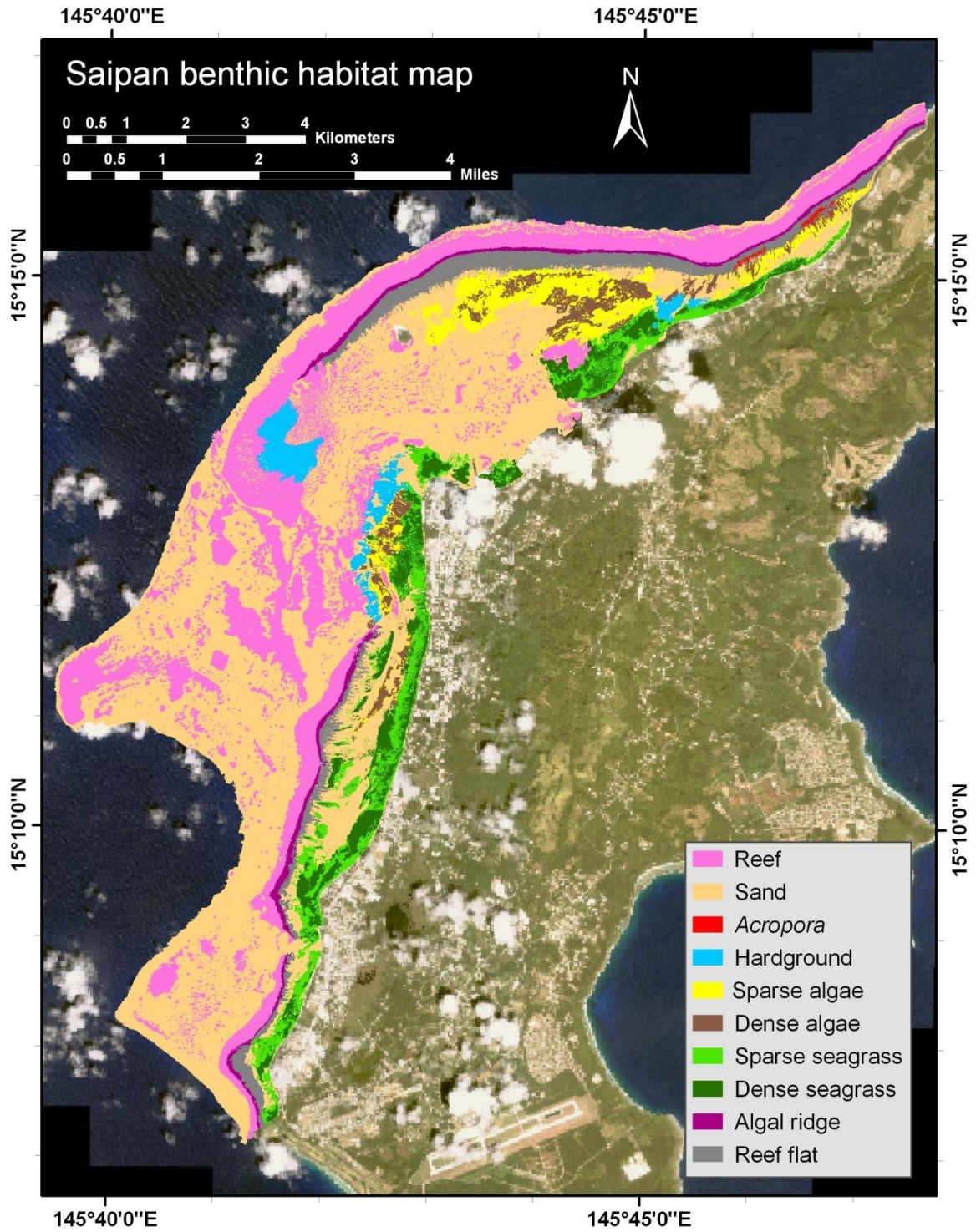
Mangrove mangles thrive along tidal muds with high organic contents and are commonly found in bays and inlets, which are protected from high wave energy. These trees obtain fresh water from sea water by secreting excess salt through their leaves or blocking absorption of salt at their roots. The mangrove forests near Andavadoaka consist of five species including: *Avicennia marina* (right), *Bruguiera gymnorrhiza*, *Ceriops tagal*, *Rhizophora mucronata* (left), and *Sonneratia alba*. This habitat class was mapped for management purposes but not analyzed as part of this study.



Mud

Intertidal lime muds that are completely submerged at high tide. This class fringes the perimeter of lagoonal embayments and is prevalent adjacent to mangrove mangles in the southern coastal zone of the study area.

C. Saipan



Acropora

Mostly dead *Acropora* (Staghorn coral) stands that exist only in the northeast portion of the Tanapag lagoon. This intricate coral framework is located leeward of the reef flat.



Reef

Aggregated reef framework including the windward northwest reef, the outer western reef, and patch reefs (4-150 meter diameters). The outer western reef is not as well developed (less wave energy) than the windward reef and it has high macro-algae (*Gelidiella acerosa*, *Asparagopsis taxiformis*, and *Padina minor*) cover with few corals. Mid-lagoon aggregate reefs are primarily composed of *Heliopora coerulea* (Blue Fire Coral) and *Pocillopora damicornis* (Lace Coral), as well as coralline and turf algae. Patch reef are composed of varying percentages of corals, turf algae, macro-algae, and coralline algae.



Hardground

The deep hardground at the base of the channel is a gradient from fully developed aggregate reef to patch reefs. The western hardground is an algal-dominated basement with a patchy distribution and low wave energy; this hardground region represents a gradient from the outer western reef framework to seagrass/macro-algae beds that rest atop sand sheets.



Algal ridge

This high wave energy habitat is colonized by coralline algae, macro-algae (*Turbinaria turbinata*), and sparse corals (*Pocillopora spp.*). These corals are typically fast growers with strong skeletons. *Pocillopora spp.* rank second for their contribution to reef structures only to *Acropora spp.*



Reef flat

The seaward portion of the reef flat is a flat expanse of dead reef rock and rubble which is partially or entirely exposed at low tide (depths of < 1 m) and covered by encrusting coralline algae and macro-algae (*Gelidiella acerosa*, *Asparagopsis taxiformis*, *Turbinaria turbinata*, and *Padina minor*). As you move towards the lagoon the reef flat remains shallow but becomes less algae-dominated and increasingly inhabited by 5-30% live coral cover consisting of *Isopora spp.* and *Porites spp.* The inner reef flat is also partially composed of coralline algae with patches of coral debris and sand in between the coral colonies.



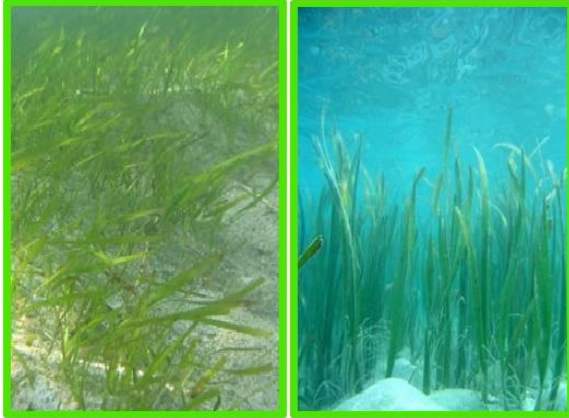
Dense seagrass

Seagrass meadows with 50-100% cover; dominant species include *Enhalus acoroides* and *Halodule uninervis*. Mixed among the seagrasses are macro-algae patches composed of *Gelidiella acerosa* and *Halimeda macroloba*. Concentrations of macro-algae are higher where nutrient runoff is prevalent (*i.e.* close to pollution sources along the coasts).



Sparse seagrass

Enhalus acoroides and *Halodule uninervis* dominate, but with patchier distributions with 10–50% cover. Left image is sparse *Halodule uninervis* and right image shows sparse *Enhalus acoroides*.



Dense algae

Sand sheets with dense cover of *Halimeda macroloba* and turf algae.



Sparse algae

Sparse turf algae colonize sand sheets with occasional macro-algae patches.



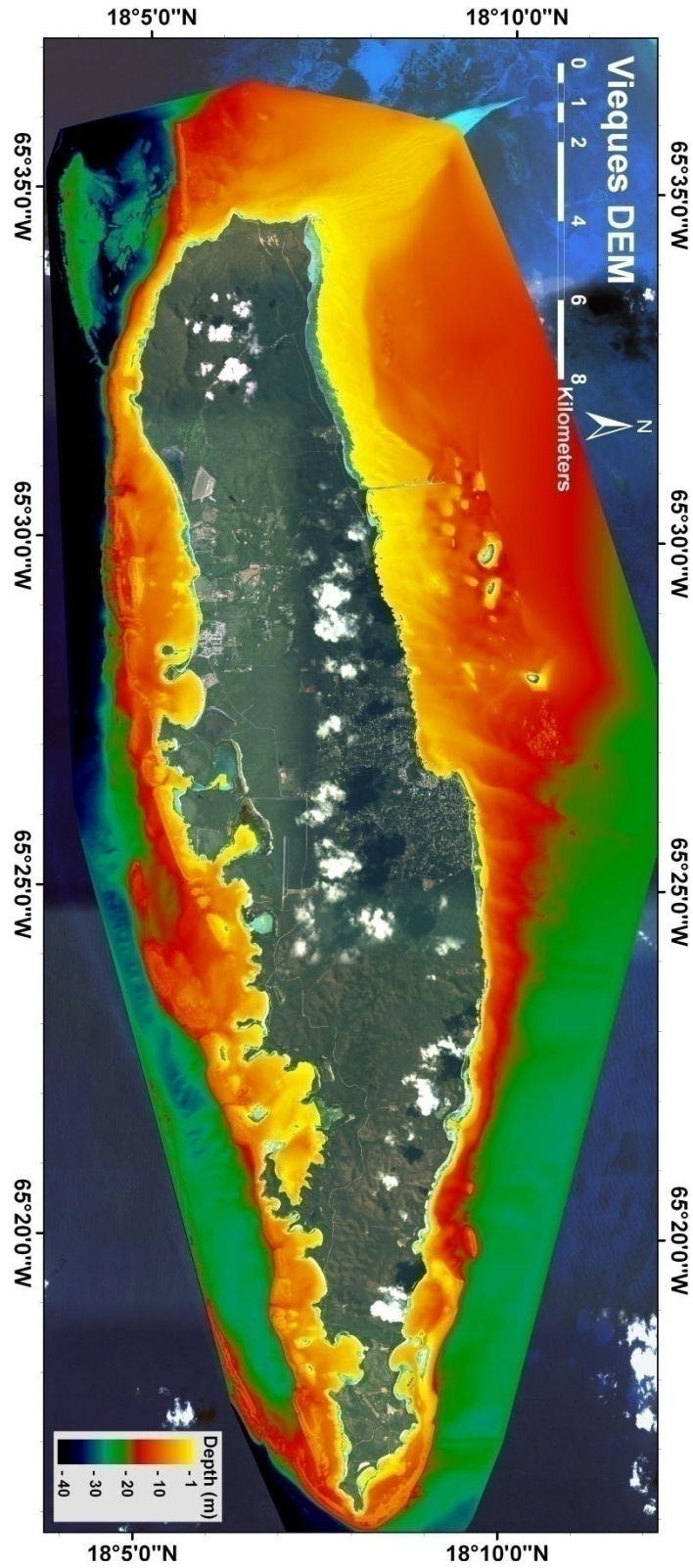
Sand

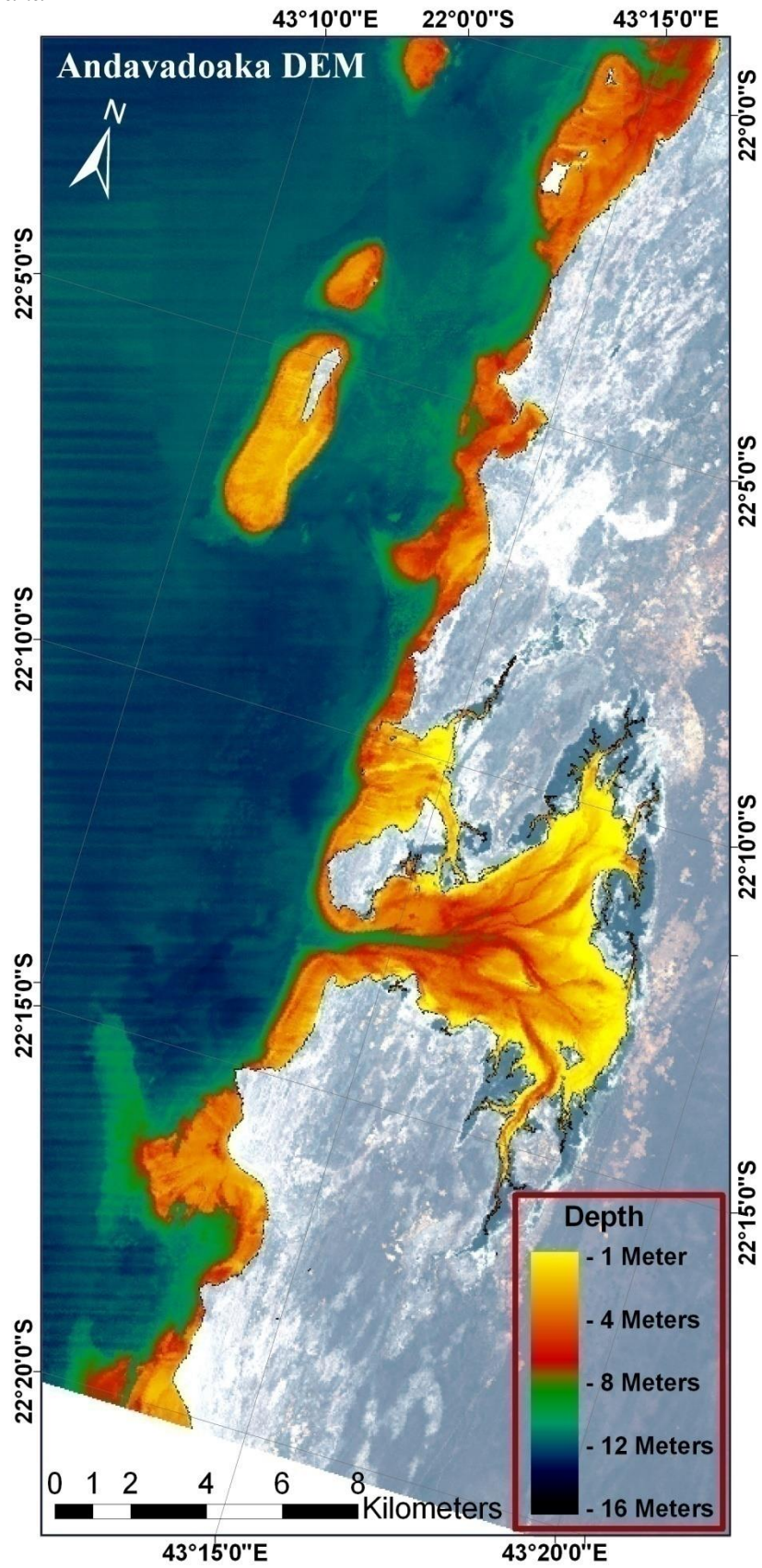
Uncolonized sand sheets between 1-30 meters depth.



Appendix II: DEMs

A. Vieques





C. Saipan

